



Medtronic Cardiac Surgery Technologies
7601 Northland Drive
Minneapolis, MN 55428.1088 USA
www.medtronic.com

October 21, 2004

Division of Dockets Management
Food and Drug Administration
6530 Fishers Lane, Room 1061 (HFA-305)
Rockville, MD 20852

RE: Post Comments to the following Dockets:
- Docket No. 02N-0534: Medical Device User Fee and Modernization Act (MDUFMA) &
- Docket No. 03N-0161: Medical Devices; Reprocessed Single-Use Devices; Termination
of Exemptions from Premarket Notification; Requirement for Submission of Validation
Data

To Whom It May Concern:

Medtronic, Inc. requests that you post the attached document to the above listed do docket. We
have included both a hard copy and electronic copy for your ease.

If you have any questions, please feel free to contact me directly.

Sincerely,

Scott Cundy
Director Regulatory, Clinical, & Quality
Medtronic Cardiac Surgery Technologies
(763) 391-9941 Phone
(763) 391-9279 Fax

03N-0161

SUP 1



U.S. Food and Drug Administration



[FDA Home Page](#) | [Search FDA Site](#) | [A-Z Index](#) | [Contact FDA](#)

Contact Division of Dockets Management

Mailing Address: Division of Dockets Management
Food and Drug Administration
5630 Fishers Lane, Room 1061 (HFA-305)
Rockville, MD, 20852

**Visit Division of Do
Management**

[Map and Direction
Nearest Metro](#)

Email: fdadockets@oc.fda.gov

Phone: 301-827-6860

Fax: 301-827-6870

TTY/TDD Users: 1-800-735-2258

[FDA Home Page](#) | [Search FDA Site](#) | [A-Z Index](#) | [Contact FDA](#) | [Privacy](#) | [Accessibility](#)

FDA/Website Management Staff
Web page created by wms 2003-JAN-06. Design by zwr.
Page updated 2003-OCT-03 jb

Observations of New and Reprocessed Octopus 3[®] Tissue Stabilizers and Octopus4[®] Tissue Stabilizers

Report on Observations of New and Reprocessed Octopus 3[®] Tissue Stabilizers and Octopus 4[®] Tissue Stabilizers

The objective of this study was to evaluate new sterile and reprocessed sterile Medtronic Octopus 3[®] and Octopus 4[®] Tissue Stabilizers (see attached product PDF files). A report dated May 24, 2004 contained information and data describing the differences observed between new sterile and reprocessed sterile Medtronic Octopus 3[®] and Octopus 4[®] Tissue Stabilizers. In that report a total of four devices were assessed, one new sterile Medtronic Octopus 3[®], one new sterile Medtronic Octopus 4[®], one reprocessed sterile Medtronic Octopus 3[®] (SterilMed) and one reprocessed sterile Medtronic Octopus 4[®] (Alliance). Subsequent to that report, eight additional reprocessed Medtronic Octopus 3[®] and Octopus 4[®] Tissue Stabilizers from the same two reprocessors were examined using similar microscopic and molecular techniques. On June 7, 2004 the additional reprocessed Medtronic Octopus 3[®] and Octopus 4[®] Tissue Stabilizers were received. Results of eight of those are contained in this study for a total of twelve devices, two new sterile devices and ten reprocessed devices.

Upon arrival, all units appeared unopened and were in original, sealed packaging. The units were hand delivered in good condition and received personally. Anti-tampering seals were all intact. The units were observed and tested by a variety of light and electron microscopic examination methods and DNA analysis and this report represents these findings.

A study code was assigned to each of the devices so that individuals performing the testing were blind as to the condition or the reprocessor. This report will refer to the device by the study ID code as follows:

Device	Reprocessor	Study ID
Octopus 3 [®]	New-not reprocessed	MT-104-1
Octopus 4 [®]	New-not reprocessed	MT-104-2
Octopus 3 [®]	SterilMed	MT-104-3
Octopus 4 [®]	Alliance	MT-104-4
Octopus 3 [®]	Alliance	MT-104-5
Octopus 3 [®]	SterilMed	MT-104-7
Octopus 3 [®]	SterilMed	MT-104-8
Octopus 3 [®]	SterilMed	MT-104-9
Octopus 4 [®]	Alliance	MT-104-10
Octopus 4 [®]	Alliance	MT-104-11
Octopus 4 [®]	Alliance	MT-104-13
Octopus 4 [®]	Alliance	MT-104-16

Our findings describe little to no debris on the new Medtronic Octopus 3[®] study ID# MT-104-1, Medtronic Octopus 4[®] study ID# MT-104-2, or the reprocessed Medtronic Octopus 4[®] study ID# MT-104-4 in the headlink region when observed by light and scanning electron microscopes. The debris present in these devices appeared to be non-organic and what appeared to be the same materials typical of the manufacturing process.

All of the other reprocessed Octopus 3[®] Tissue Stabilizers and Octopus 4[®] Tissue Stabilizers observed in this study clearly demonstrated the presence of artifacts, defects, bioburden and contamination including etching of the metal surfaces, cell profiles, hair, fibers, and protein and nucleic acid labeled material on the headlink region when compared to new sterile devices. Additional DNA testing by PCR analysis of the material confirmed the presence of human DNA in several pods of the reprocessed Octopus 3[®] Tissue Stabilizers and Octopus 4[®] Tissue Stabilizers.

All devices in this report will be referred to by the study ID number. In the course of this study, extensive observations and over 4000 images were completed. This report contains only a relatively small number of those images. The images included are representative of the observations overall.

Each of the units was to be evaluated by methods outlined below and contained in the MT104 Protocol.doc document. There were numerous digital images and video sequences collected during the testing that were utilized in the evaluation but not contained in this report. These images will be provided with all devices, documents and packing materials upon the completion of the study.

PROTOCOL FOR EVALUATION

A. Opening of Devices

1. Photos of intact packaging and devices
2. Retain packaging materials
3. Video

B. Microscopy (areas of interest - done before dismantling)

1. Headlink
 - a. Complete view
 - b. Joints
2. Pods
 - a. Back side
 - b. Suction side
3. Arm with sheath
4. Handle

C. Separation of Headlink from Arm

1. Photos of dismantled pieces

D. Low Voltage Scanning Electron Microscopy (SEM) on Headlink

1. Any suspicious areas based on optical microscopy
2. Suction side of pods

E. Hypotube Interior Exposed

1. Document setup and process
 - a. Photos
 - b. Written description
2. Cut open hypotube, preserving designated portion(s) for SEM

F. SEM Exposed Surfaces of Hypotube

1. Suggested magnifications of 50x, 250x, 1000x and higher
2. Particular attention to particles and residue
3. Record images

I. Particle/Residue Specimen Evaluation Identification

1. Performed only if particles or residue are found during SEM examination
2. If residue is found, Medtronic will meet to discuss the best approach to identify. Approach may vary dependent upon the nature of the residue.
3. An addendum will be written to the protocol when completed.

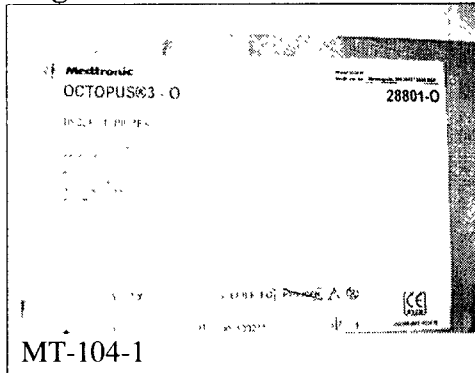
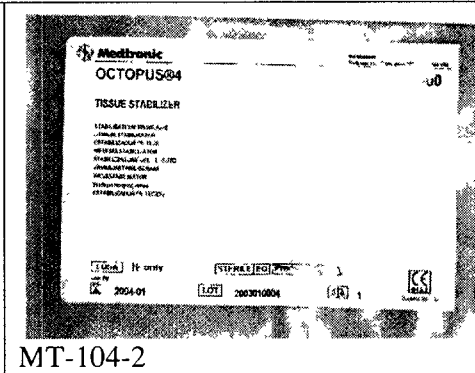
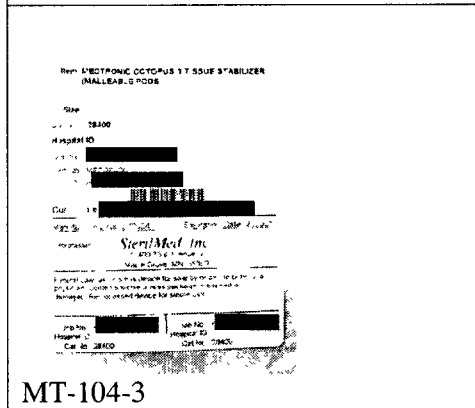
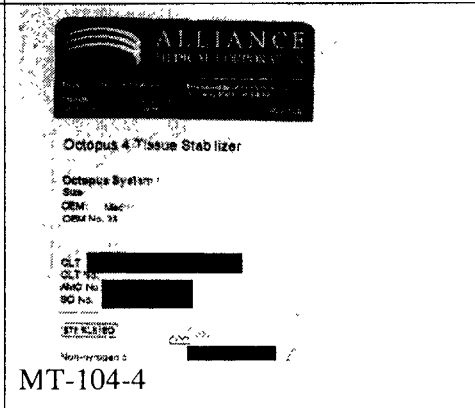
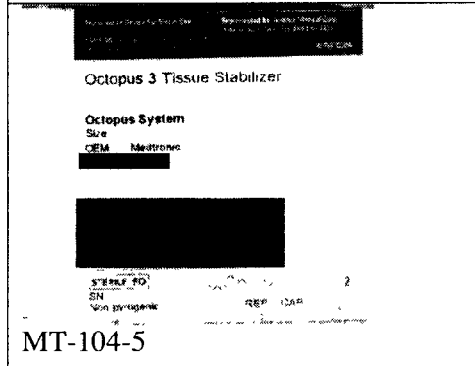
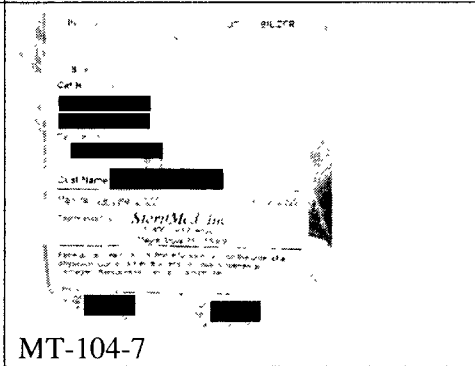
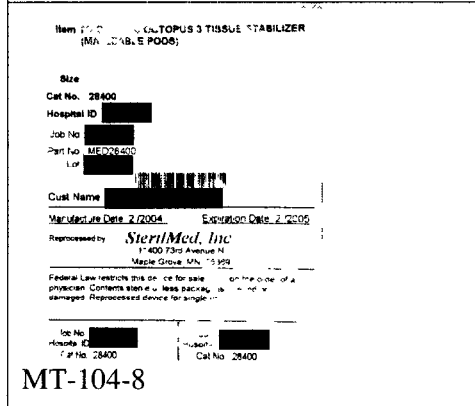
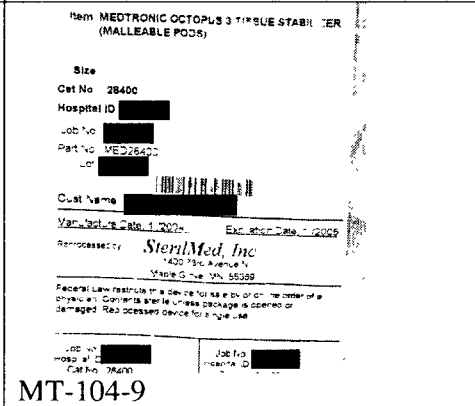
Units evaluated in this report

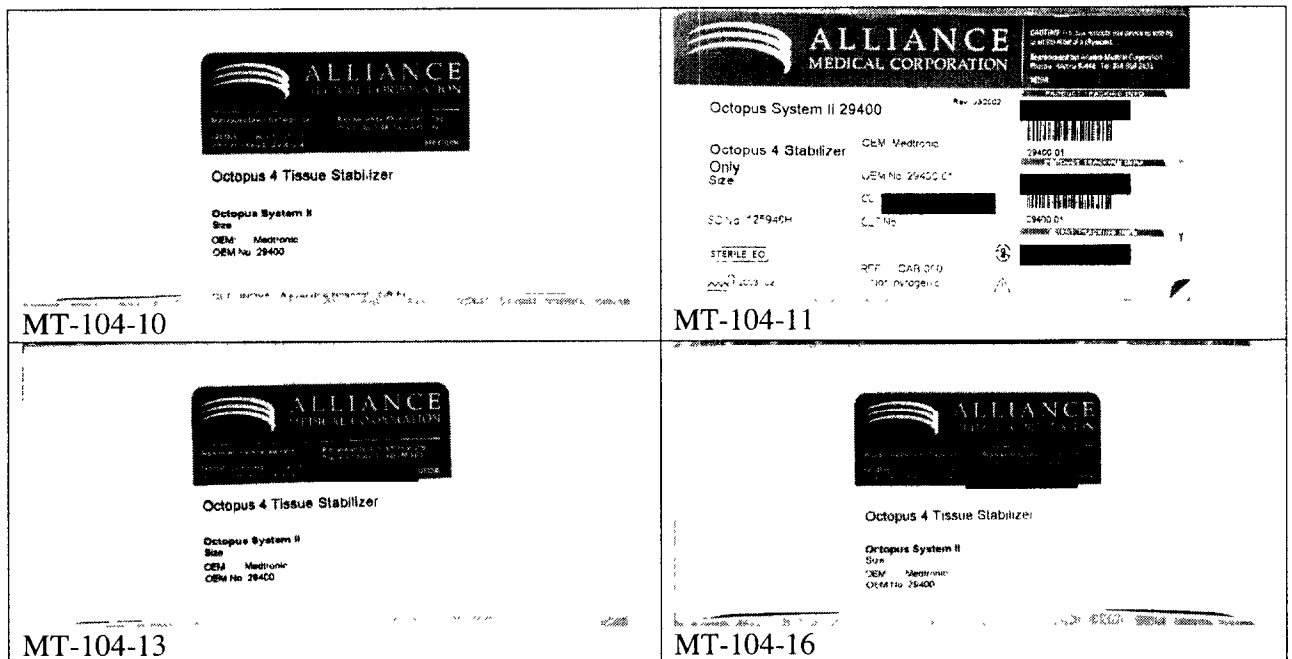
All of the devices evaluated in this study were identified as either new sterile or reprocessed devices from hospitals that requested Medtronic to provide them with the data on the cleanliness of these devices. The table below is the key used to identify the devices within the testing laboratory.

Table I. Study code

Study ID	Device	Reprocessor
MT-104-1	Octopus 3 [®]	New-not reprocessed
MT-104-2	Octopus 4 [®]	Alliance
MT-104-3	Octopus 3 [®]	SterilMed
MT-104-4	Octopus 4 [®]	New-not reprocessed
MT-104-5	Octopus 3 [®]	Alliance
MT-104-7	Octopus 3 [®]	SterilMed
MT-104-8	Octopus 3 [®]	SterilMed
MT-104-9	Octopus 3 [®]	SterilMed
MT-104-10	Octopus 4 [®]	Alliance
MT-104-11	Octopus 4 [®]	Alliance
MT-104-13	Octopus 4 [®]	Alliance
MT-104-16	Octopus 4 [®]	Alliance

Figure 1. The devices were labeled as follows:

 <p>Medtronic OCTOPUS®3 - 0 Cat No. 28801-0</p>	 <p>Medtronic OCTOPUS®4 TISSUE STABILIZER Cat No. 28801-0</p>
 <p>Item: MEDTRONIC OCTOPUS 3 TISSUE STABILIZER (MALLEABLE PODS) Cat No. 28400 Reprocessed by: SteriMed, Inc.</p>	 <p>ALLIANCE OCTOPUS 4 Tissue Stabilizer Cat No. 28400</p>
 <p>Item: MEDTRONIC OCTOPUS 3 TISSUE STABILIZER (MALLEABLE PODS) Cat No. 28400 Reprocessed by: SteriMed, Inc.</p>	 <p>Item: MEDTRONIC OCTOPUS 3 TISSUE STABILIZER (MALLEABLE PODS) Cat No. 28400 Reprocessed by: SteriMed, Inc.</p>
 <p>Item: MEDTRONIC OCTOPUS 3 TISSUE STABILIZER (MALLEABLE PODS) Cat No. 28400 Reprocessed by: SteriMed, Inc.</p>	 <p>Item: MEDTRONIC OCTOPUS 3 TISSUE STABILIZER (MALLEABLE PODS) Cat No. 28400 Reprocessed by: SteriMed, Inc.</p>



Instrumentation used in the study

Sample Handling

Samples were handled with care to prevent modifications, damage and contamination. Sealed packaging was opened and documented by digital video (not included in this report). Standard laboratory practices, including sterile latex or nitrile gloves were always worn when handling the devices. Images of the devices were documented by non-contact methods. Units, all original packing materials and data has been retained and stored in a secure location.

Digital Cameras

Digital video was taken using a Sony DCR-TRV90 camera and recorded to mini-DV tape. Digital still images were taken using a Nikon CoolPix 995 or 4500 digital camera. A Nikon SMZ-1500 stereoscope equipped with a Nikon CoolPix digital camera was also used to image the devices and procedures.

Variable Pressure Scanning Electron Microscopy

A Hitachi S-3500N scanning electron microscope equipped with Environmental Secondary Electron Detector, Absorbed Electron EBIC detector, Robinson Backscattered Electron Detector, standard Secondary Electron Detector, Infrared ChamberScope,

EDAX Phoenix x-ray microanalysis system with Super Ultra-thin window, 10mm Compact Detector Unit, elemental mapping, spectral processing, multi-point analysis, an Emitech K-1150 Cryogenic System, with cryo-prep unit, airlock interface to SEM and sputter-coater. The system was operated in variable pressure mode such that imaging can be accomplished without any prior specimen processing. Conventional preparation techniques for scanning electron microscopy (SEM) necessarily involve dehydration, which in turn, usually necessitates a prior chemical treatment known as fixation. The main advantage of the variable pressure SEM is that it offers the opportunity of observation and microanalysis of samples under conditions that are closely related to the natural state. Other than separating the head from the tubing, no additional modifications or treatments were done to the sample prior to viewing by SEM. Preparations were viewed using 5 keV in 15Pa variable pressure mode and photographs were digitally recorded.

Confocal Microscopy

Unmodified and subsequently treated (stained for DNA and/or protein) units were viewed by fluorescence using a BioRad MRC-1024 confocal microscope attached to a Nikon Diaphot inverted microscope (BioRad Labs, Hercules, CA) equipped with a 15 mW Krypton/Argon laser. Excitation filters allowing 488 nm or 568 nm or combinations of both laser lines were used. Room temperature was maintained throughout the experiment. The samples were viewed using either a 4x, 0.15 n.a.; 10x, 0.4 n.a. or 20x, 0.75 n.a. objectives. Digital images were collected on a Compaq ProSignia model 300 personal computer using LaserSharp version 3.2 software (BioRad Labs., Hercules, CA). Stored digital images were analyzed using Image Pro Plus version 4.5 software (Media Cybernetics, Silver Springs, MD 20910). Prints were made utilizing Adobe PhotoShop version 7.0 and a Fujix Pictography 3000 digital image printer (Fuji North America, Elmsford, NY 10523) or Xerox Phaser 8200 color printer.

Fluorescence Microscopy

A Nikon E800 research grade microscope, along with a CoolSnap HQ 12 bit monochrome camera connected to a Pentium IV 2.6 GHz personal computer using Image Pro Plus version 4.5 software (Media Cybernetics, Silver Springs, MD 20910) was used to capture high resolution, low-light fluorescence images. This upright microscope is equipped with phase, DIC, darkfield and epi-fluorescence optics. The system has the capacity to capture still and high frame rate images to digital formats. Additionally, time-lapse images can be recorded digitally for future analysis, if required. Digital images can be captured and analyzed using a number of image processing software applications, including Media Cybernetics ImagePro Plus 4.5, ImageJ and VayTek VoxBlast digital deconvolution. The microscope is also equipped with AFA (Advanced Fluorescence Acquisition) software and hardware that is an add-on module which plugs into Image-Pro Plus and Scope-Pro[®] software products. It uses the

microscope and peripheral control capabilities of Scope-Pro to configure the system for image captured of transmitted and /or fluorescent images in a 3D or 4D series. This system was used to preview DAPI labeled devices.

DNA Analysis

Following initial imaging and prior to disassembly and cutting of the tubes, samples of content from designated pods (see Table III) of the new and reprocessed Octopus 3[®] and Octopus 4[®] devices were collected using sterile swabs. DNA was identified using a Quiagen DNeasy tissue kit (cat # 69502 Quiagen, Valencia, CA) as per kit instructions. Briefly, following swabbing of an individual pod, the swab end was treated with proteinase K at 70°C for 1 hour to lyse cellular material. 200 μ l of Buffer AL was added and sample vortexed. 200 μ l of EtOH was added and vortexed. The entire sample was placed into DNeasy mini spin column and spun at 6000g for 1 minute. The collection tube was discarded. 500 μ l of Buffer AW1 was added and spun at 6000g for 1 minute. The flow-through and tube was discarded. 500 μ l of Buffer AW2 was added and spun at 20,000 x g for 3 minutes. The column was washed 2 times with 200 μ l of Buffer AE, incubated for 1 minute and spun at 6000 x g for 1 minute.

A single-copy 536 bp human β -globin fragment was amplified from each sample using standard PCR protocols, and the products electrophoresed on a 10% polyacrlamide/TBE gel and stained with ethidium bromide (Molecular Probes). Gels were photographed using a BioDocIt gel documentation system (UVP Inc.).

Briefly, PCR was preformed by using one hundred picograms of DNA in quadruplicate 20 μ l parallel PCR assays using a Perkin Elmer 9700 thermal cycler. The fluorescence of 0.25x SYBR-Green (Molecular Probes, Eugene, OR) was measured at each amplification step. Sixty cycles of PCR were carried out using the HotStar *Taq* polymerase system (Qiagen, Valencia, CA) with the primer pairs below at the specified annealing temperatures.

Primer: TTT AGT GGG GTA GTT ACT CCT

Product length 536, $T_a=60.4$, Read Temp=77.5

This primer is designed to amplify the genes corresponding to β -globin region of human genome DNA. This primer is used as the positive control for confirming the presence and the acceptability of the extracted DNA to template. PCR and gel electrophoresis performed by external staff.

Procedures, Testing and Results

Opening of Devices

Digital photos and video were taken to document the opening and unpacking of the devices. All packing materials were saved. The devices were stored in a secure location while not being analyzed.

Microscopy (areas of interest - done before dismantling)

All devices had intact anti-tamper seals. The outer packaging was opened by cutting the seal at the end of the boxes of the Alliance reprocessed devices or opening the polymer outer packaging in the SterilMed or Medtronic devices. The devices have a transparent outer package permitting the initial macro imaging was done prior to packaging removal.

Initial stereoscopic inspection of the reprocessed Octopus 3[®] and Octopus 4[®] devices revealed a light colored material in numerous openings of the metal tubing in the pods. Fibers and or hairs were also observed. Cracks and defect in the plastic surrounding the hypotubes were observed. Some tube openings were blocked. These artifacts were not observed in the new devices or reprocessed device MT-104-4. Visual and macro inspection did not reveal obvious signs of foreign material in other regions of the device, with the exception of the ball joint. Extensive imaging studies were not performed on the devices away from the headlink area. The vast majority of images collected are from the headlink and ball joint regions.

Separation of Headlink from Arm

Following initial inspections described above, the headlinks were removed from the packaging and separated from the devices by removing the retaining clip with a small flat blade cleaned screwdriver and cutting the vacuum tubing with a cleaned razor blade. Additional inspections of pods of the headlink region of the reprocessed devices confirm the presence of material in the openings of some of the hypotubes. There are also what appear to be hairs and colored fibers present in some devices.

Low Voltage Scanning Electron Microscopy (SEM) on Headlink

Variable pressure SEM confirms the presence of foreign material in the openings of several hypotubes. There are indications of erosion of the openings and surface of the hypotubes. The foreign material on the surface at times appears to be cellular in size and shape. Some openings of the hypotubes are blocked.

Confocal and Fluorescence Microscopy Evaluation

The exterior of the hypotube regions of the reprocessed Tissue Stabilizers were observed by confocal and fluorescence microscopy to assist in the identification of the material. Some autofluorescence was observed in the regions of the openings of the hypotube with the most material, however autofluorescence cannot determine composition of unknown material. Images were collected before and after nucleic acid and protein specific stains were applied. The material in the openings and on the surface of the hypotube was positive for DNA and protein stains.

Samples collected for DNA Analysis

At least two of the exteriors of the hypotube pod regions of new and reprocessed Tissue Stabilizers were swabbed to collect the material for DNA analysis using the Quiagen DNeasy analysis kit.

Hypotube Interior Exposed

The headlinks of five devices were hand delivered to University of Minnesota St. Paul Apparatus Shop to further disassemble the device, remove the hypotube from the headlink and open the hypotube interior. Once removed the hypotube was placed into an aluminum jig and the interior was exposed using a Bridgeport milling machine by machining a pair of parallel slits enabling the removal of a piece of the tube exposing the interior. The machining was done at low speeds by removing nine to ten, 0.001 inches of material per pass in order to minimize heat and debris. The perforated section could then be removed by hand.

SEM and Light Micrographs of the Exposed Surfaces of Hypotube

Scanning electron microscopy and light microscopy was done to observe the inner surfaces of the hypotubes of the devices. The interior of the hypotube regions of the reprocessed devices was observed and additional material was found in the interior. Foreign material is also present on the inner openings and surfaces of several hypotubes.

Images

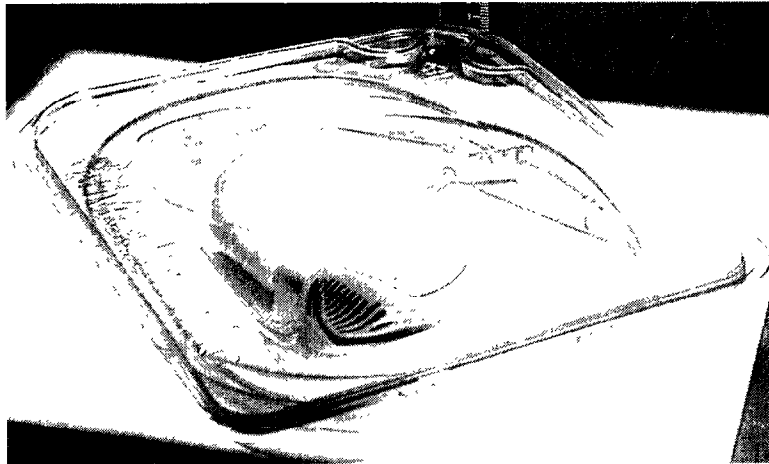


Figure 2. Example of Octopus 3® - Medtronic Sales Stock – indicated as sterile, unopened from the warehouse. Outer packaging removed (MT-104-1).

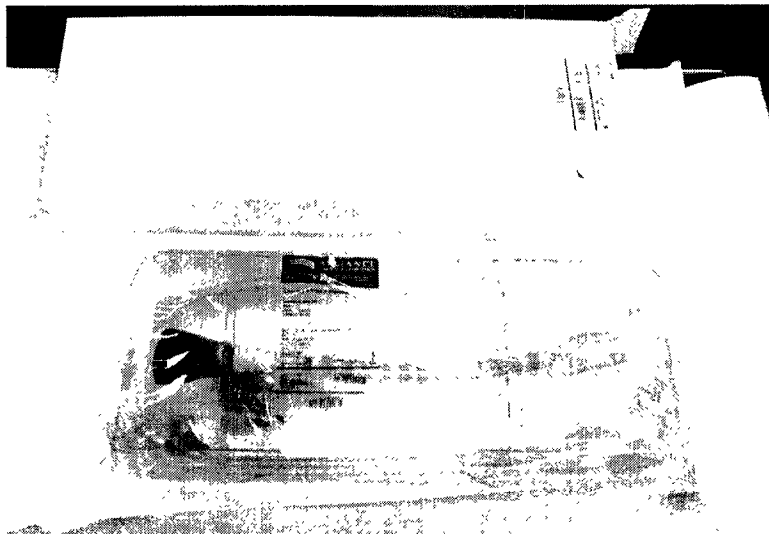


Figure 3. Example of Octopus 4® - used and reprocessed device and packaging. Outer packaging removed (MT-104-4).

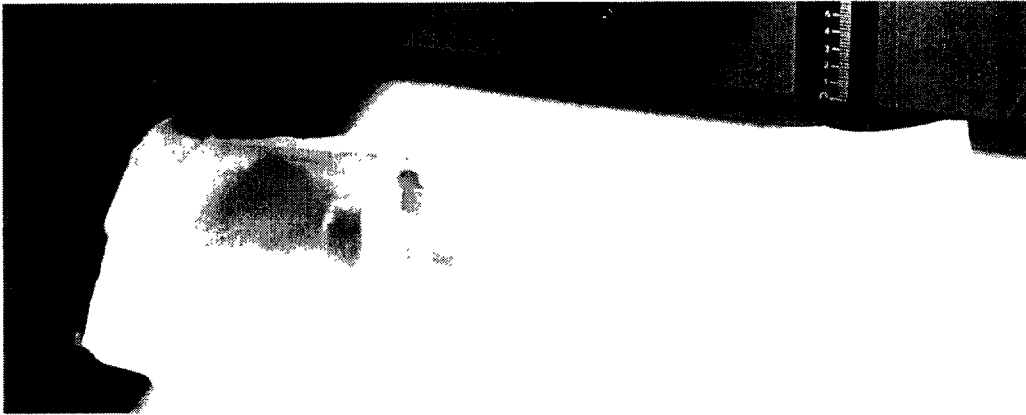


Figure 4. Example of Octopus 3[®] - Used and reprocessed device – sterile, unopened from reprocessor. Outer packaging removed (MT-104-3).

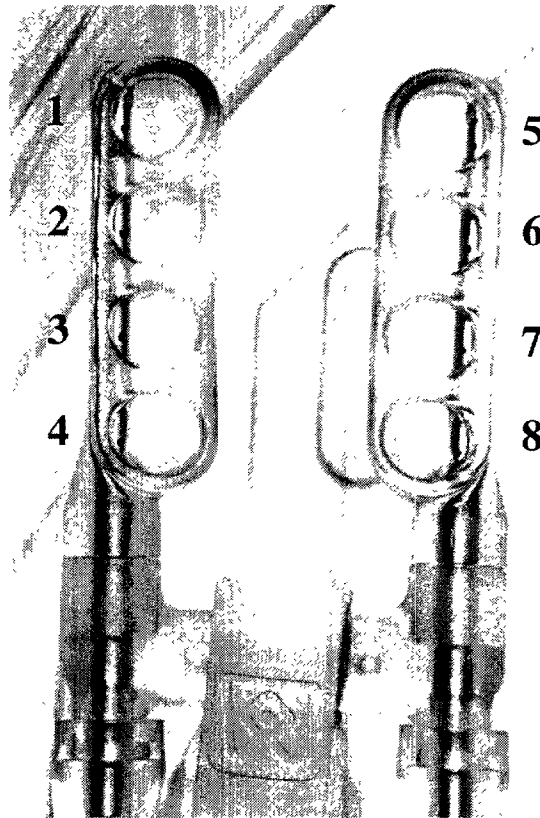


Figure 5. Overview of headlink region of an Octopus3[®] (MT-104-1). Numbers indicate pod number referenced in this report for both Octopus3[®] and Octopus4[®] devices.

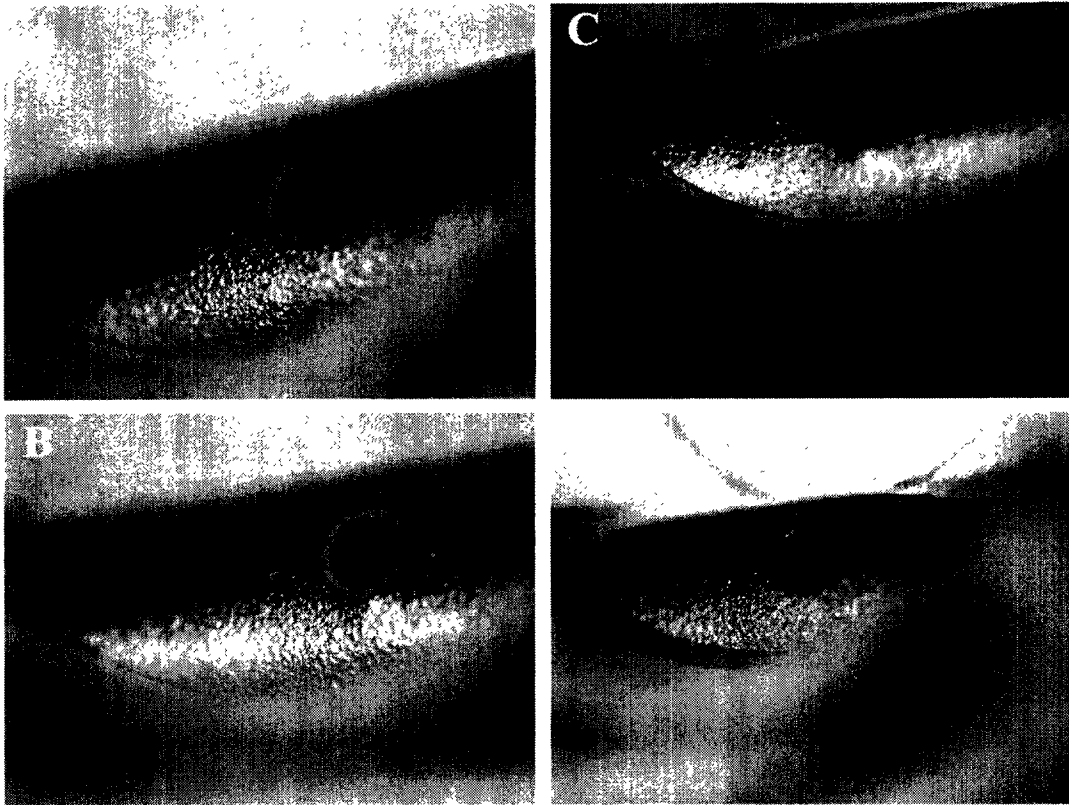


Figure 6. **Reprocessed Octopus 3[®]** - Used and reprocessed device – close-up view of openings in four of the eight pods of the head region. Presence of a light colored foreign material noticed in openings of A, B, and C (MT-104-3). This material was not observed in the new devices.

Pod Head Dismantling

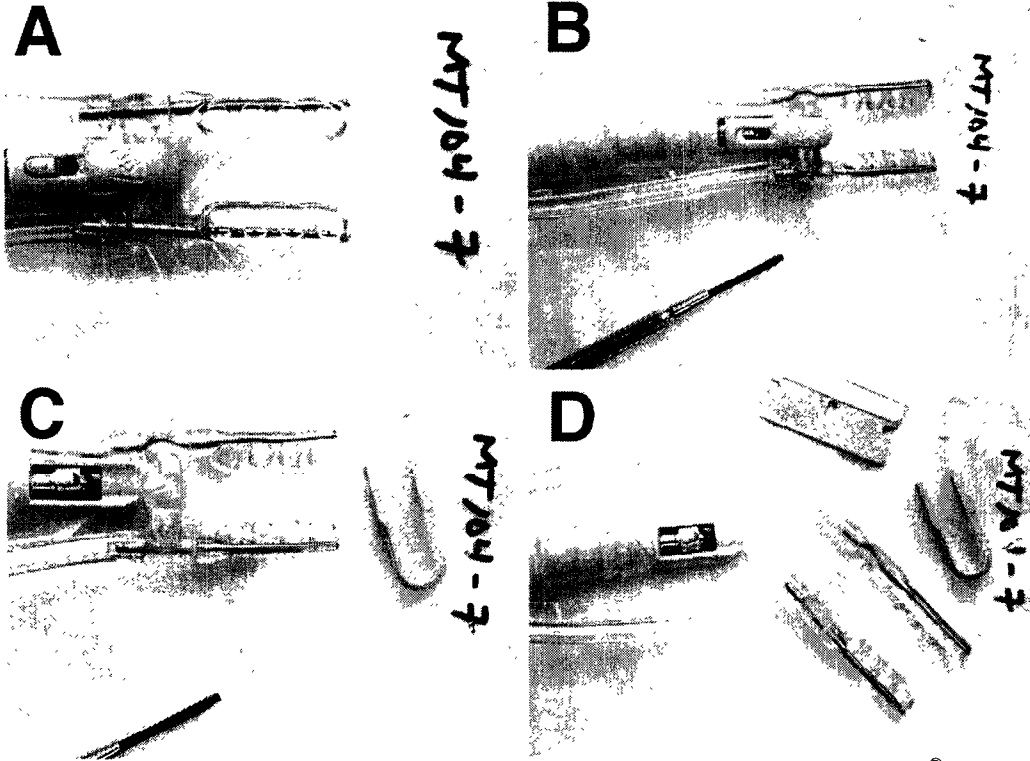


Figure 7. Example of pod - headlink dismantling (MT-104-7). All Octopus[®] devices were dismantled in a similar manner. This permitted viewing of the interior of hypotubes and ball joint regions as well as observation in the variable pressure scanning electron and confocal microscopy.

Ball Joint Observations

Pod heads were separated from the flexible arm in order to continue microscopic evaluations. The heads were separated from the arm by removing the retaining clip and using a sterile razor blade to cut the tubing (see Figure 7). Once the pod head was removed the arm was examined for corrosion and debris in the region of the ball joint at the end of the flexible arm. Cutting the plastic arm end surrounding the ball joint using a jeweler's saw then further exposed the ball joint. The exposed ball joint was then examined by stereomicroscopy and digital images recorded.

Corrosion and debris did not appear obvious in new sterile Octopus[®] devices. There is discoloration of the metal, presumably due to heat generated during a grinding/polishing process following the attachment of the integral cable to the ball joint. Example images are below:

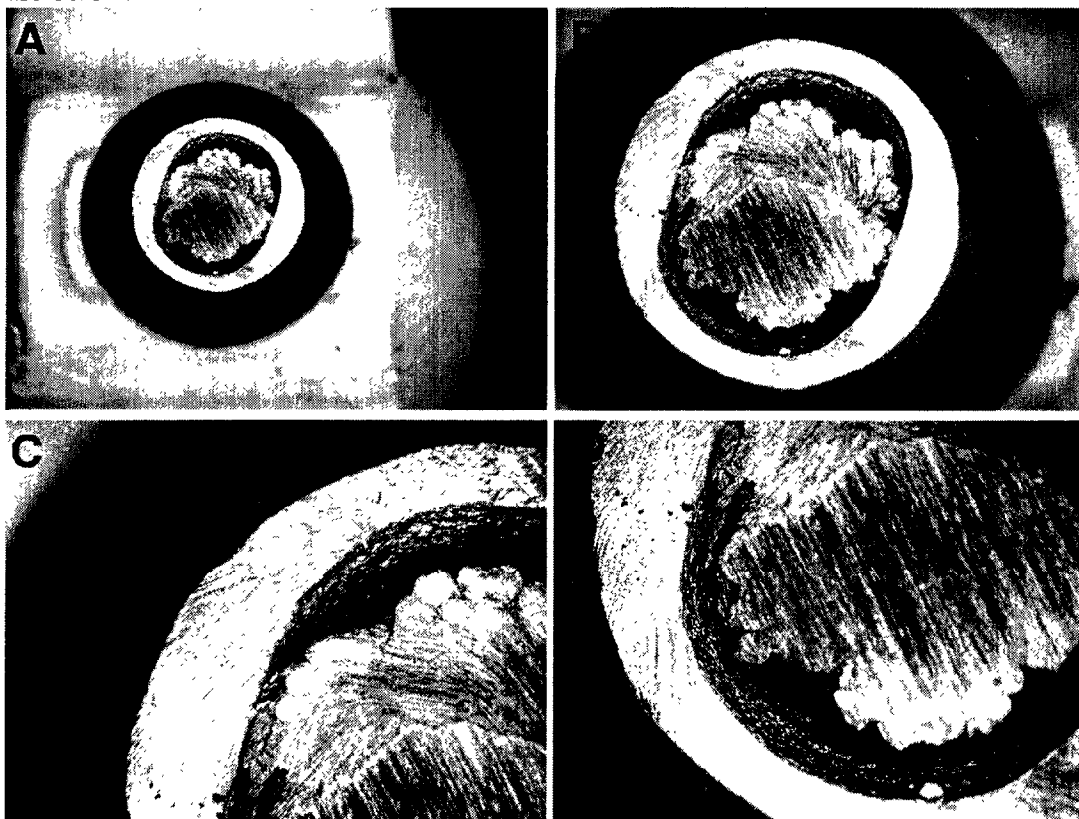


Figure 8. Ball joint region from a new sterile **Octopus 4[®]** (MT-104-4). No corrosion or debris was observed.

Reprocessed devices study IDs MT-104-3, 7, 8 and 9 (SterilMed) all had discoloration and significant corrosion in the cable attachment area of the ball joint region. All of the units had obvious bioburden and debris including hair or hair-like fibers (arrowheads) in the region of the ball joint. Example images from MT-104-7, 8 and 9 are below (arrowheads indicate hair, note extensive corrosion):

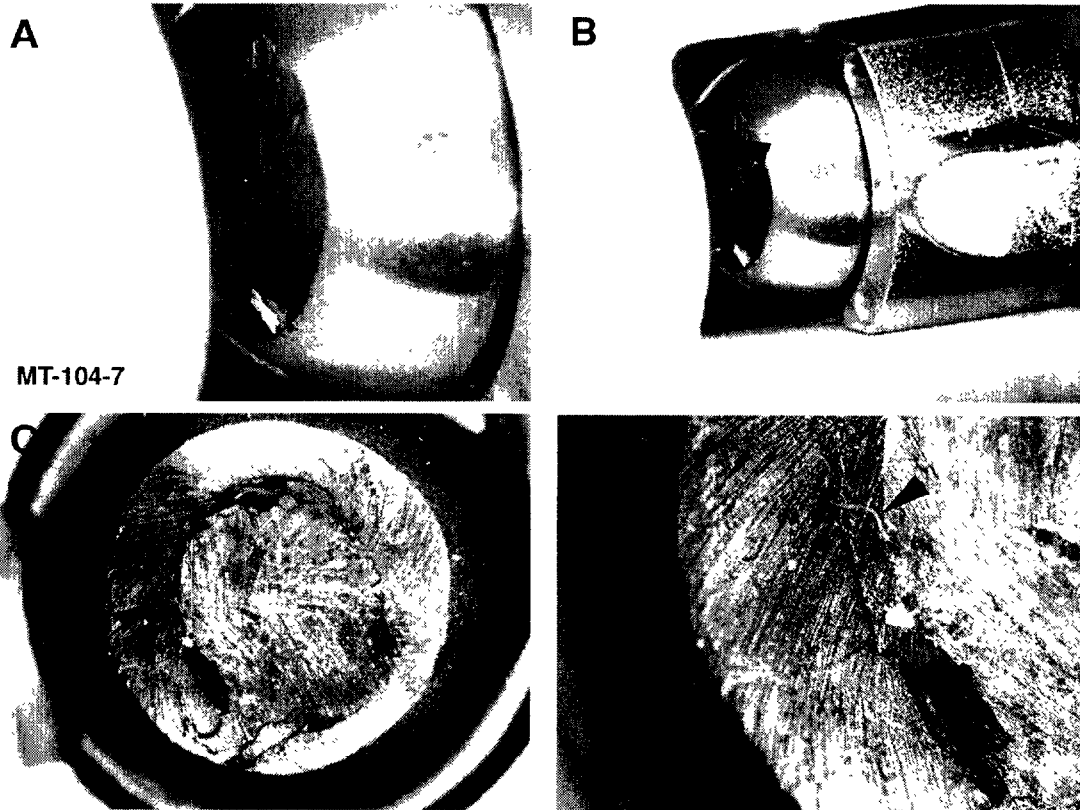


Figure 9. Stereomicroscopy images from **reprocessed device MT-104-7**. Arrowheads indicate hair, note extensive corrosion. Hair identified by cuticular scales and has been stained by the corrosion indicating its presence at the time of corrosion formation.

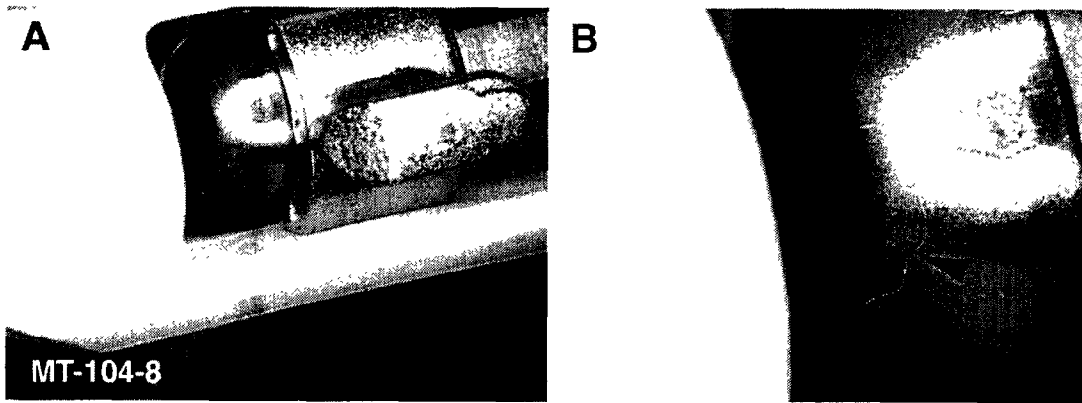


Figure 10. Stereomicroscopy images from reprocessed device MT-104-8. Arrowhead indicates hair or hair-like fiber.

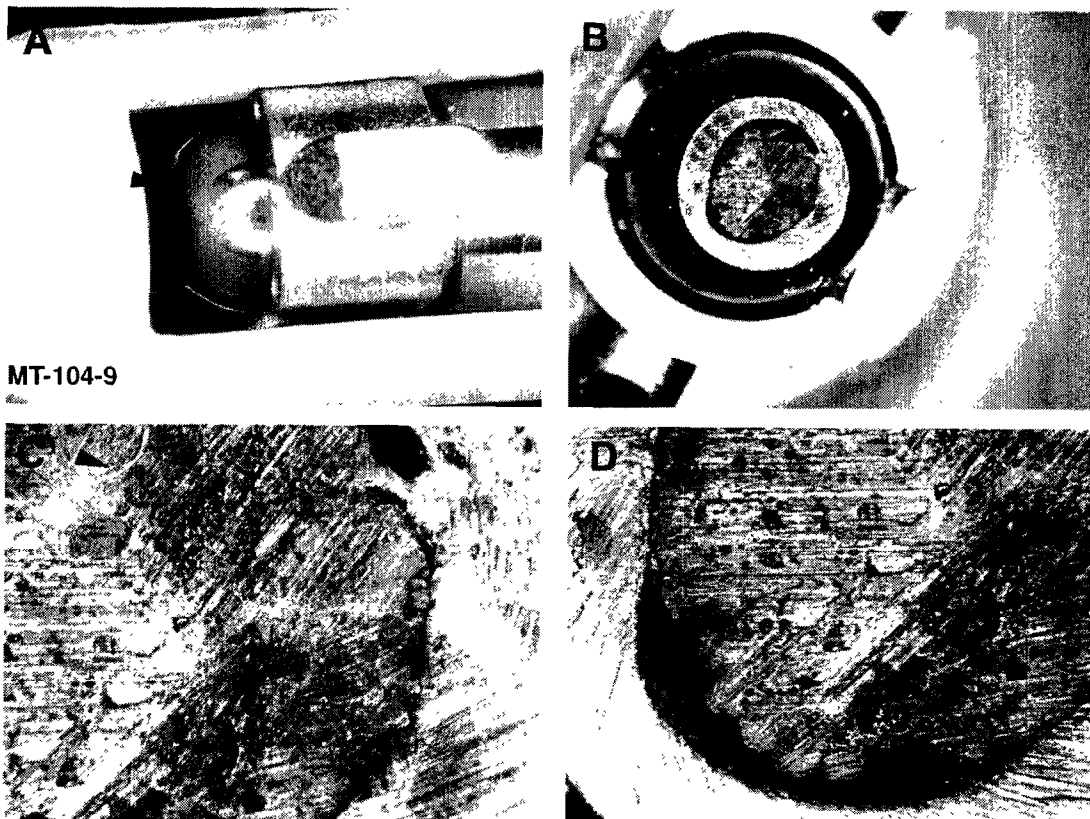


Figure 11. Stereomicroscopy images from reprocessed device MT-104-9. Arrowheads indicate hair, note extensive corrosion.

Significantly less corrosion and metal discoloration did appear on reprocessed Octopus[®] devices identified as MT-104-4, 5, 10, 11, 13 and 16 (Alliance) when compared to device IDs MT-104-3, 7, 8 and 9 (SterilMed). Example images from MT-104-5 and 10 are below:

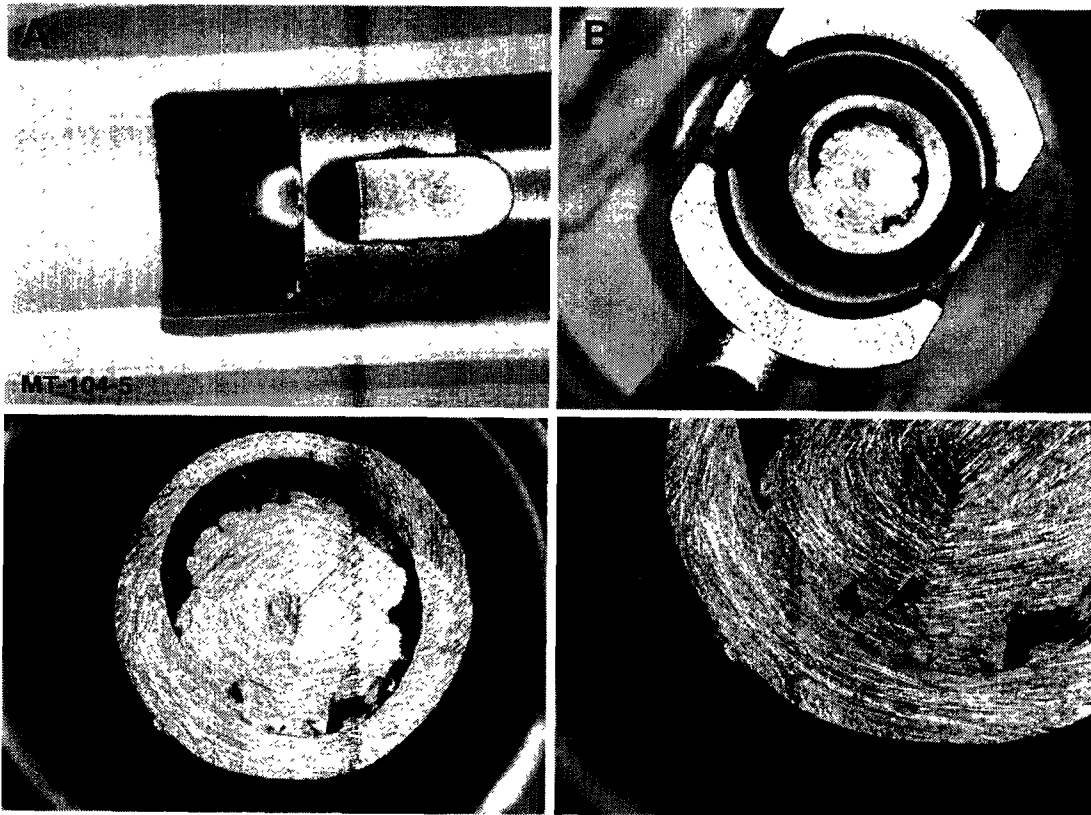


Figure 12. Minor corrosion and metal discoloration (arrowhead) as compared to new on reprocessed Octopus4[®] (MT-104-5).

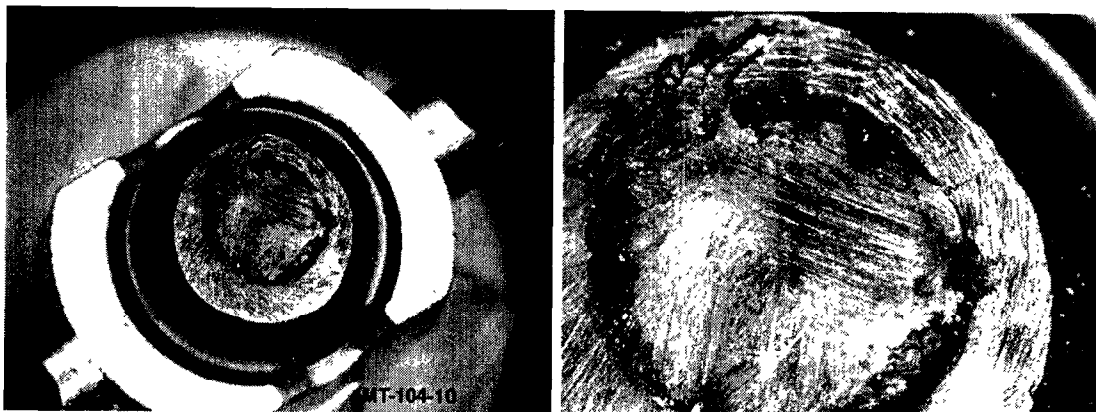


Figure 13. Minor corrosion and metal discoloration as compared to new on reprocessed Octopus4[®] (MT-104-10).

Physical Defects - Blocked Hypotube Openings

MT-104-10 and 13 have partially or completely blocked hypotube openings (arrows). Example images are below of MT-104-13:

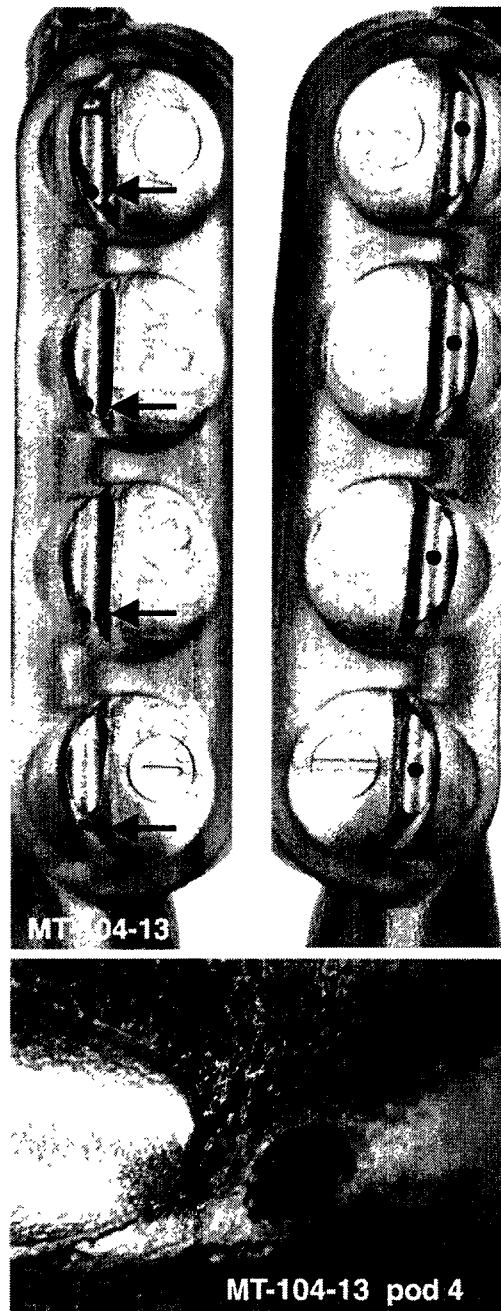


Figure 14. Reprocessed device MT-104-13 with blocked pod openings (arrows).

Scanning Electron Microscopy

Preparations were viewed using a Hitachi S-3500N scanning electron microscope equipped with an Emitech K1150 cryogenic preparation and EDAX X-ray microanalysis system. The head from the unit was removed by cutting the tubing with a cleaned razor blade and releasing it from the arm by removing the retaining clip (see Figure 7). The unit was then transferred to the stage in the scanning electron microscope specimen chamber the pressure was set to 15 Pa. The entire headlink for each device was viewed and images digitally recorded at the desired magnification.

Representative images from the devices are indicated in Figures 15-75.

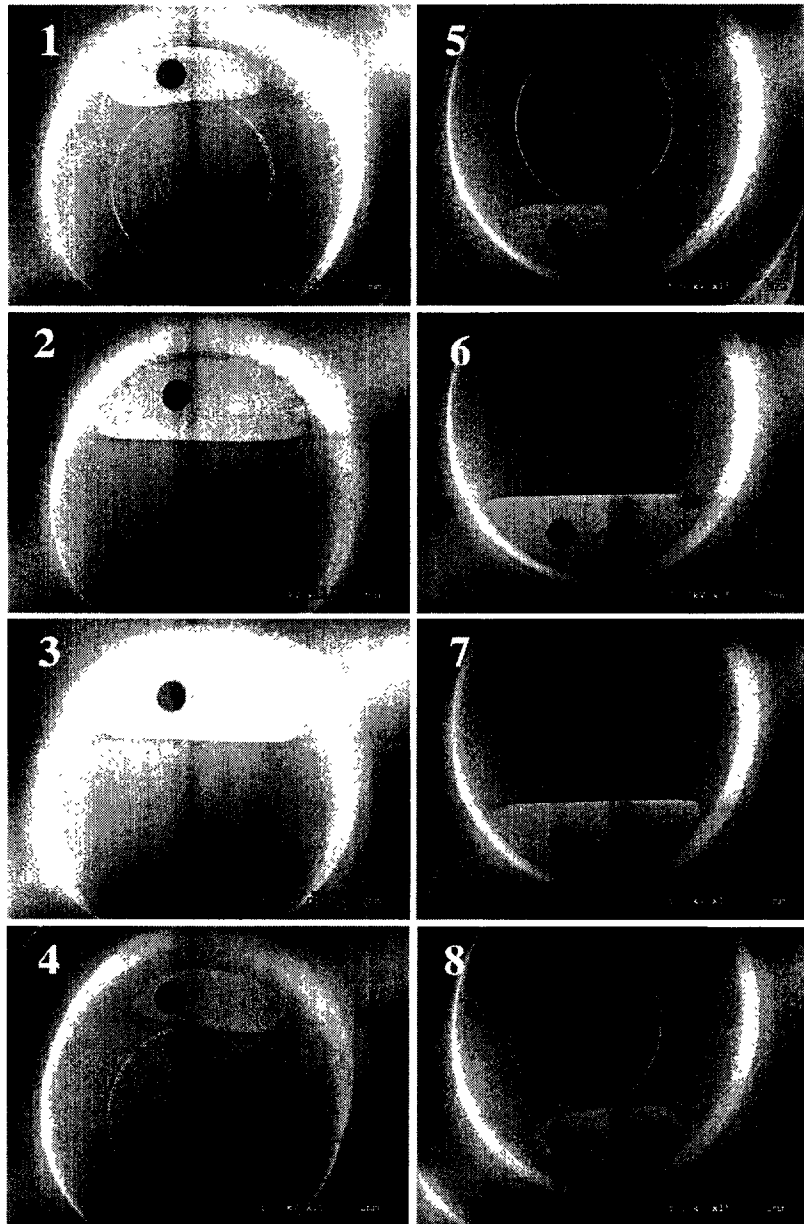


Figure 15. Series of images collected from Hitachi S3500N variable pressure scanning electron microscope in the areas of the pods on the **new Octopus 3[®] (MT-104-1)**. The images show uniform surface structure in the wells and tubing. There are what appear to be small pieces of the same material as the pod in some wells (e.g. #2 and #6). The numbers indicate the pod # (see Figure 5). Scale bar in each image.

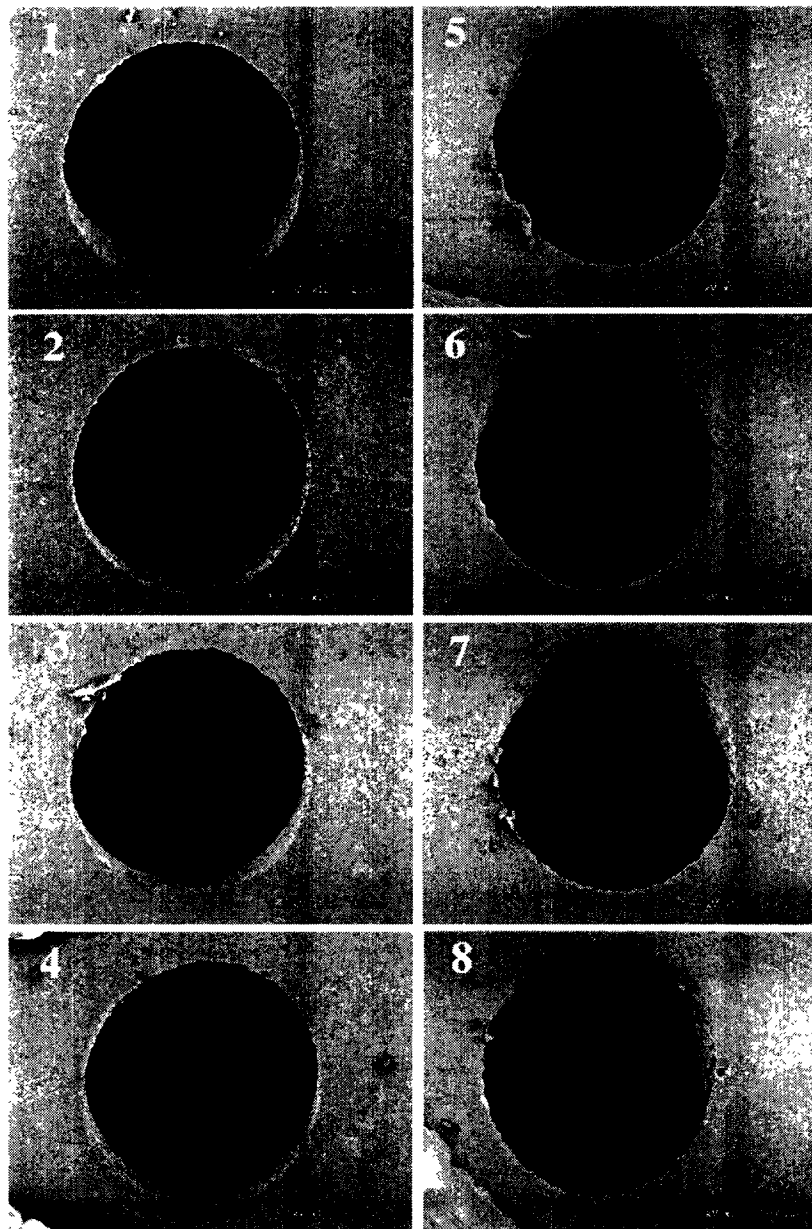


Figure 16. Series of images collected from Hitachi S3500N variable pressure scanning electron microscope in the areas of the orifices in the tubing within each pod on the **new Octopus 3[®] (MT-104-1)**. The images show uniform surface structure on the metal surface of the tubing. The openings appear to be uniform in size and composition. There are what appear to be small pieces of debris in some wells (e.g. #3, #7 and #8). The debris does not appear organic. The numbers indicate the pod # (see Figure 5). Scale bar in each image.

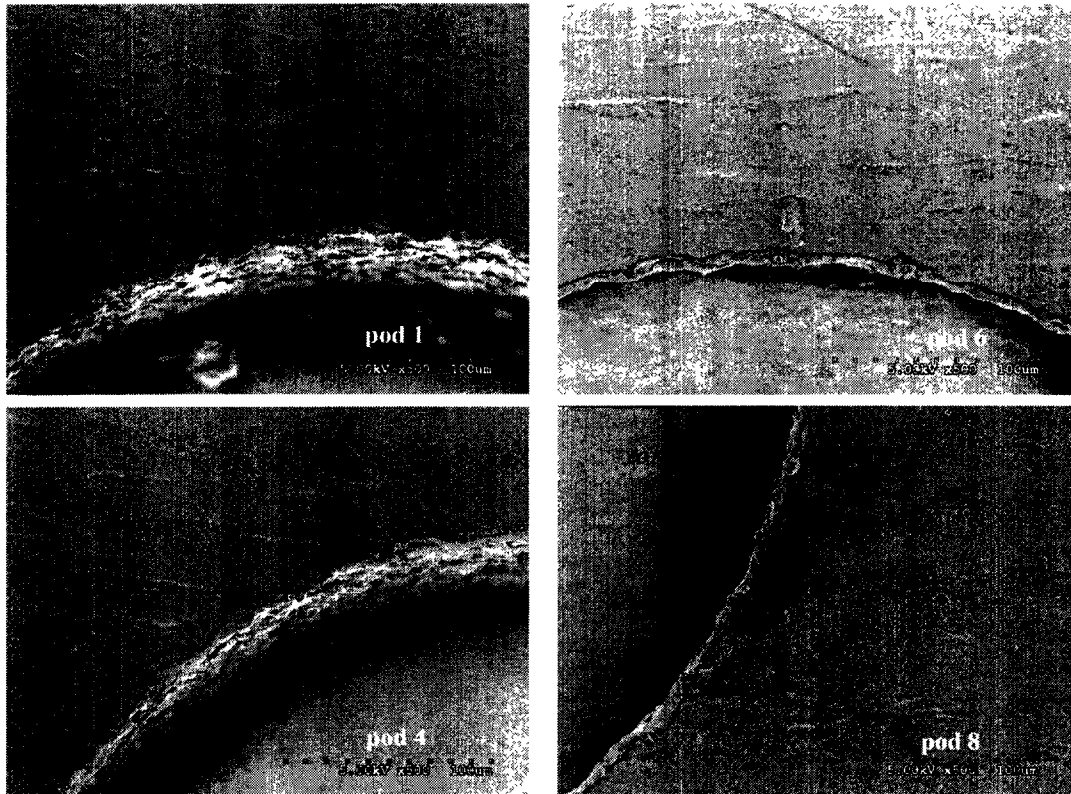


Figure 17. Series of images collected from Hitachi S3500N variable pressure scanning electron microscope of the inner surfaces following cutting in the areas of the orifices in the hypotube on the **new Octopus 3[®]** (MT-104-1). The images show relatively uniform surface structure on the metal surface of the tubing. The openings appear to be uniform in size and composition. There are what appear to be small pieces of debris in some wells. The debris does not appear organic. The label indicates the pod # (see Figure 5). Scale bar in each image.

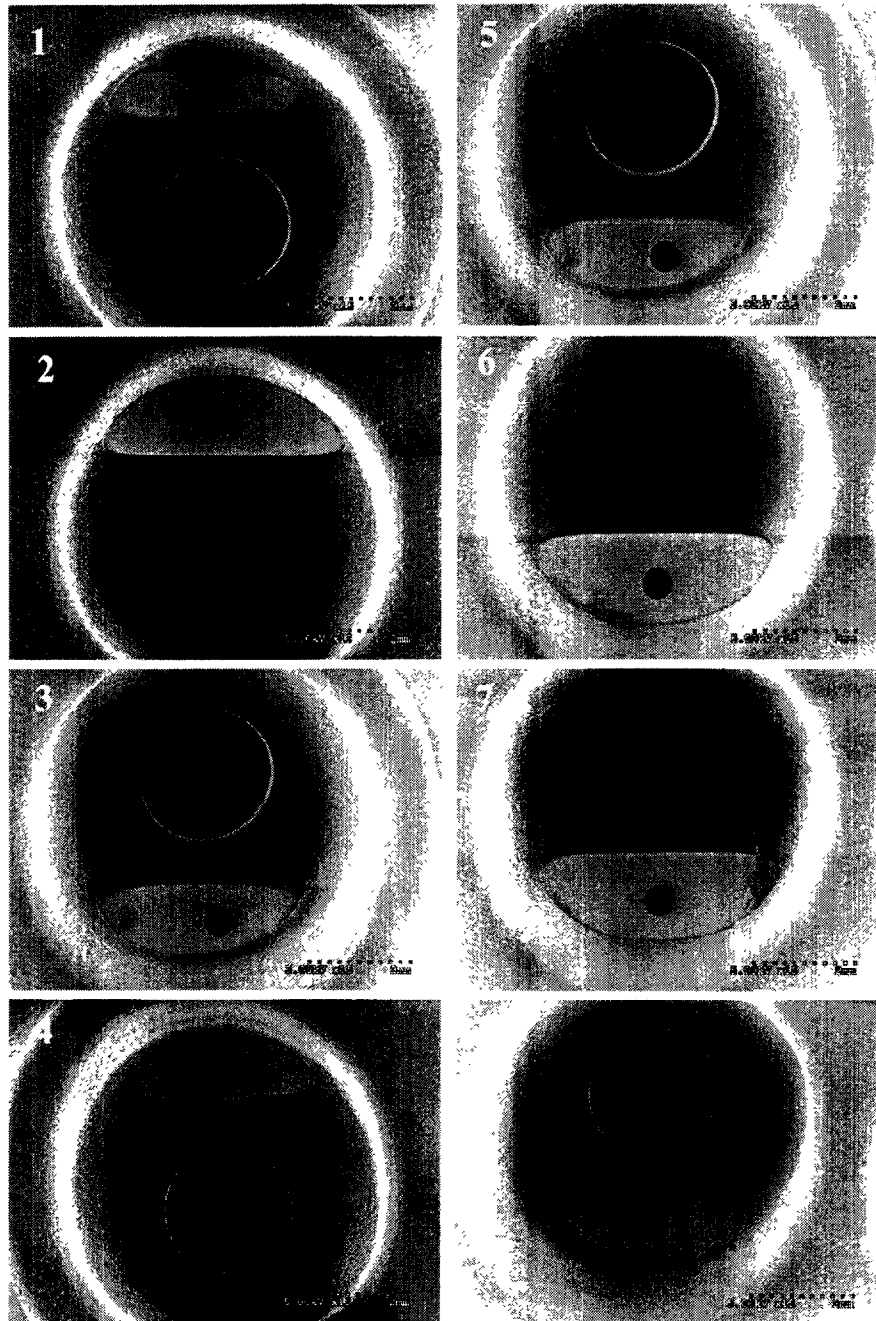


Figure 18. Series of images collected from Hitachi S3500N variable pressure scanning electron microscope in the areas of the pods on the **new Octopus 4[®] (MT-104-2)**. The images show uniform surface structure in the wells and tubing. There are what appear to be small pieces of the same material as the pod in some wells (e.g. #1 and #7). The numbers indicate the pod # (see Figure 5). Scale bar in each image.

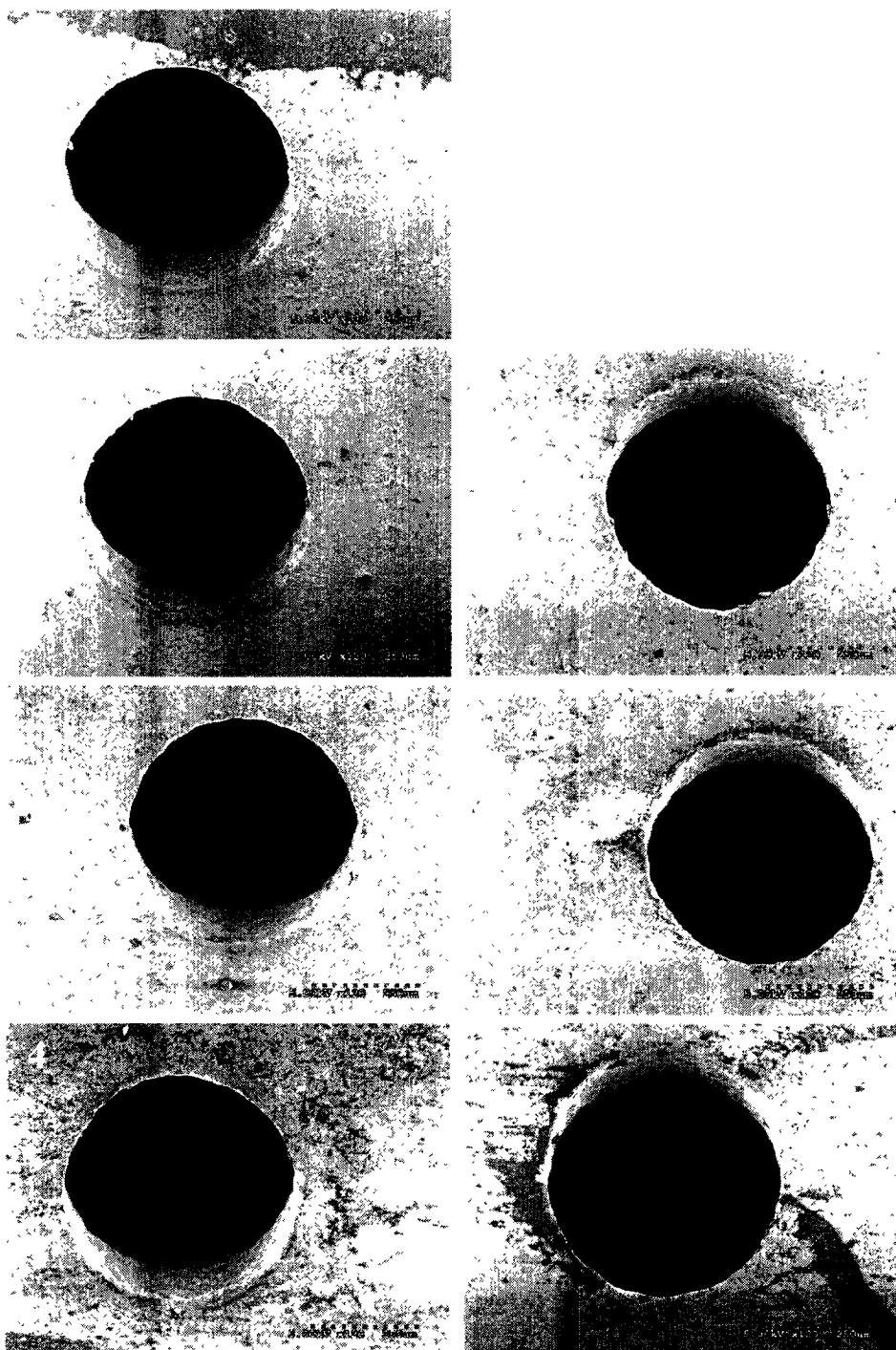


Figure 19. Series of images collected from Hitachi S3500N variable pressure scanning electron microscope in the areas of the pods on the **new Octopus 4[®] (MT-104-2)**. The images show uniform structure of the holes in the tubing. The numbers indicate the pod # (see Figure 5). Scale bar in each image.

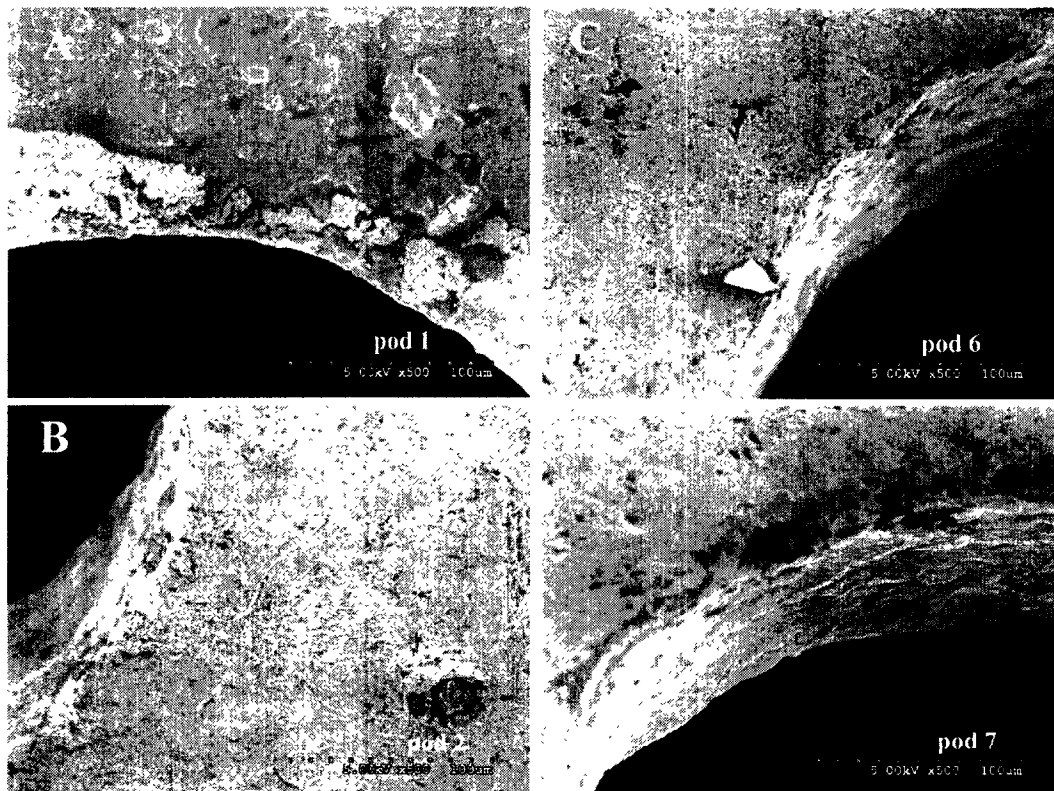


Figure 20. Series of images collected from Hitachi S3500N variable pressure scanning electron microscope in the areas of the pods on the new Octopus 4[®] (MT-104-2). The images show structure of regions near the holes in the tubing from 4 of the 8 pods. The other pods show similar features. The numbers indicate the pod # (see Figure 5). Scale bar in each image.

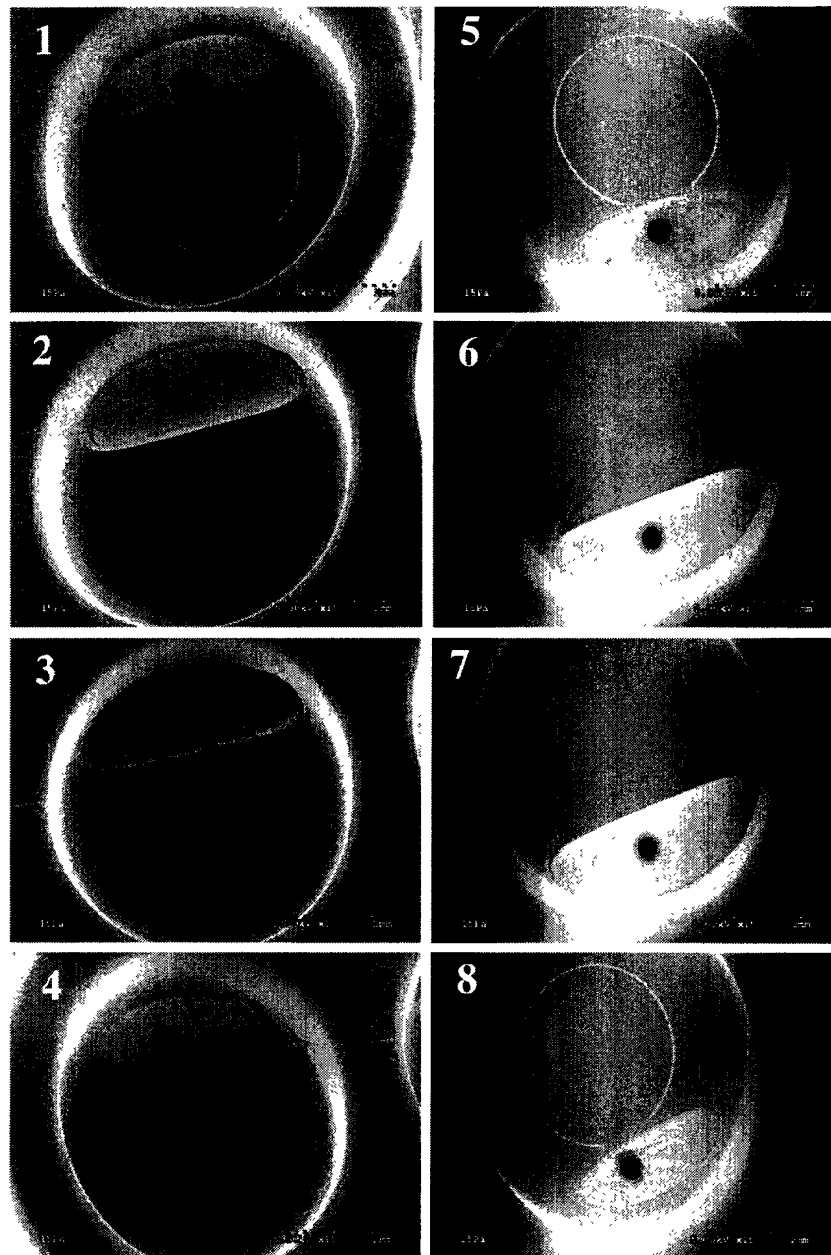


Figure 21. Series of images collected from Hitachi S3500N variable pressure scanning electron microscope in the areas of the pods on the **reprocessed Octopus 3[®] MT-104-3**. The images show irregularities on surface structure in the wells and tubing. There are irregularities and debris present in the orifices of the tubing. The numbers indicate the pod # (see Figure 5). Scale bar in each image.

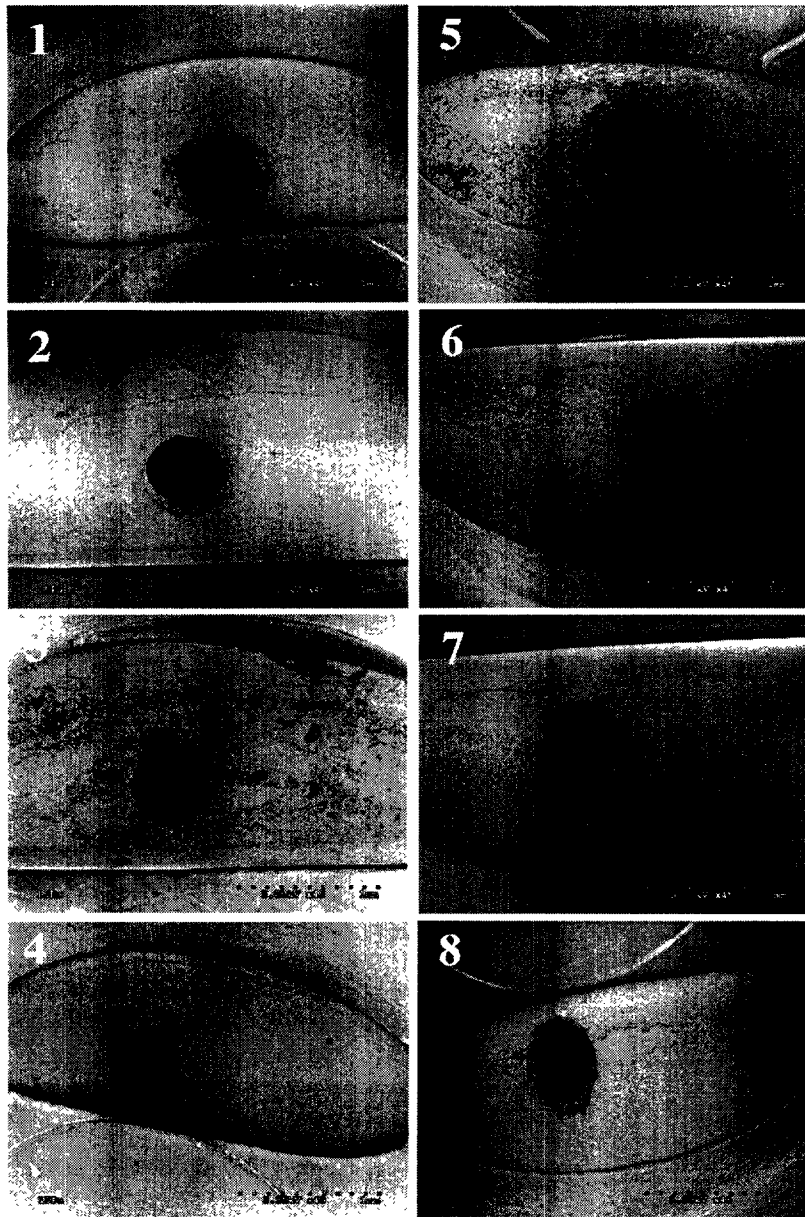


Figure 22. Series of images collected from Hitachi S3500N variable pressure scanning electron microscope in the areas of the tubing within the pods on the **reprocessed Octopus 3[®] MT-104-3**. The images show irregularities on surface structure of the tubing (e.g. in all pods to varying degrees). There is debris and irregularities present in the orifices of the tubing (e.g. in #1, #3, #5, #6, #7 and #8). The orifices are not as uniform in shape when compared to the “new” Octopus 3[®] (Figure 15). The numbers indicate the pod # (see Figure 5). Scale bar in each image.

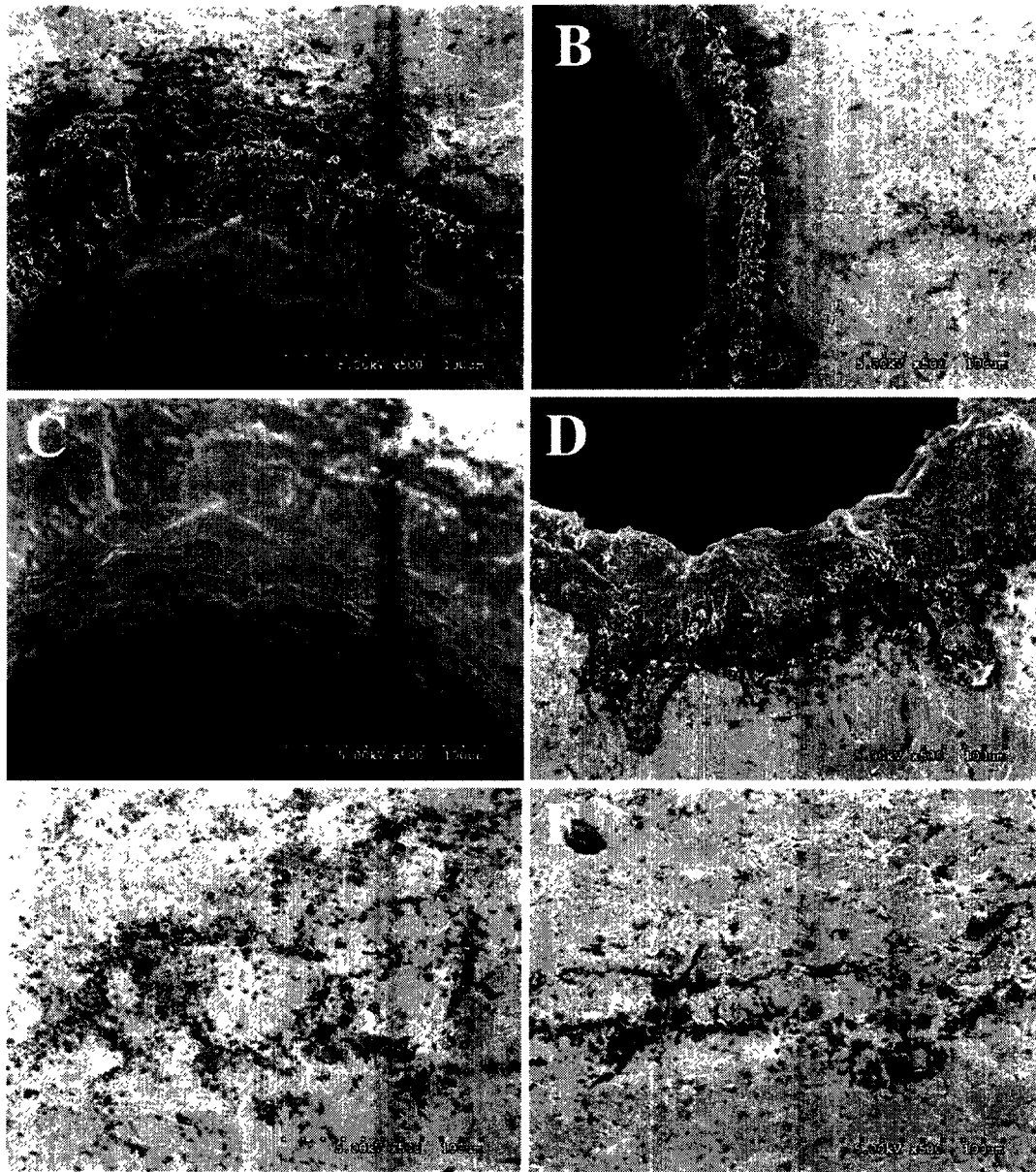


Figure 23. Series of images collected from Hitachi S3500N variable pressure scanning electron microscope of the tubing within pod #8 on the **reprocessed Octopus 3[®] MT-104-3**. The images show irregularities to varying degrees on surface structure of the tubing in all pods. A-D is debris present in the orifices of the tubing. Note bioburden material coating the opening of the tubing orifice and the irregular shape. E and F are images showing debris and contamination on the surface of the metal tubing. Scale bar in each image.

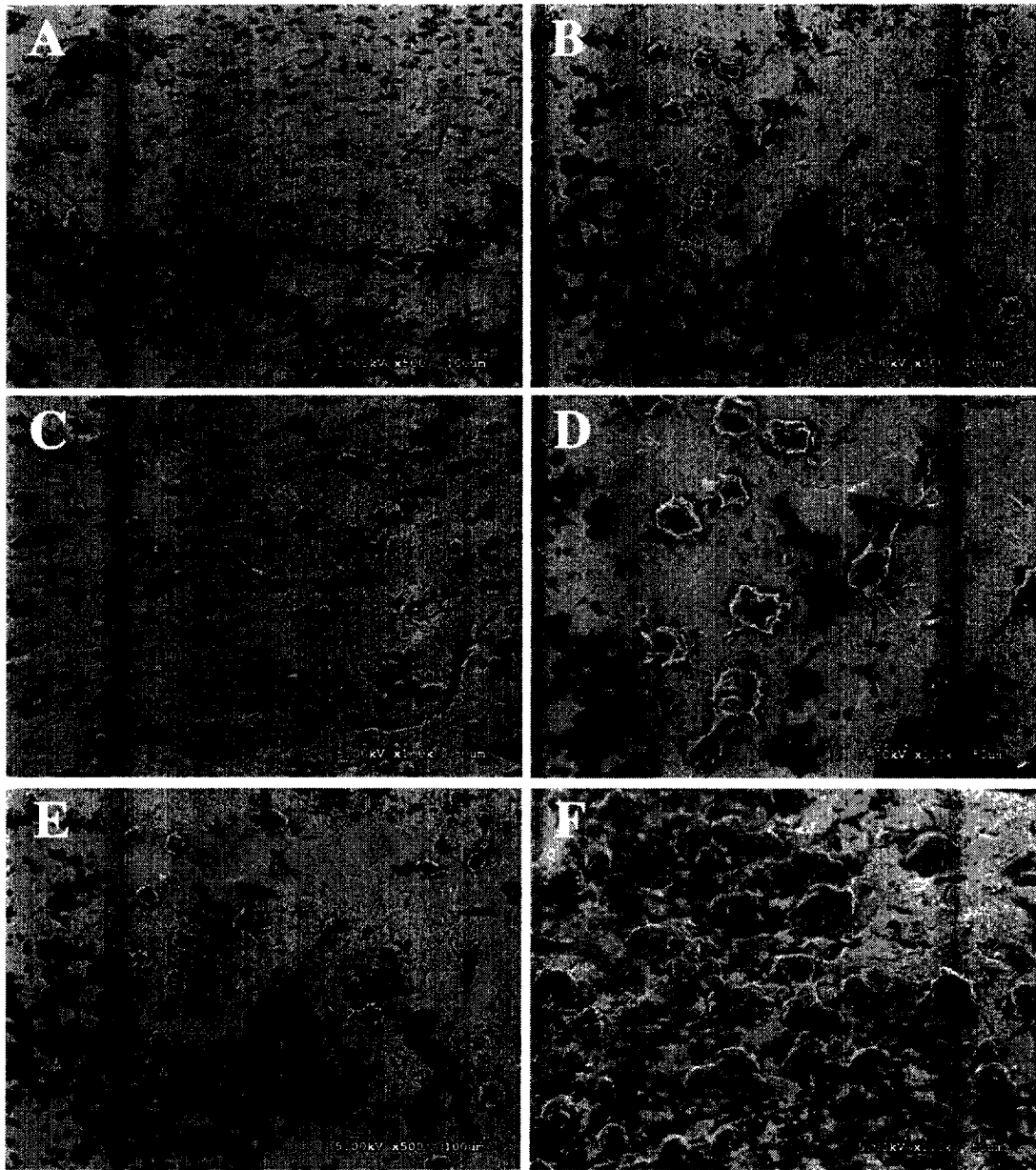


Figure 24. Series of images collected from Hitachi S3500N variable pressure scanning electron microscope of the tubing within pod #5 on the **reprocessed Octopus 3[®] MT-104-3**. The images show various irregularities and contamination on the surface structure of the tubing. All images show foreign debris, bioburden and contamination present on the surface of the tubing when compared to “new”. B, D, E and F are images show what clearly appear to be mammalian cells on the surface of the metal tubing. Scale bar in each image.

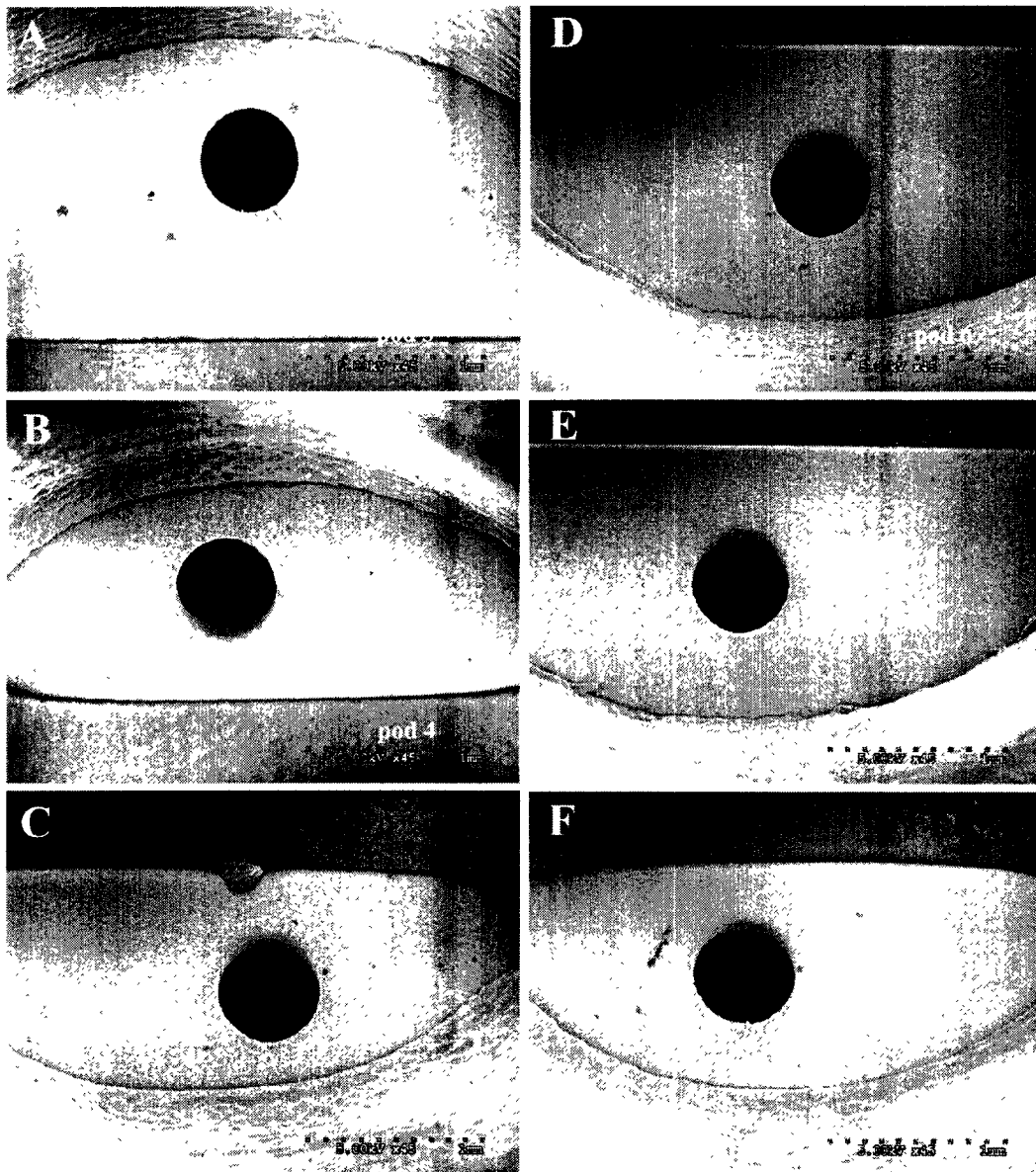


Figure 25. Series of images collected from Hitachi S3500N variable pressure scanning electron microscope in the areas of the pods on the **reprocessed Octopus 4[®] MT-104-4**. The images show uniform structure of the holes in the hypotube. There are what appear to be small pieces of the same material as the pod in some wells (e.g. pod #5 and #8). The numbers indicate the pod # (see Figure 5). Scale bar in each image.

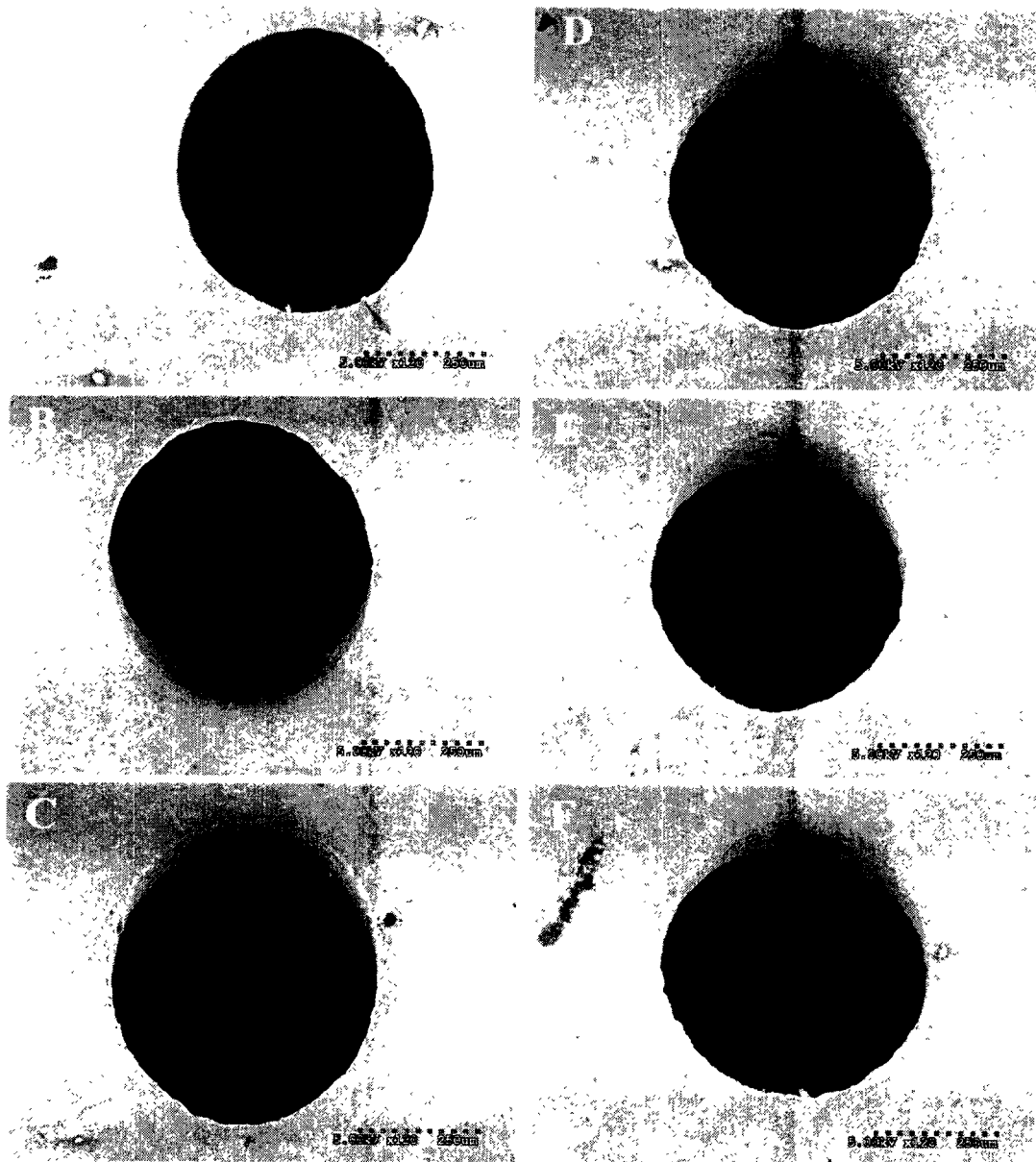


Figure 26. Series of images collected from Hitachi S3500N variable pressure scanning electron microscope in the areas of the pods on the **reprocessed Octopus 4[®] MT-104-4**. The images show uniform structure of the holes and hypotube surfaces. The numbers indicate the pod # (see Figure 5). Scale bar in each image.

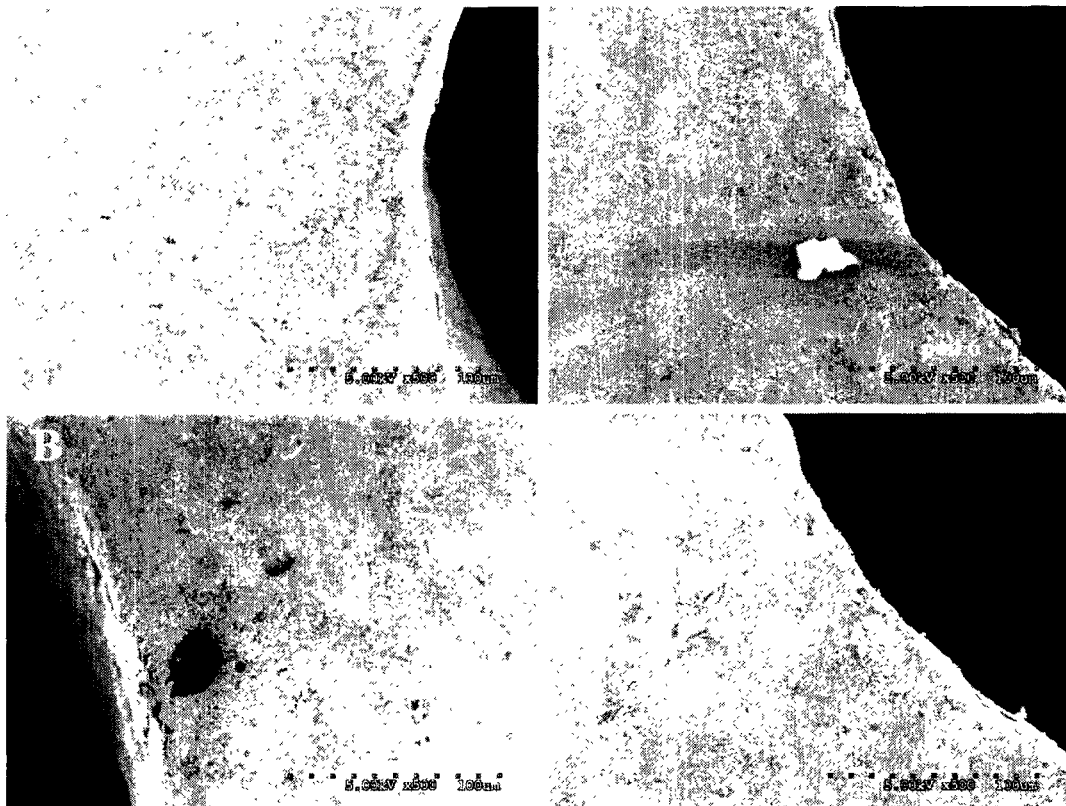


Figure 27. Series of images collected from Hitachi S3500N variable pressure scanning electron microscope in the areas of the pods on the **reprocessed Octopus 4[®] MT-104-4**. The images show uniform structure and inner and outer surfaces of the holes in the hypotube. The numbers indicate the pod # (see Figure 5). Scale bar in each image.

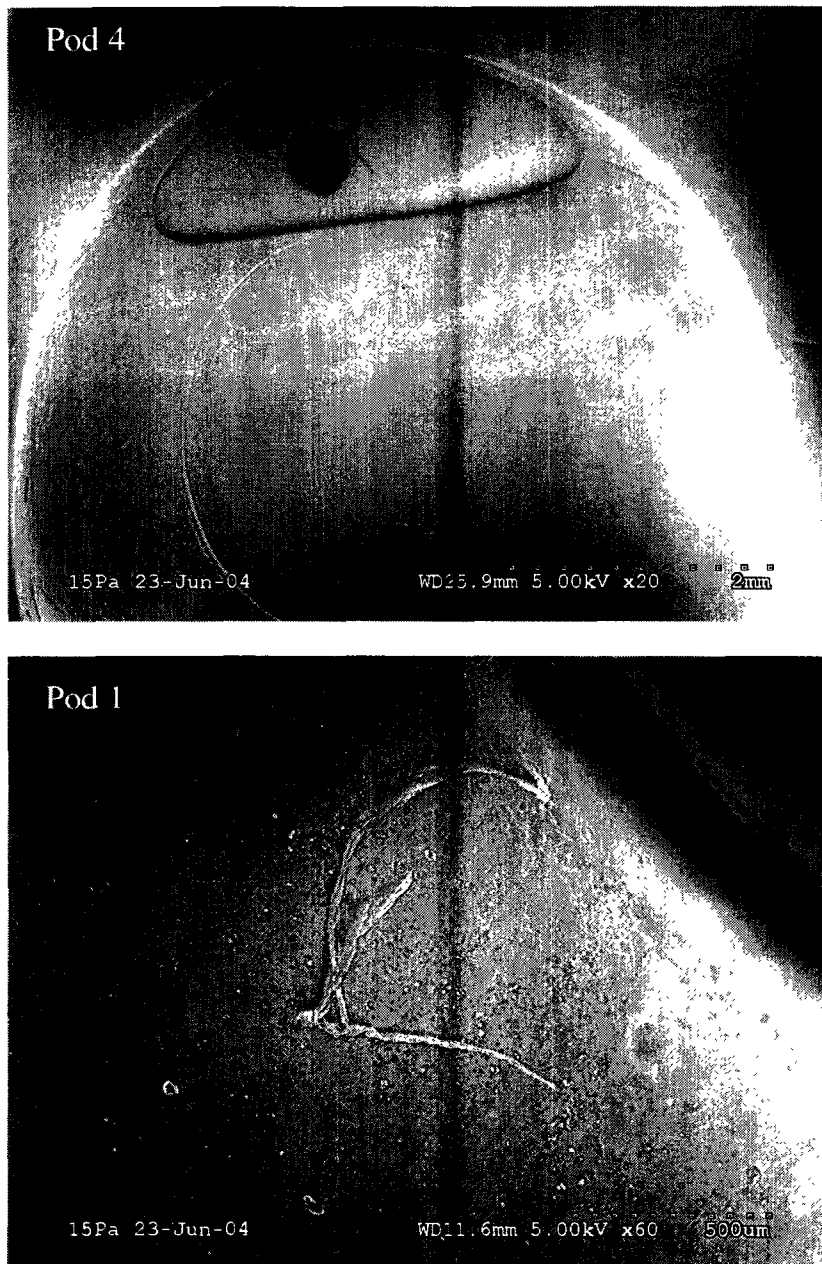


Figure 28. Images collected from Hitachi S3500N variable pressure scanning electron microscope in the areas of the pods on the **reprocessed Octopus 3[®] MT-104-5**. The images show hair-like fibers on surface of the hypotubing near the opening. There is also debris present in the surface of the tubing. The numbers in the upper left indicate the pod # (see Figure 5). Scale bar in each image.

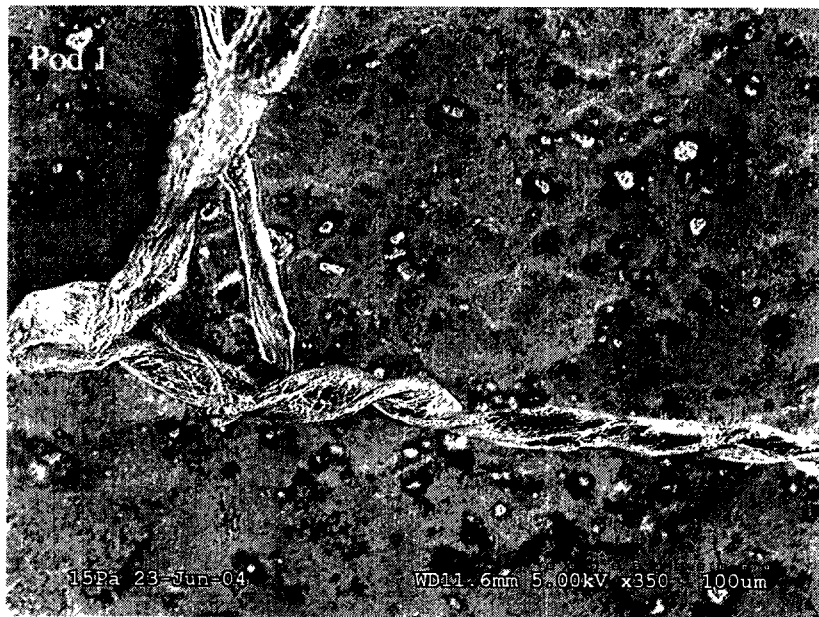


Figure 29. Image collected from Hitachi S3500N variable pressure scanning electron microscope in the areas of pod 1 on the **reprocessed Octopus 3[®] MT-104-5**. The images show hair-like fibers on surface of the hypotubing near the opening. There is also debris present in the surface of the tubing. The number in the upper left indicates the pod # (see Figure 5). Scale bar in each image.

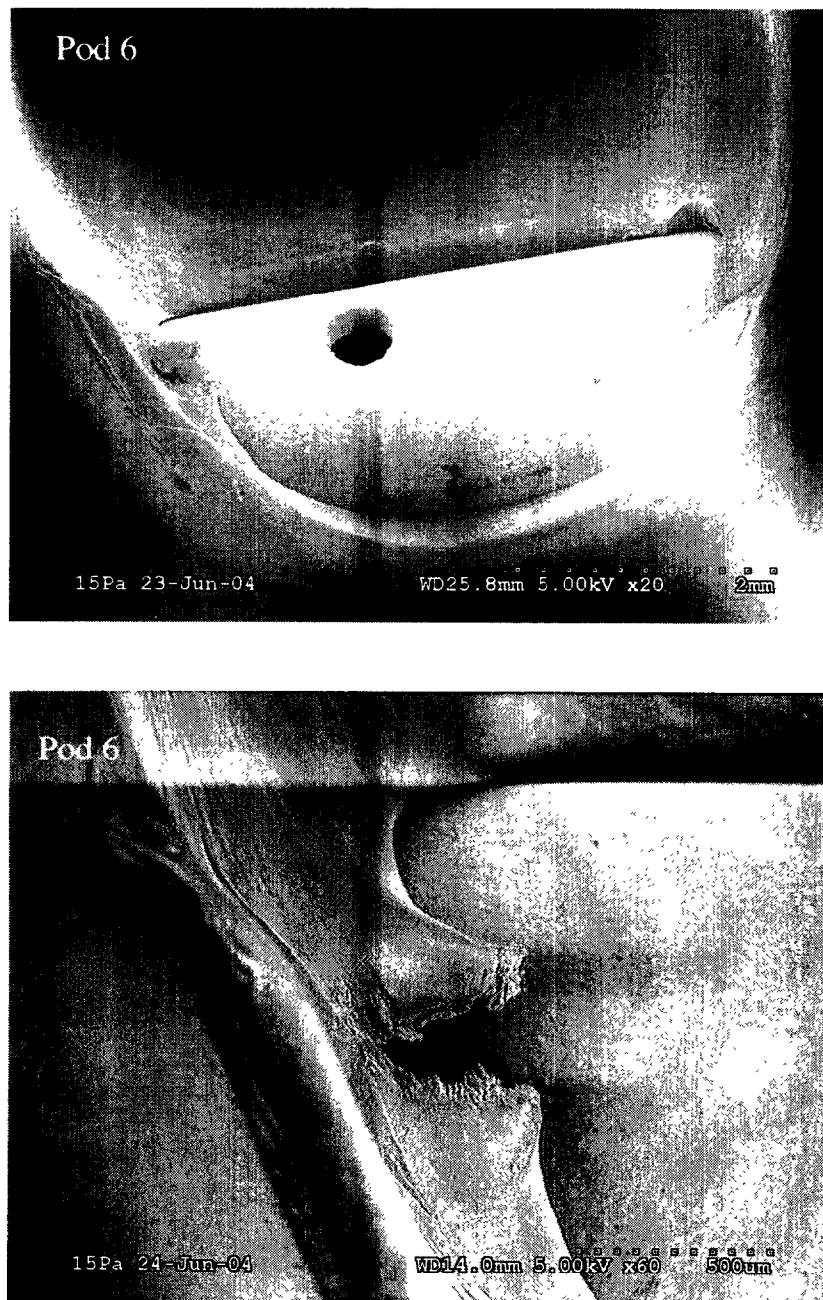


Figure 30. Image collected from Hitachi S3500N variable pressure scanning electron microscope in the areas of pod 6 on the **reprocessed Octopus 3[®] MT-104-5**. The images show a tear of the material surrounding the hypotube. There is also debris present in the surface of the tubing (upper panel). The number in the upper left indicates the pod # (see Figure 5). Scale bar in each image.

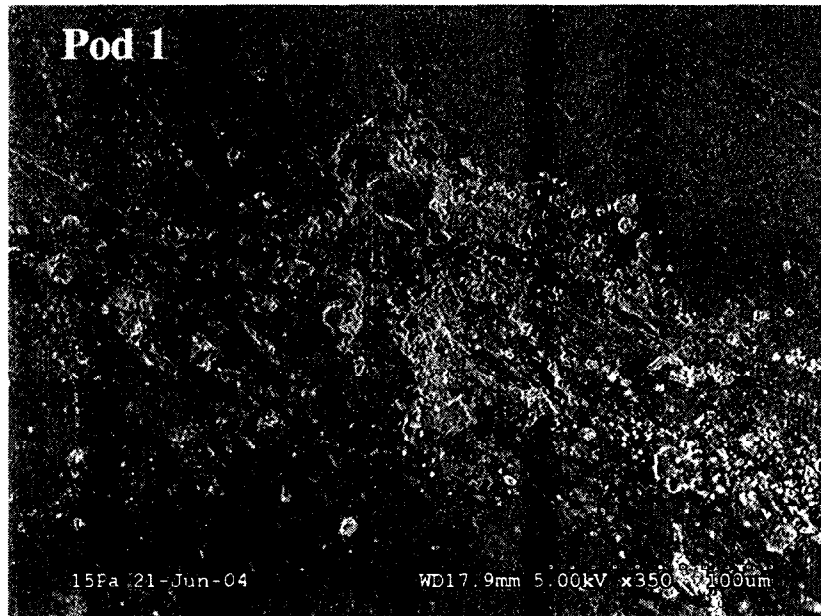


Figure 31. Image collected from Hitachi S3500N variable pressure scanning electron microscope in the areas of pod 1 on the **reprocessed Octopus 3[®] MT-104-7**. The images show debris on surface of the hypotube. The number in the upper left indicates the pod # (see Figure 5). Scale bar in each image.

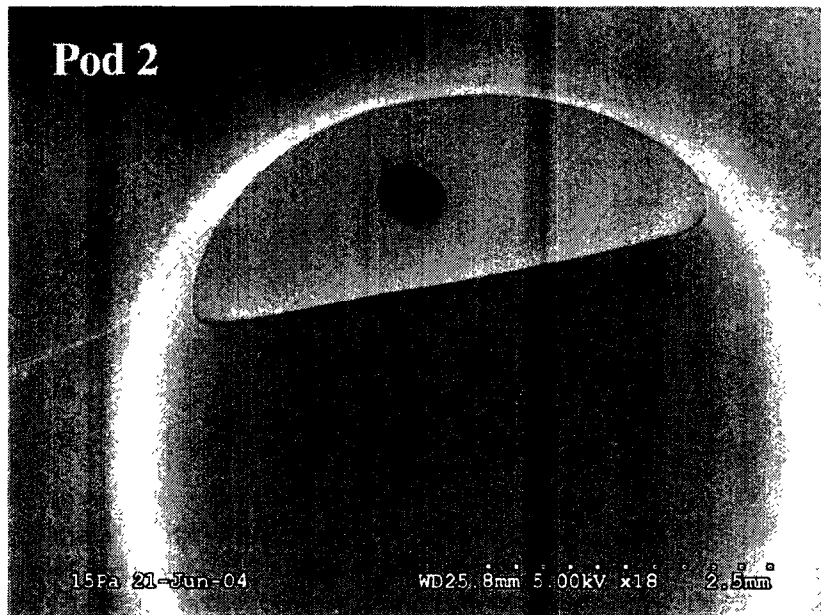


Figure 32. Image collected from Hitachi S3500N variable pressure scanning electron microscope in the areas of pod 2 on the **reprocessed Octopus 3[®] MT-104-7**. The number in the upper left indicates the pod # (see Figure 5). Scale bar in each image.

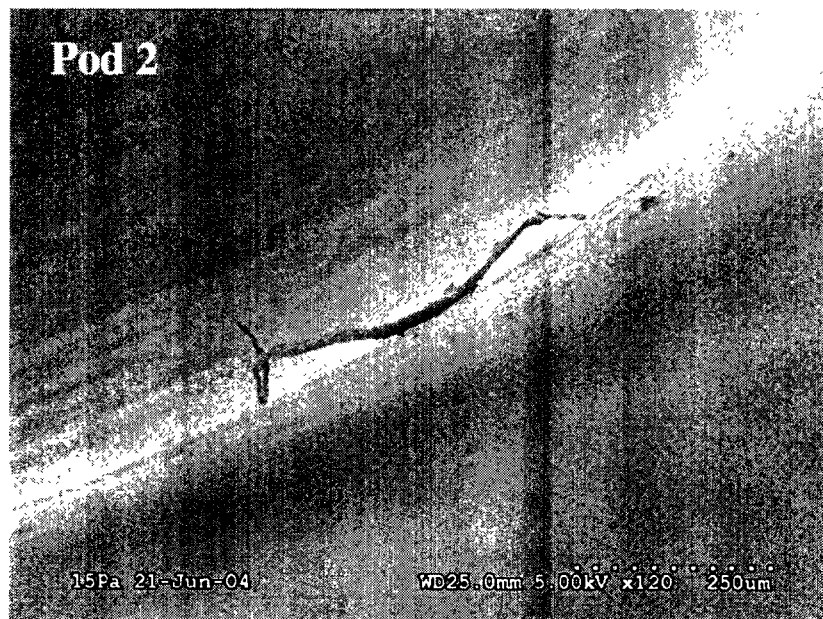


Figure 33. Image collected from Hitachi S3500N variable pressure scanning electron microscope in the areas of pod 2 on the **reprocessed Octopus 3[®] MT-104-7**. The images show hair-like fiber on surface of the pod. The number in the upper left indicates the pod # (see Figure 5). Scale bar in each image.

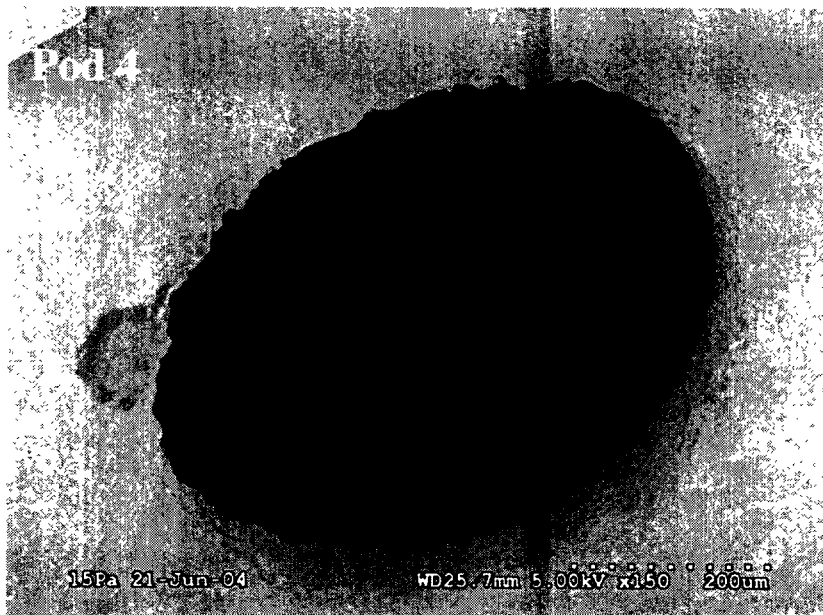


Figure 34. Series of images collected from Hitachi S3500N variable pressure scanning electron microscope of the tubing within pod 4 on the **reprocessed Octopus 3[®] MT-104-7**. Note material near the opening of the tubing orifice and the irregular shape. Scale bar in each image

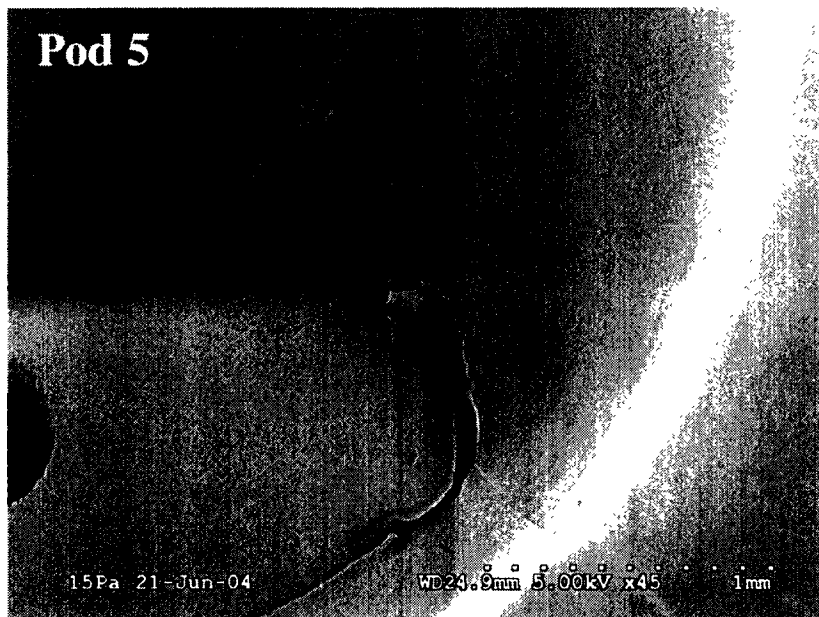


Figure 35. Image collected from Hitachi S3500N variable pressure scanning electron microscope in the areas of pod 5 on the **reprocessed Octopus 3[®] MT-104-7**. The images show a tear of the material surrounding the hypotube. There is also debris present. The number in the upper left indicates the pod # (see Figure 5). Scale bar in each image.

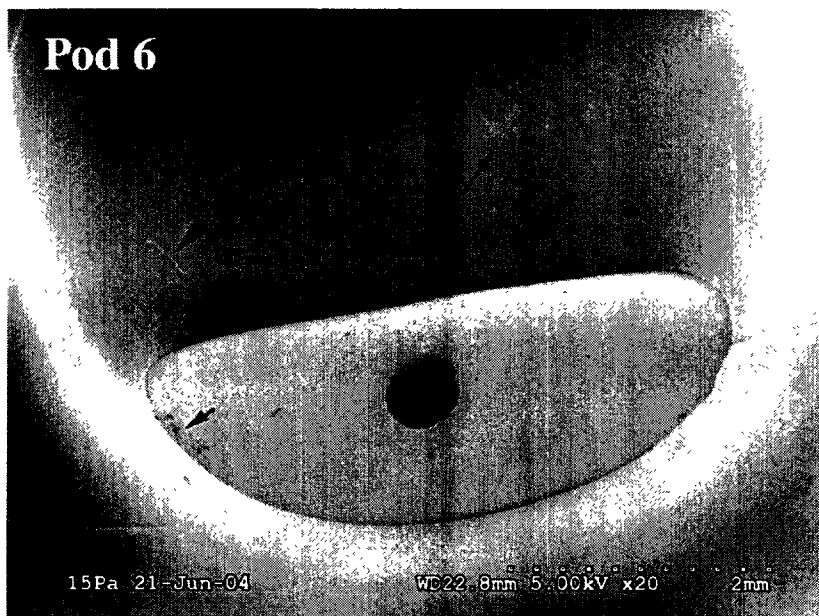


Figure 36. Image collected from Hitachi S3500N variable pressure scanning electron microscope in the areas of pod 6 on the **reprocessed Octopus 3[®] MT-104-7**. The images show a fiber (arrowhead) and debris on surface of pod and hypotube (arrows). The number in the upper left indicates the pod # (see Figure 5). Scale bar in each image.

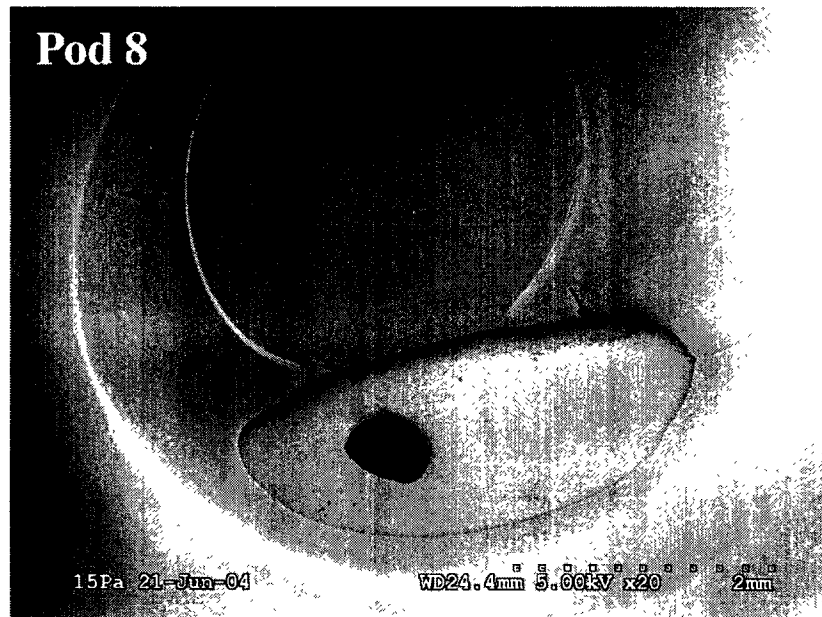


Figure 37. Image collected from Hitachi S3500N variable pressure scanning electron microscope in the areas of pod 8 on the **reprocessed Octopus 3[®] MT-104-7**. The images show debris on surface of pod and hypotube (arrows). Note gap between the hypotube and the pod. The number in the upper left indicates the pod # (see Figure 5). Scale bar in each image.

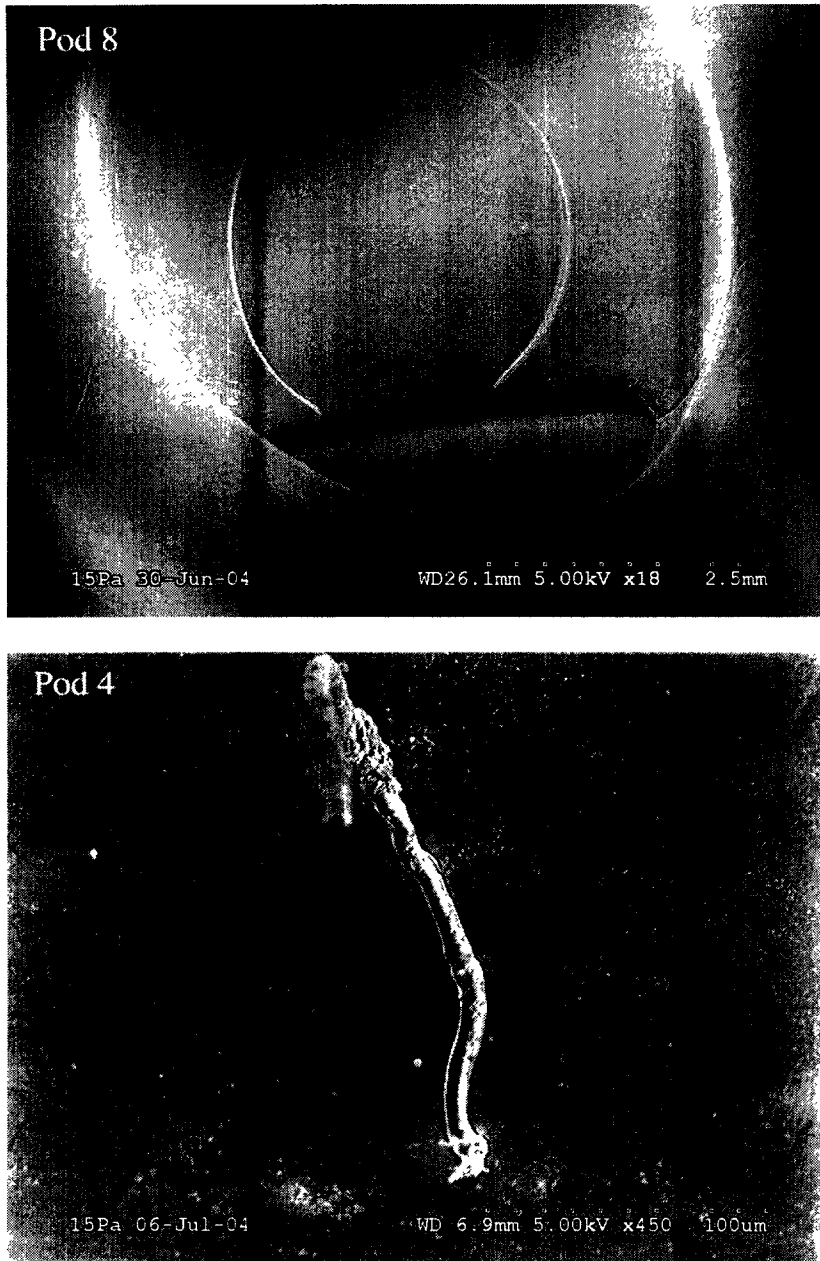


Figure 38. Series of images collected from Hitachi S3500N variable pressure scanning electron microscope of the **reprocessed Octopus 3[®] MT-104-8**. The images show several irregularities on surface structure of the tubing including a gap in the area of the pod surrounding the tubing. There is a fiber and irregularities present in the pod of the tubing. Scale bar in each image.



Figure 39. Image collected from Hitachi S3500N variable pressure scanning electron microscope of the **reprocessed Octopus 3[®] MT-104-8**. The image shows spherical shaped particle on the surface of the pod. Numerous 40-60 micron diameter particles were observed on this and other devices. Scale bar in each image.

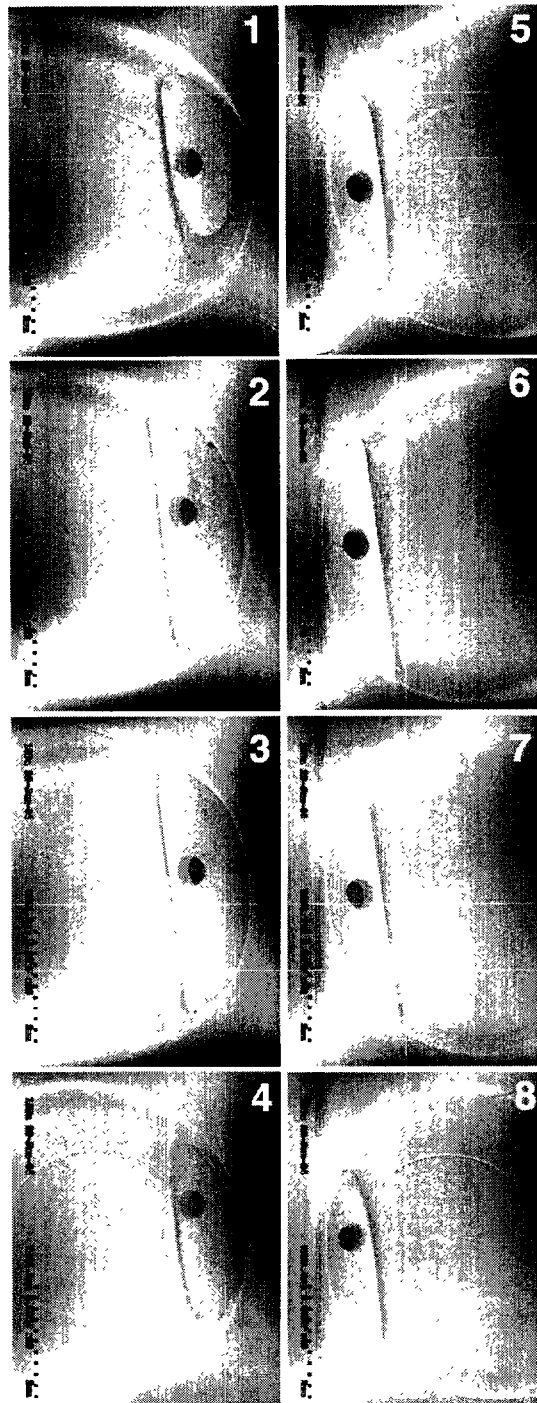


Figure 40. Series of images collected from Hitachi S3500N variable pressure scanning electron microscope in the areas of the pods on the **reprocessed Octopus 3[®] MT-104-9**. The images show irregularities on surface structure in the wells and tubing. There are irregularities and debris present in the orifices of the tubing. The numbers indicate the pod # (see Figure 5). Scale bar in each image.

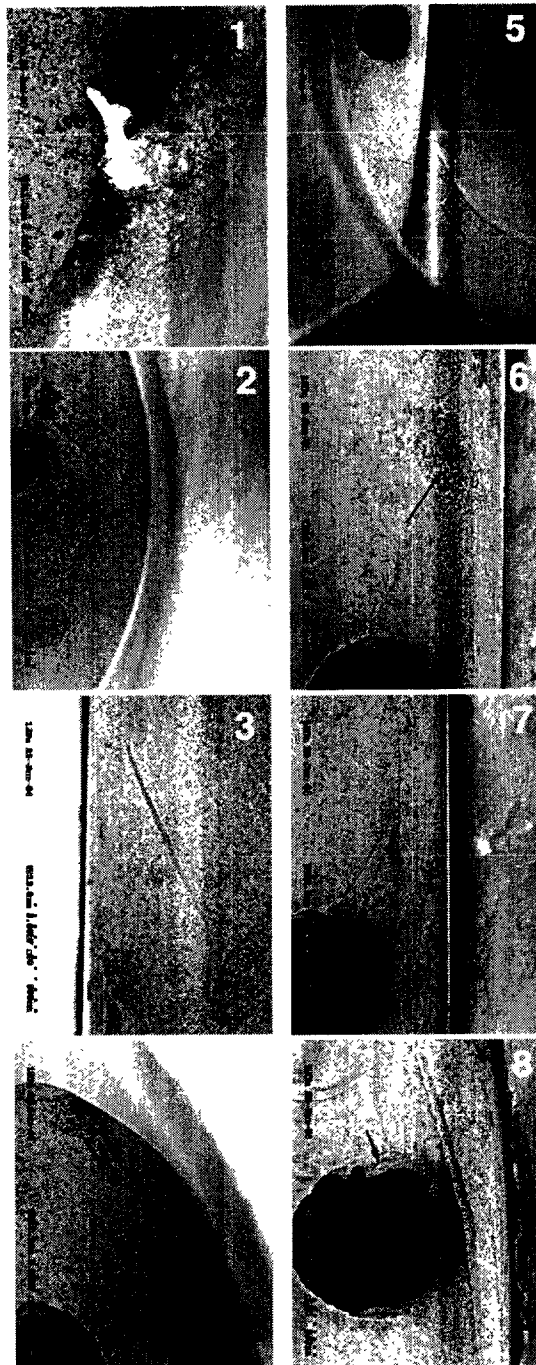


Figure 41. Series of images collected from Hitachi S3500N variable pressure scanning electron microscope in the areas of the tubing within the pods on the **reprocessed Octopus 3[®] MT-104-9**. The images show irregularities on surface structure of the tubing (e.g. in all pods to varying degrees). There is debris and irregularities present in the orifices of the tubing (e.g. in #2, #5, #6, #7 and #8). The numbers indicate the pod # (see Figure 5). Scale bar in each image.

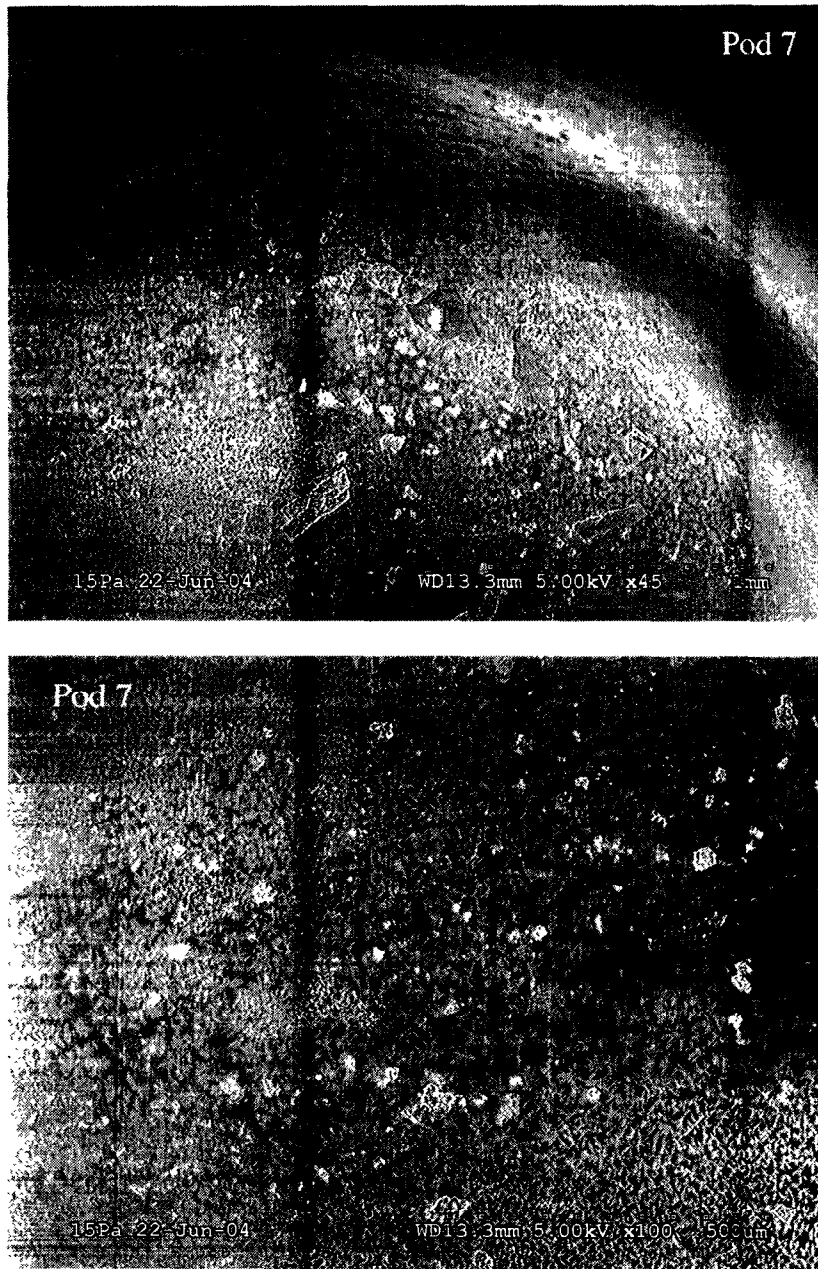


Figure 42. Images collected from Hitachi S3500N variable pressure scanning electron microscope in the areas of pod 1 on the **reprocessed Octopus 3[®] MT-104-9**. The images show bioburden and crystalline debris present in the surface of the tubing. The number in the upper corner indicates the pod # (see Figure 5). Scale bar in each image.



Figure 43. Series of images collected from Hitachi S3500N variable pressure scanning electron microscope in the areas of the tubing within the pods on the **reprocessed Octopus 3® MT-104-9**. The images show irregularities on surface structure of the tubing. There is debris and irregularities present in the orifices of the tubing. Note fiber near orifice and gouge near the opening of the hypotube. The numbers indicate the pod # (see Figure 5). Scale bar in each image.

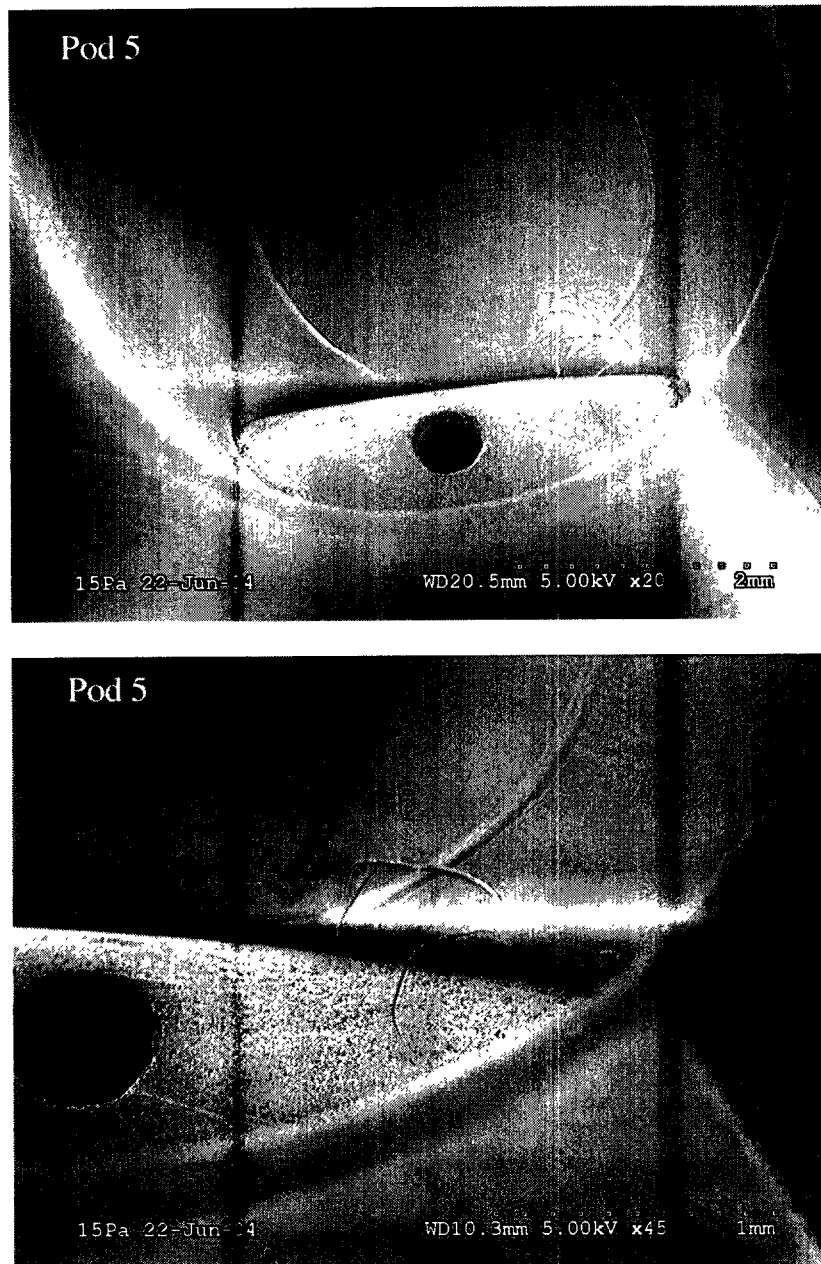


Figure 44. Series of images collected from Hitachi S3500N variable pressure scanning electron microscope in the areas of the tubing within the pods on the **reprocessed Octopus 3[®] MT-104-9**. The images show irregularities on surface structure of the tubing. Note the hair and the enlarged gap between the hypotubing and the pod. The numbers indicate the pod # (see Figure 5). Scale bar in each image.



Figure 45. Enlarged image showing cuticular bands of hair on the surface of pod #5 in figure 44 of the **reprocessed Octopus 3[®] MT-104-9**.

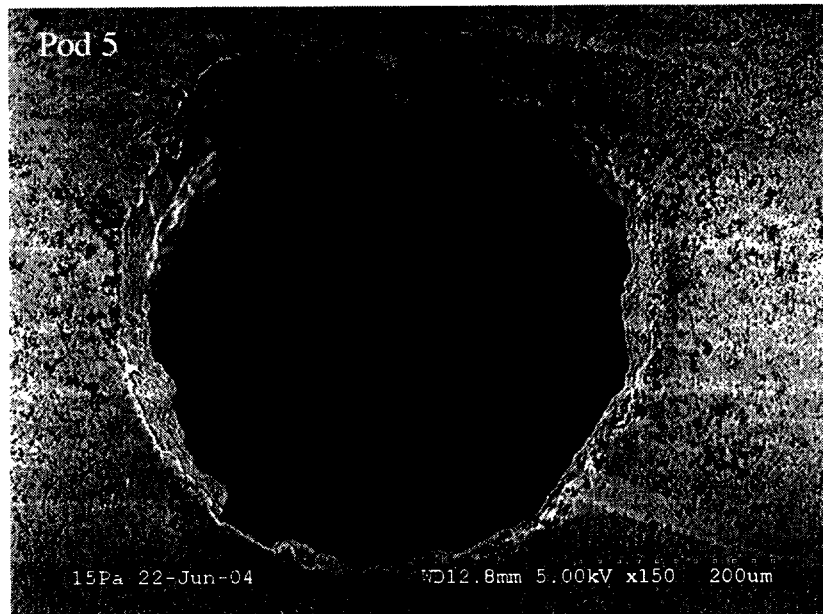


Figure 46. Image collected from Hitachi S3500N variable pressure scanning electron microscope in the areas of the hypotube opening of the **reprocessed Octopus 3[®] MT-104-9**. There is debris and irregularities present in the orifices of the tubing. The numbers indicate the pod # (see Figure 5). Scale bar in each image.

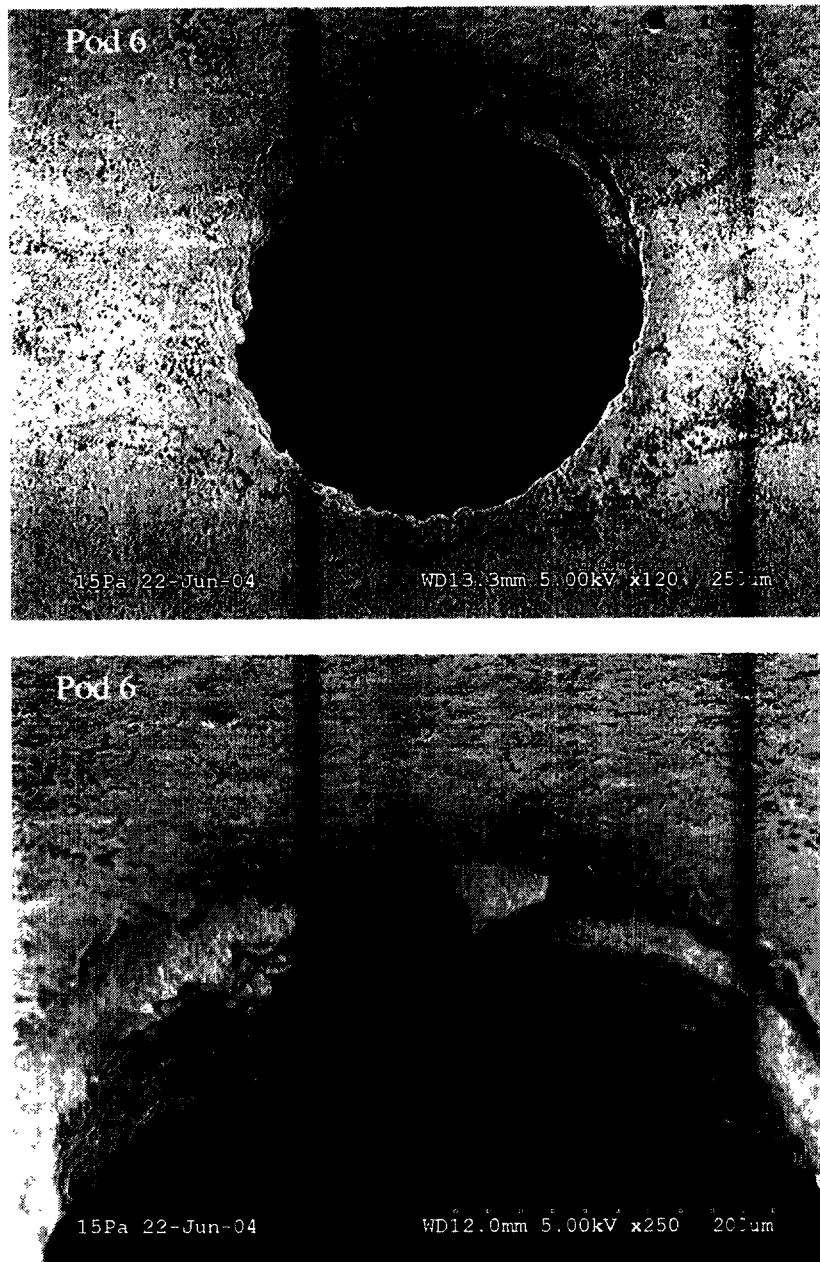


Figure 47. Image collected from Hitachi S3500N variable pressure scanning electron microscope in the areas of the hypotube opening of pod 6 of the **reprocessed Octopus 3® MT-104-9**. There is bioburden debris and irregularities present in the orifices of the tubing. The numbers indicate the pod # (see Figure 5). Scale bar in each image.

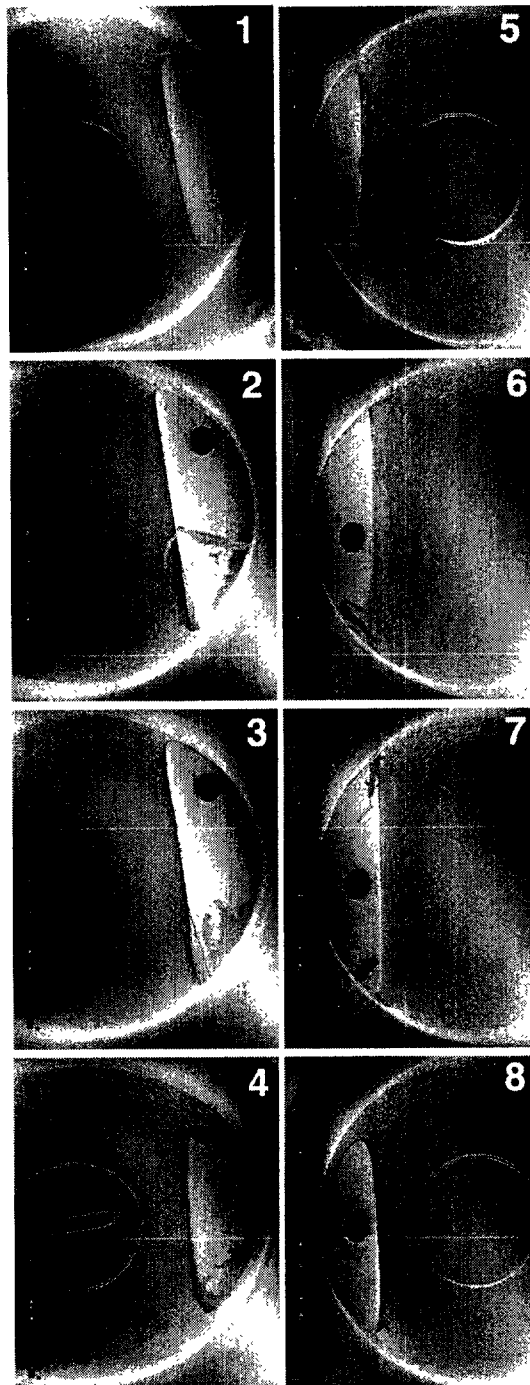


Figure 48. Series of images collected from Hitachi S3500N variable pressure scanning electron microscope of the pods on the **reprocessed Octopus 4[®] MT-104-10**. The images show various irregularities and contamination on the surface structure of the tubing and the pods. All images show foreign debris and contamination present on the surface of the tubing when compared to “new”. Scale bar in each image.



Figure 49. Images collected from Hitachi S3500N variable pressure scanning electron microscope of pod 1 on the **reprocessed Octopus 4® MT-104-10**. The images show various irregularities and contamination on the surface structure of the tubing and the pods. Bioburden debris and contamination is present on the surface of the tubing when compared to “new”. Note fiber. Scale bar in each image.

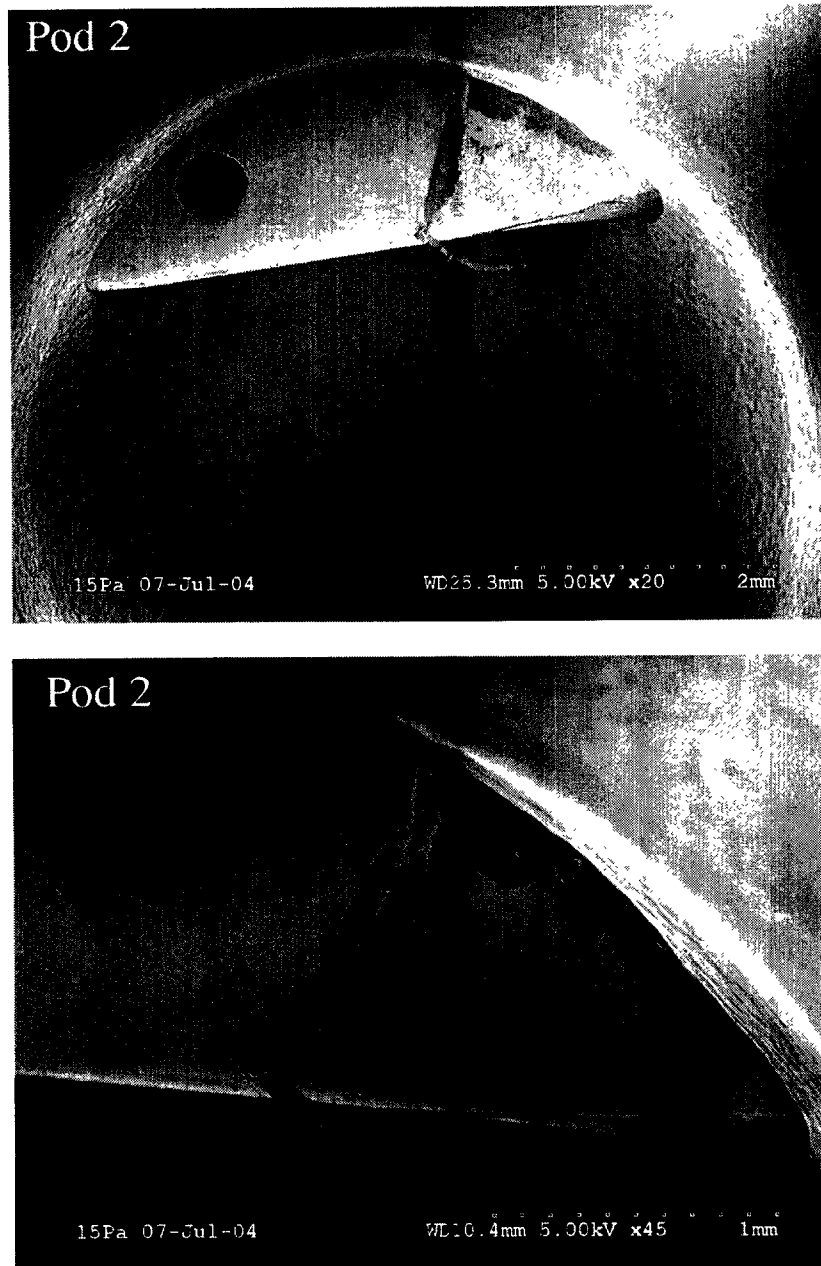


Figure 50. Images collected from Hitachi S3500N variable pressure scanning electron microscope of pod 2 on the **reprocessed Octopus 4[®] MT-104-10**. The images show various irregularities and contamination on the surface structure of the tubing and the pods. Bioburden debris and contamination is present on the surface of the tubing when compared to “new”. Note large fragment of material. Scale bar in each image.

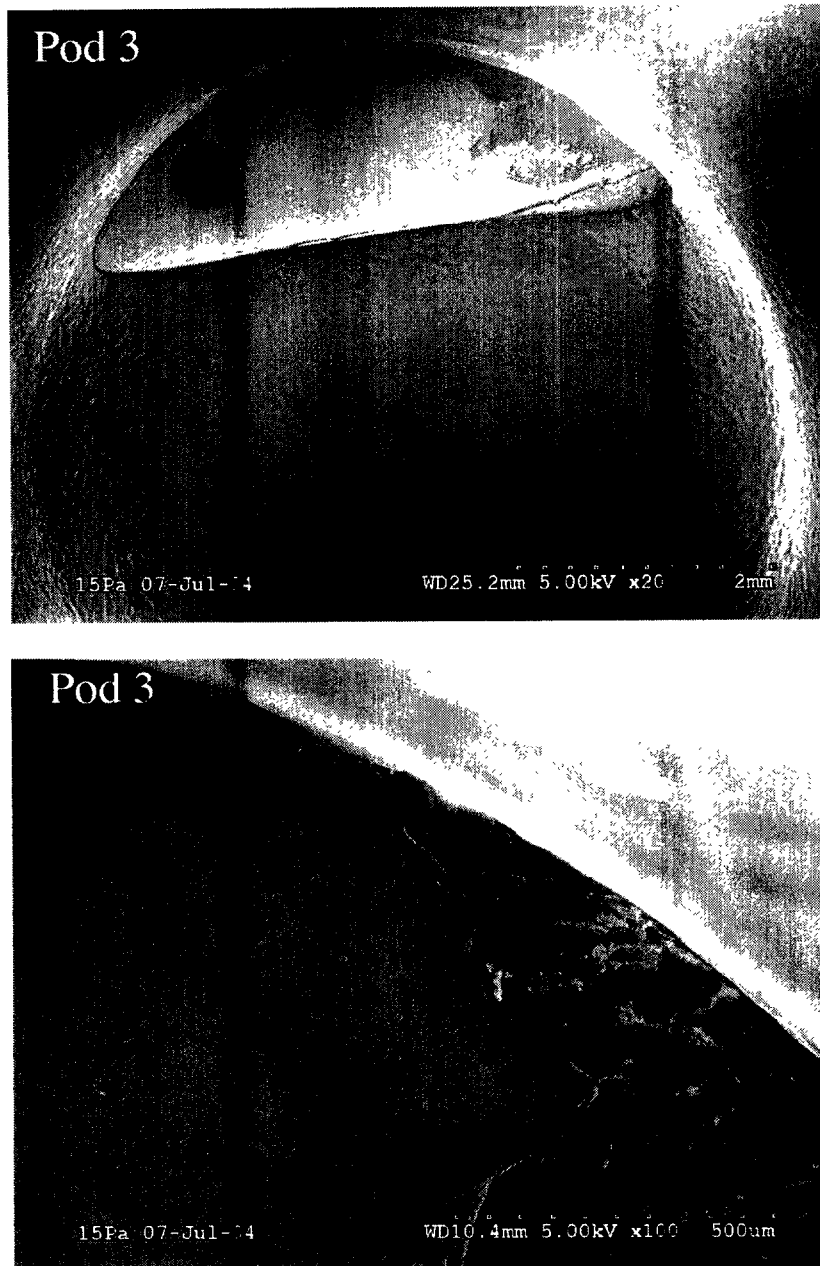


Figure 51. Images collected from Hitachi S3500N variable pressure scanning electron microscope of pod 3 on the **reprocessed Octopus 4® MT-104-10**. The images show various irregularities and contamination on the surface structure of the tubing and the pods. Bioburden debris and contamination is present on the surface of the tubing when compared to “new”. Note “sheet” of foreign material on tubing surface. Scale bar in each image.

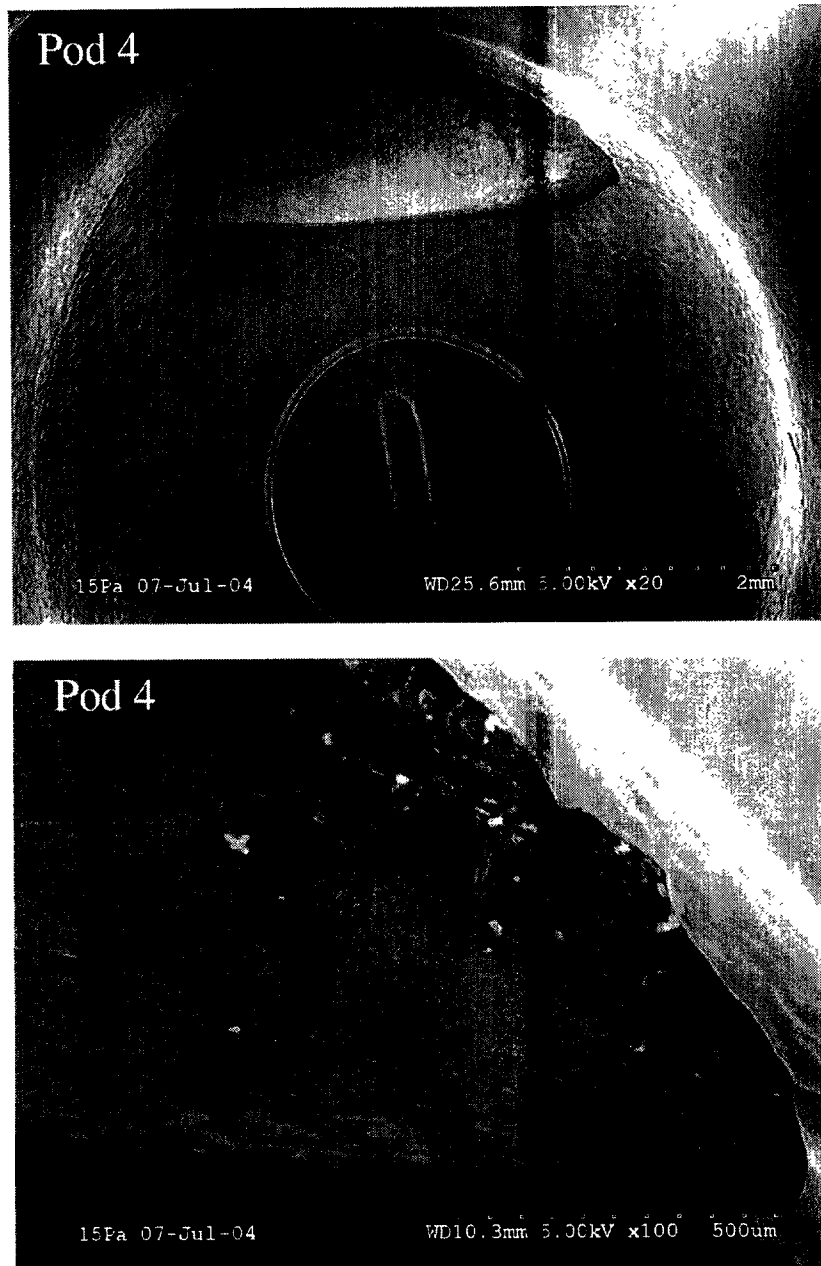


Figure 52. Images collected from Hitachi S3500N variable pressure scanning electron microscope of pod 4 on the **reprocessed Octopus 4® MT-104-10**. The images show various irregularities and contamination on the surface structure of the tubing and the pods. Bioburden debris and contamination is present on the surface of the tubing when compared to “new”. Note sheet of material on tubing, gap between pod and hypotube and the partially blocked opening. Scale bar in each image.

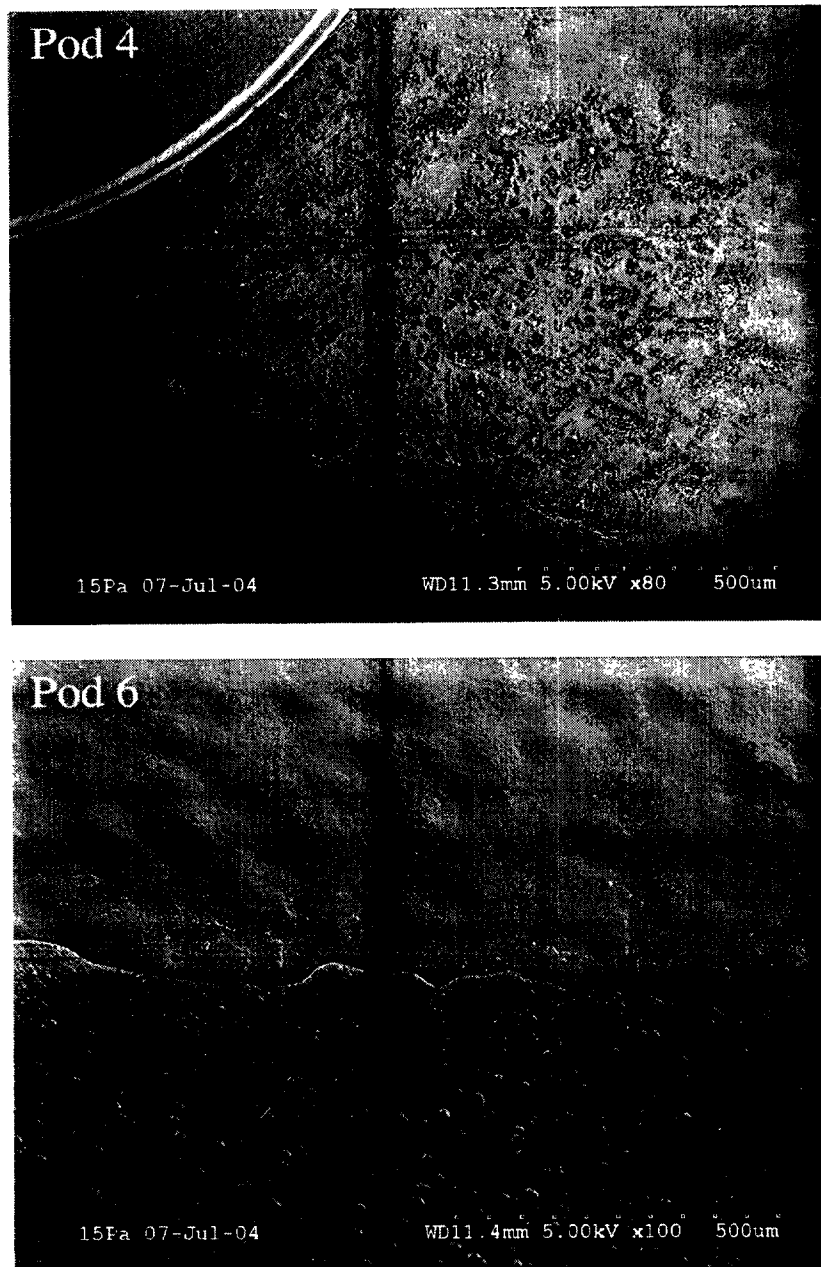


Figure 53. Images collected from Hitachi S3500N variable pressure scanning electron microscope of pods 4 and 6 on the **reprocessed Octopus 4[®] MT-104-10**. The images show contamination on the surface structure of the pods. Scale bar in each image.

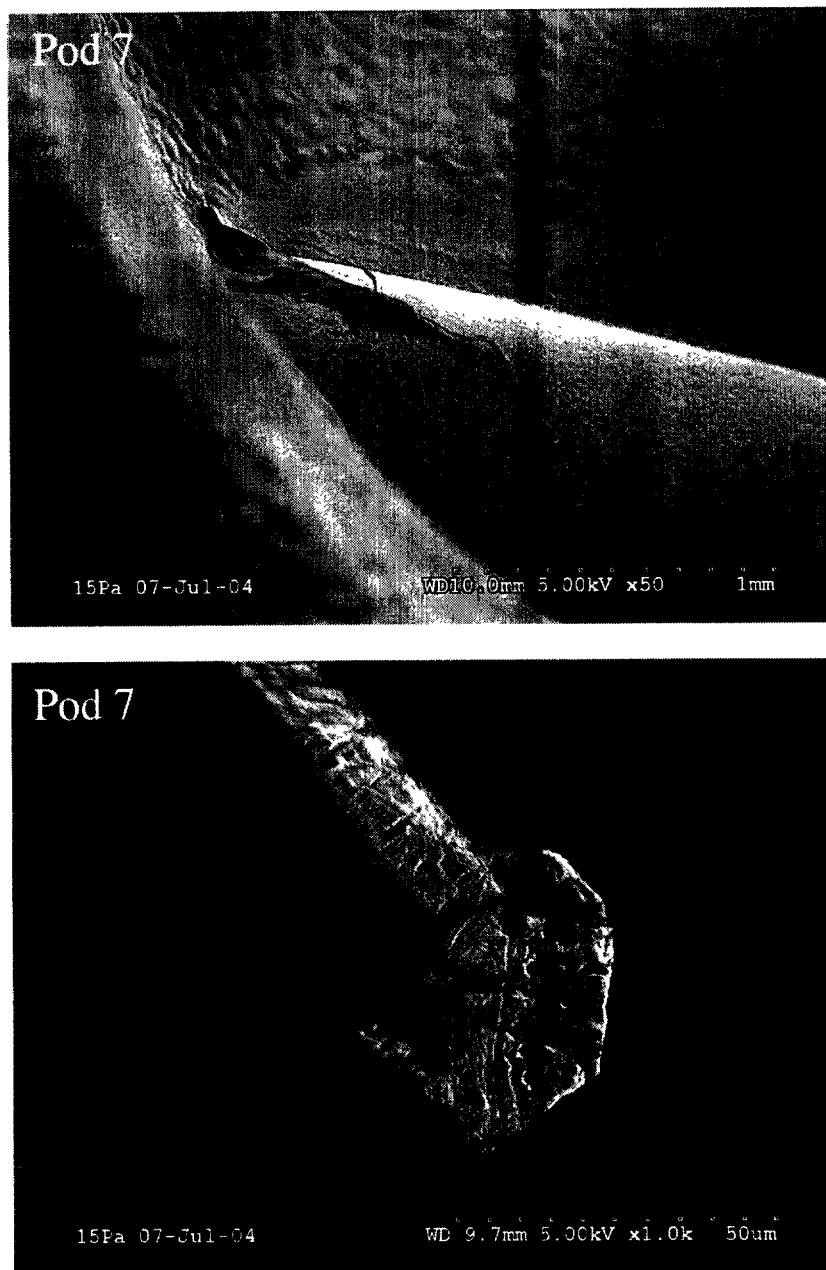


Figure 54. Images collected from Hitachi S3500N variable pressure scanning electron microscope of pod 7 on the **reprocessed Octopus 4® MT-104-10**. The images show various irregularities and contamination on the surface structure of the tubing and the pods. Note hair-like fiber in lower panel. Scale bar in each image.

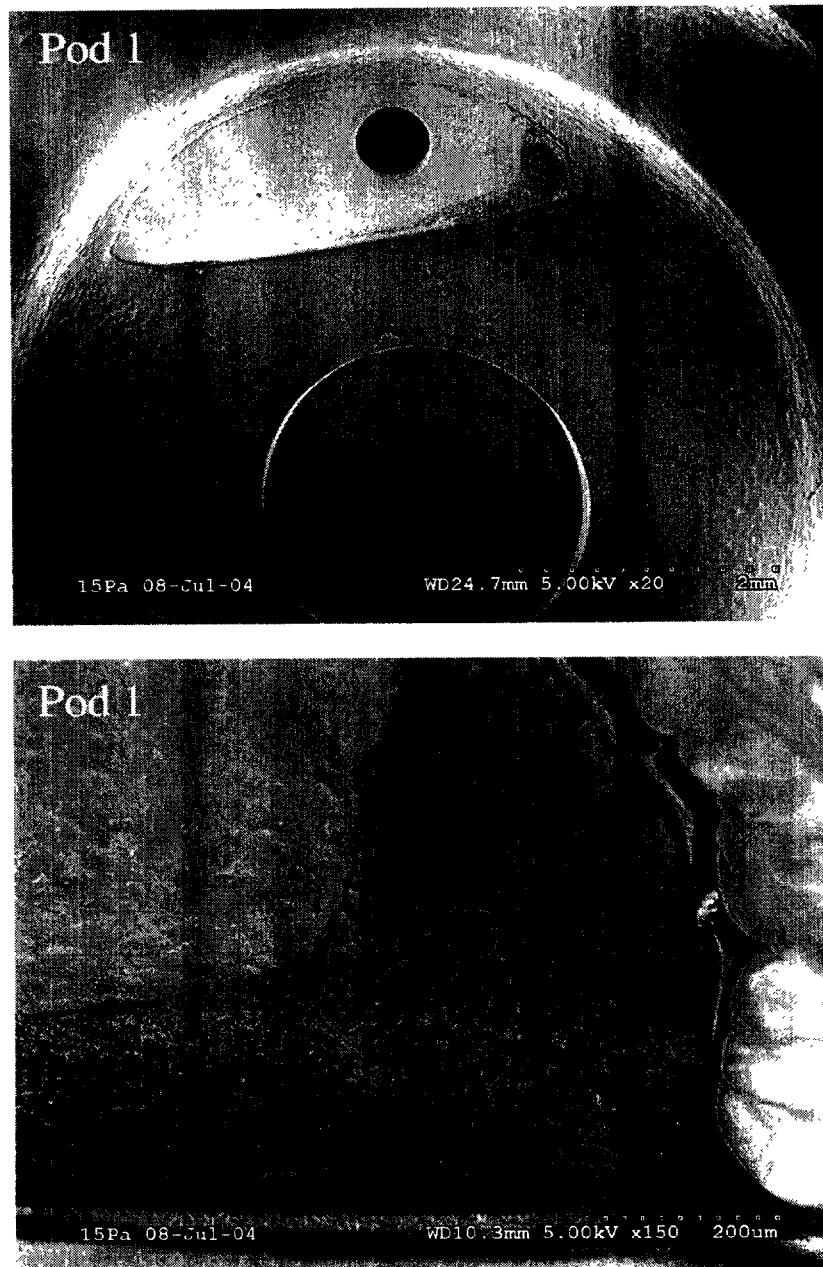


Figure 55. Images collected from Hitachi S3500N variable pressure scanning electron microscope of pod 1 on the **reprocessed Octopus 4® MT-104-11**. The images show various irregularities and contamination on the surface structure of the tubing and the pods. Bioburden debris and contamination is present on the surface of the tubing when compared to “new”. Note “sheet” of foreign material on tubing surface. Scale bar in each image.

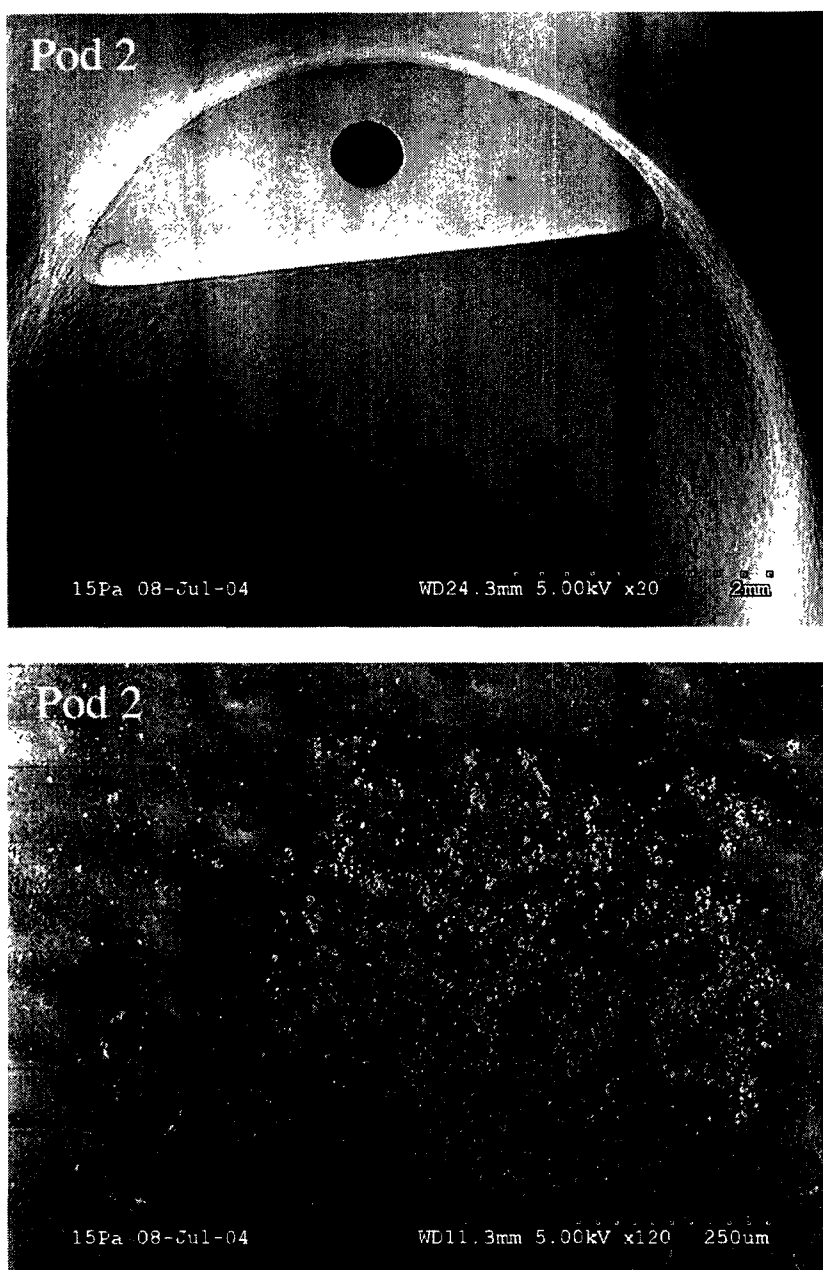


Figure 56. Images collected from Hitachi S3500N variable pressure scanning electron microscope of pod 2 on the **reprocessed Octopus 4[®] MT-104-11**. The images show various irregularities and contamination on the surface structure of the tubing and the pod. Bioburden debris and contamination is present on the surface of the pod when compared to “new”. Scale bar in each image.

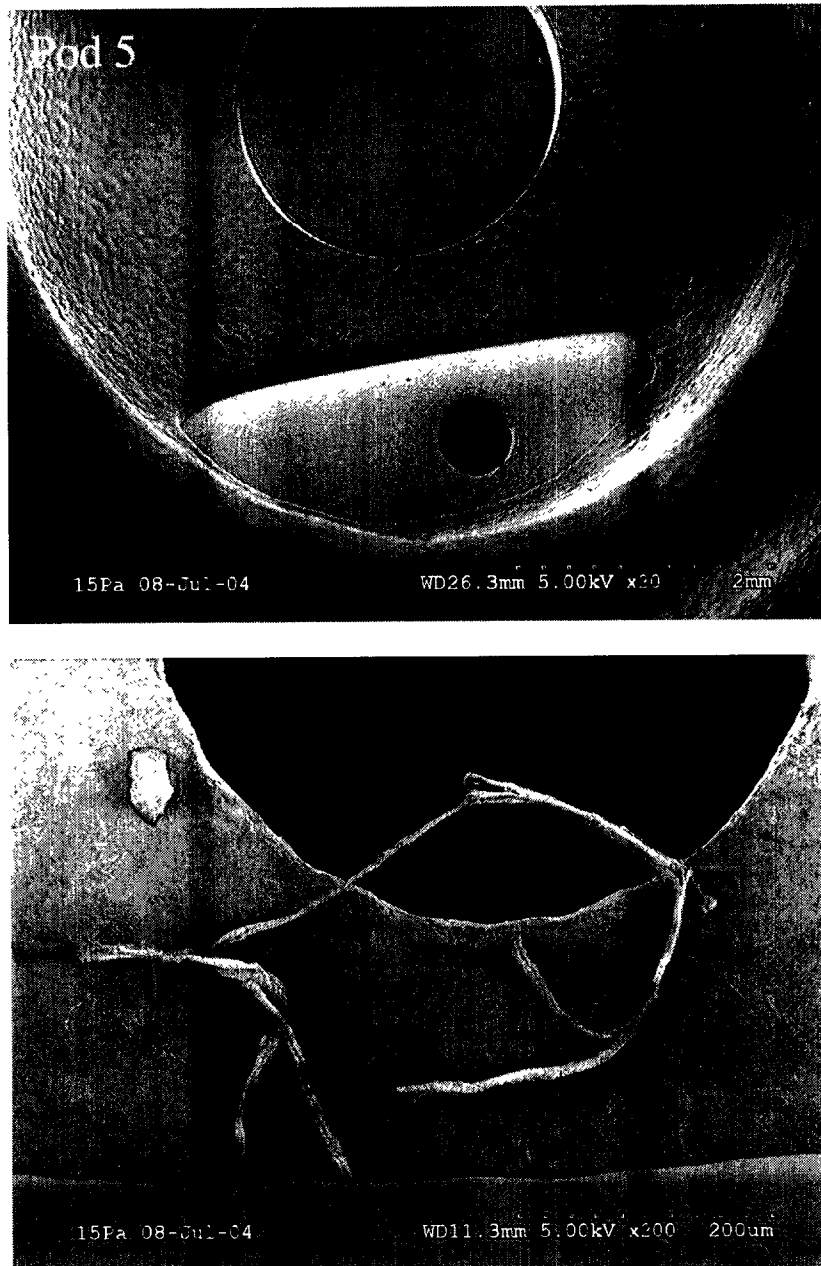


Figure 57. Images collected from Hitachi S3500N variable pressure scanning electron microscope in the areas of pod 5 on the **reprocessed Octopus 4[®] MT-104-11**. The images show hair-like fibers on surface of the hypotubing near the opening. There is also debris present in the surface of the tubing. The number in the upper left indicates the pod # (see Figure 5). Scale bar in each image.

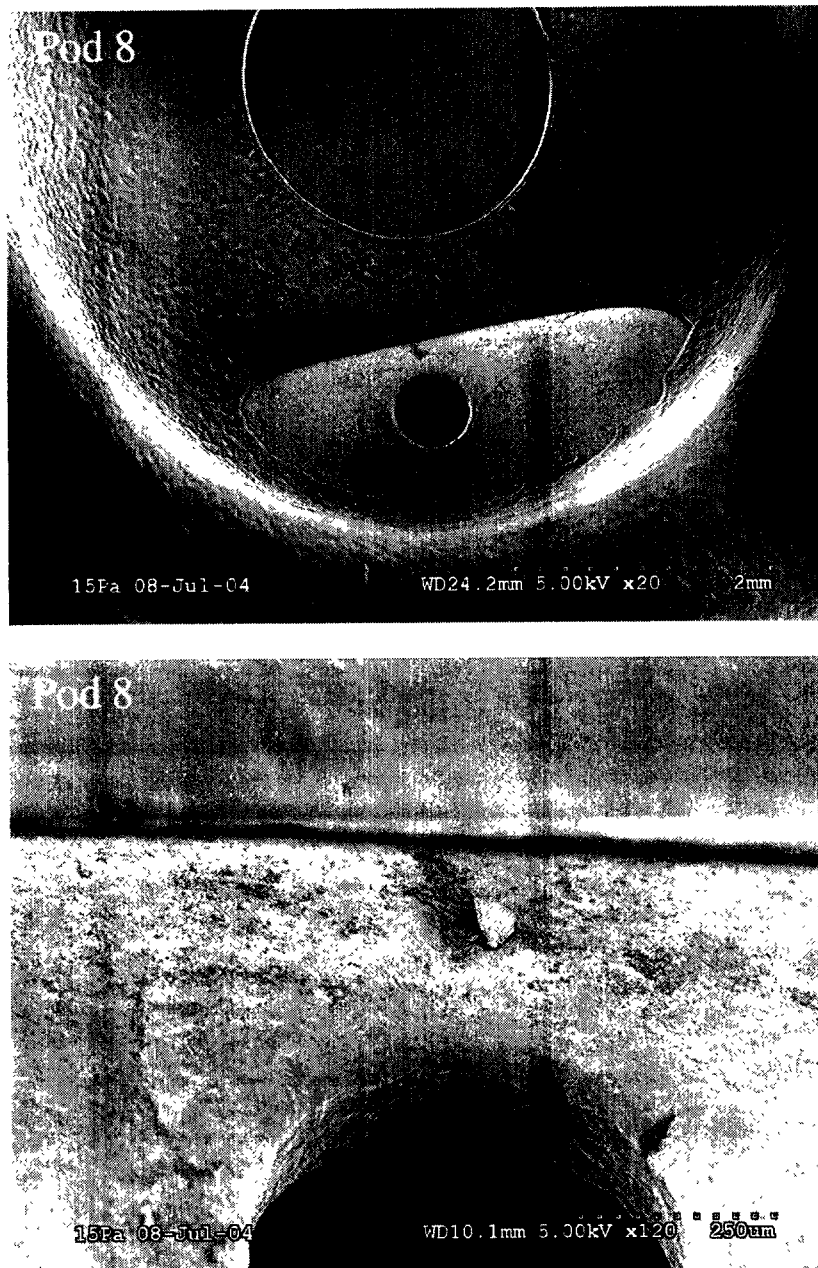


Figure 58. Images collected from Hitachi S3500N variable pressure scanning electron microscope in the areas of pod 8 on the **reprocessed Octopus 4[®] MT-104-11**. The images show contamination on surface of the hypotubing near the opening. There is also debris present on the surface of the tubing. The number in the upper left indicates the pod # (see Figure 5). Scale bar in each image.

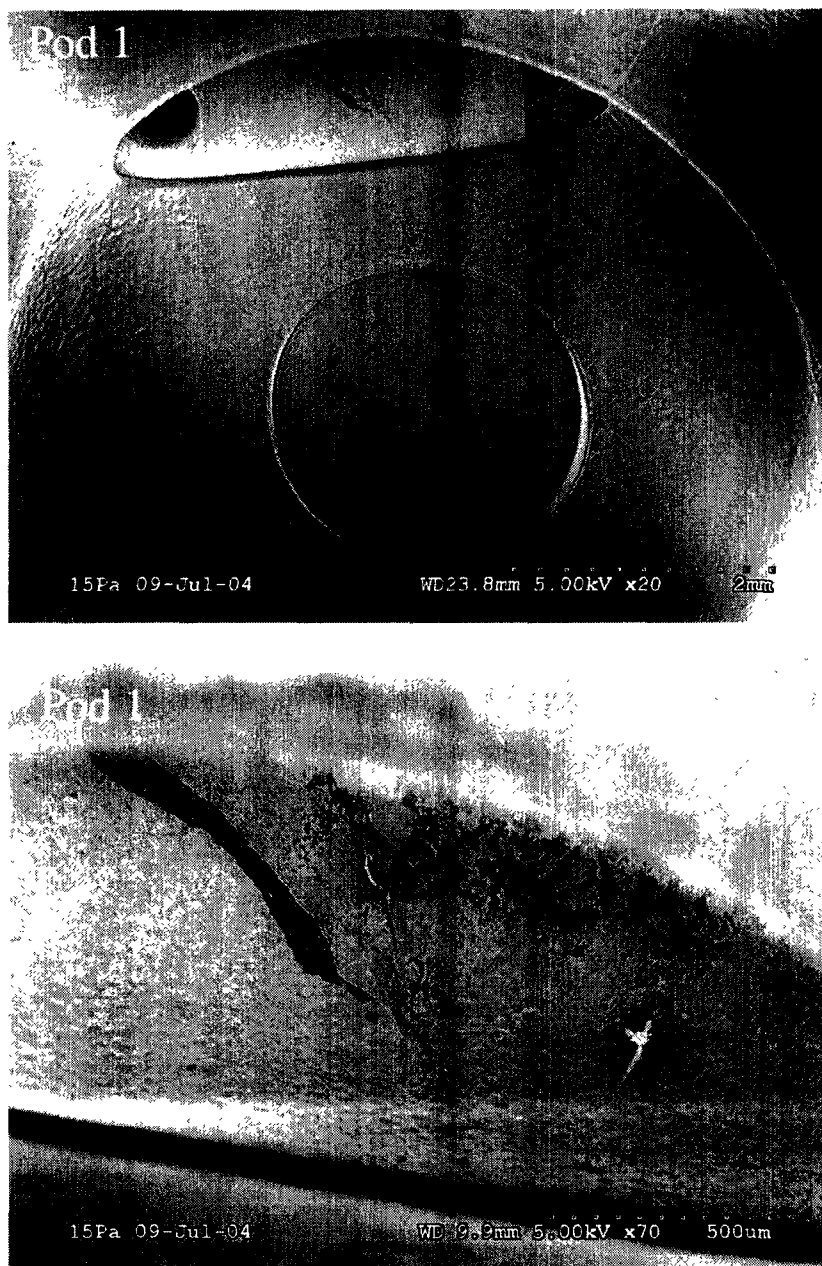


Figure 59. Images collected from Hitachi S3500N variable pressure scanning electron microscope in the areas of pod 1 on the **reprocessed Octopus 4[®] MT-104-13**. The images show contamination on surface of the hypotubing. The number in the upper left indicates the pod # (see Figure 5). Scale bar in each image.



Figure 60. Higher magnification views of debris in pod 1 on the reprocessed Octopus 4[®] MT-104-13. The number in the upper left indicates the pod # (see Figure 5). Scale bar in each image.

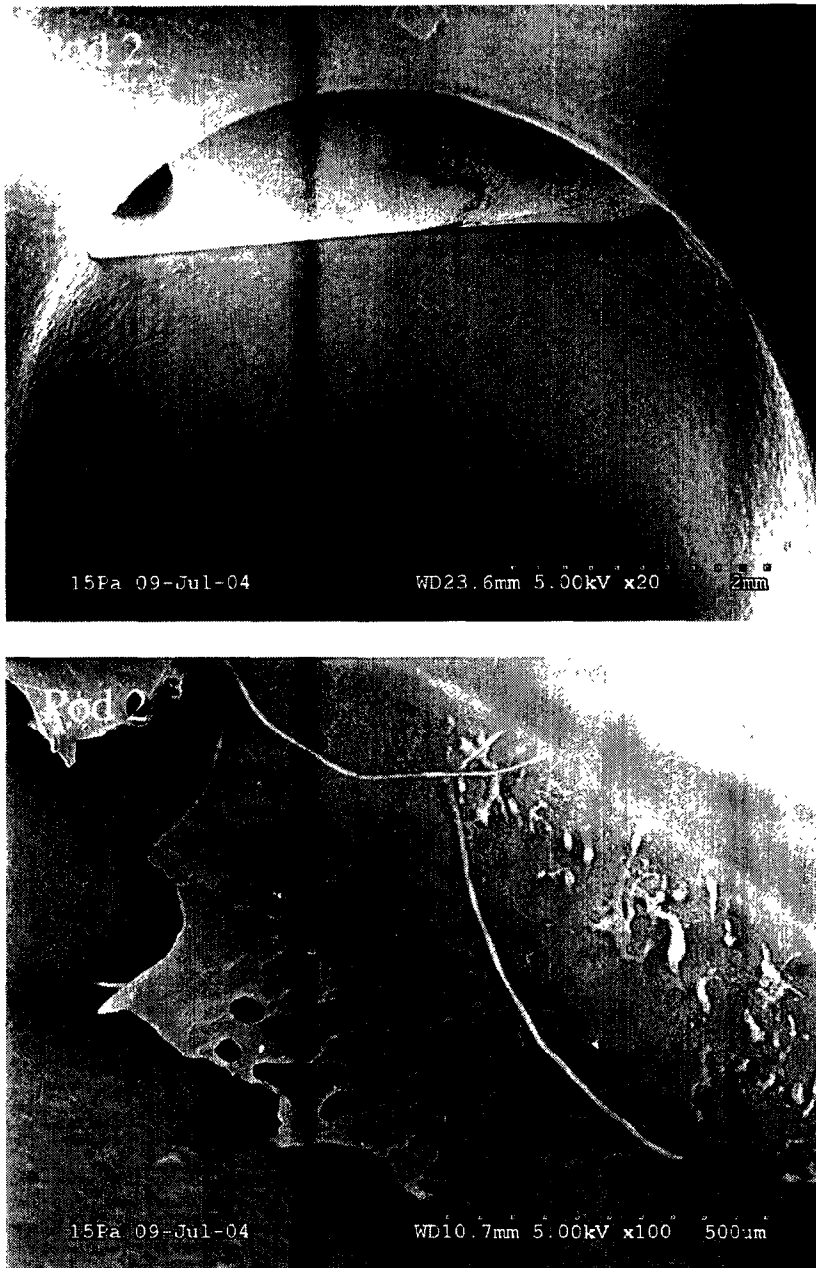


Figure 61. Images collected from Hitachi S3500N variable pressure scanning electron microscope in the areas of pod 2 on the **reprocessed Octopus 4[®] MT-104-13**. The images show contamination on surface of the hypotubing. Note sheet of bioburden and hair-like fiber. The number in the upper left indicates the pod # (see Figure 5). Scale bar in each image.

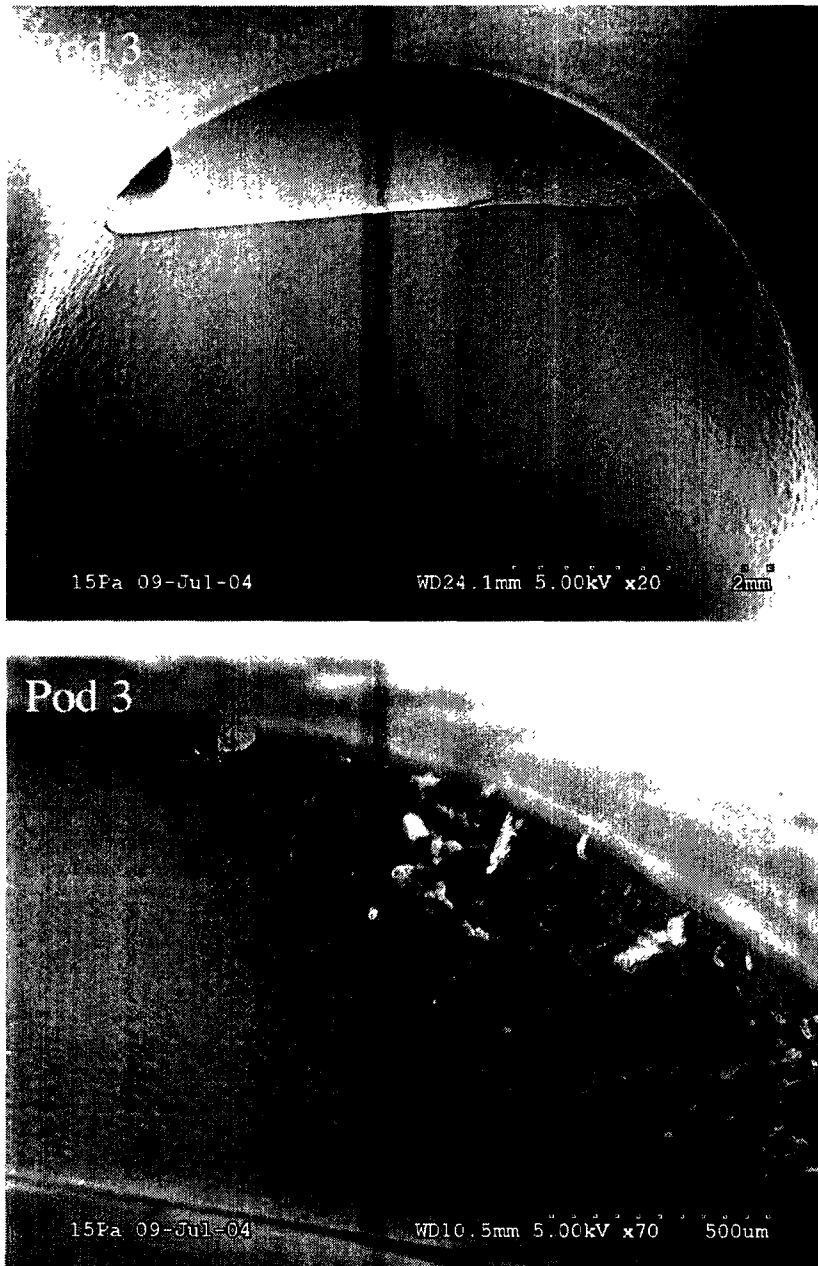


Figure 62. Images collected from Hitachi S3500N variable pressure scanning electron microscope in the areas of pod 3 on the **reprocessed Octopus 4® MT-104-13**. The images show contamination on surface of the hypotubing. Note sheet of bioburden on the hypotube. The number in the upper left indicates the pod # (see Figure 5). Scale bar in each image.

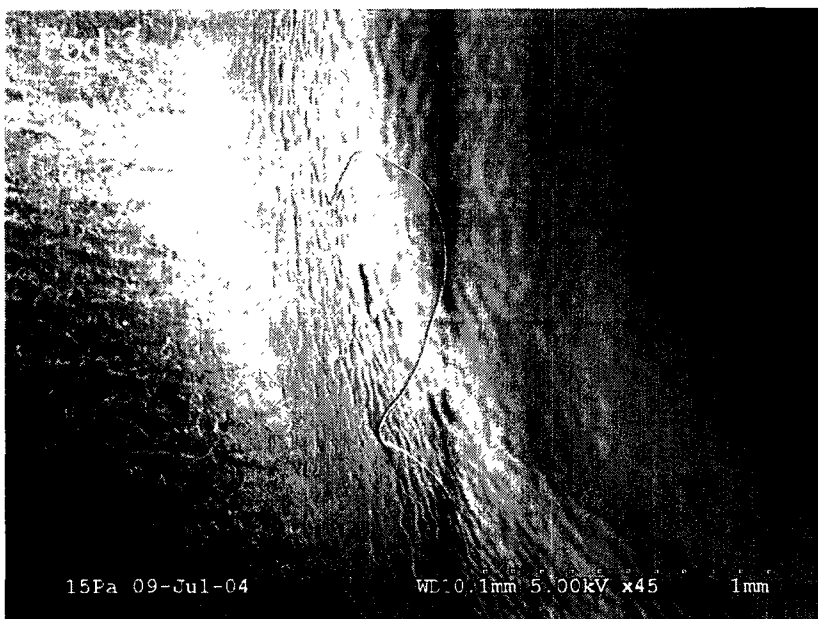


Figure 63. Images collected from Hitachi S3500N variable pressure scanning electron microscope in the areas of pod 3 on the **reprocessed Octopus 4[®] MT-104-13**. The images show hair on the pod surface and partially blocked hypotube opening. The number in the upper left indicates the pod # (see Figure 5). Scale bar in each image.

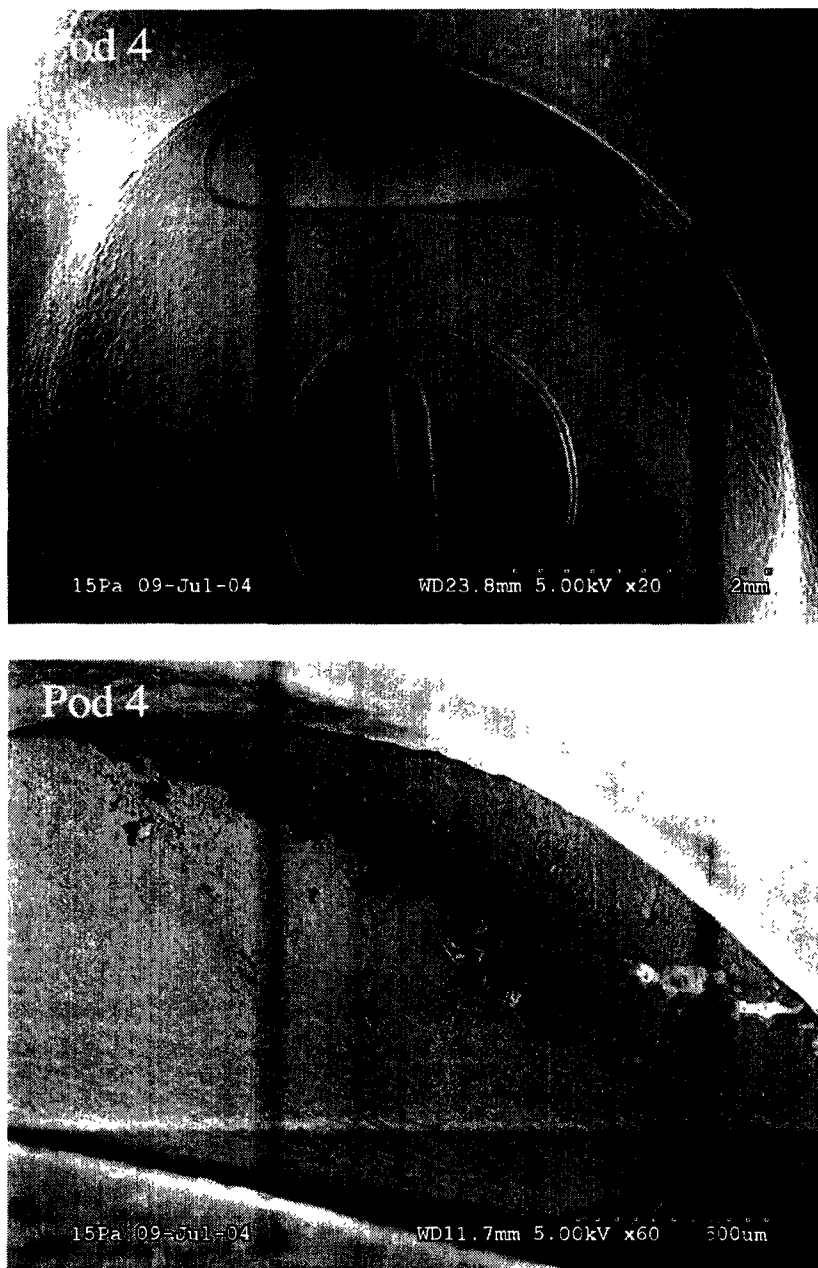


Figure 64. Images collected from Hitachi S3500N variable pressure scanning electron microscope in the areas of pod 4 on the **reprocessed Octopus 4® MT-104-13**. The images show contamination on surface of the hypotubing. The hypotube opening is completely blocked. Note sheet of bioburden and gap between hypotube and pod. The number in the upper left indicates the pod # (see Figure 5). Scale bar in each image.

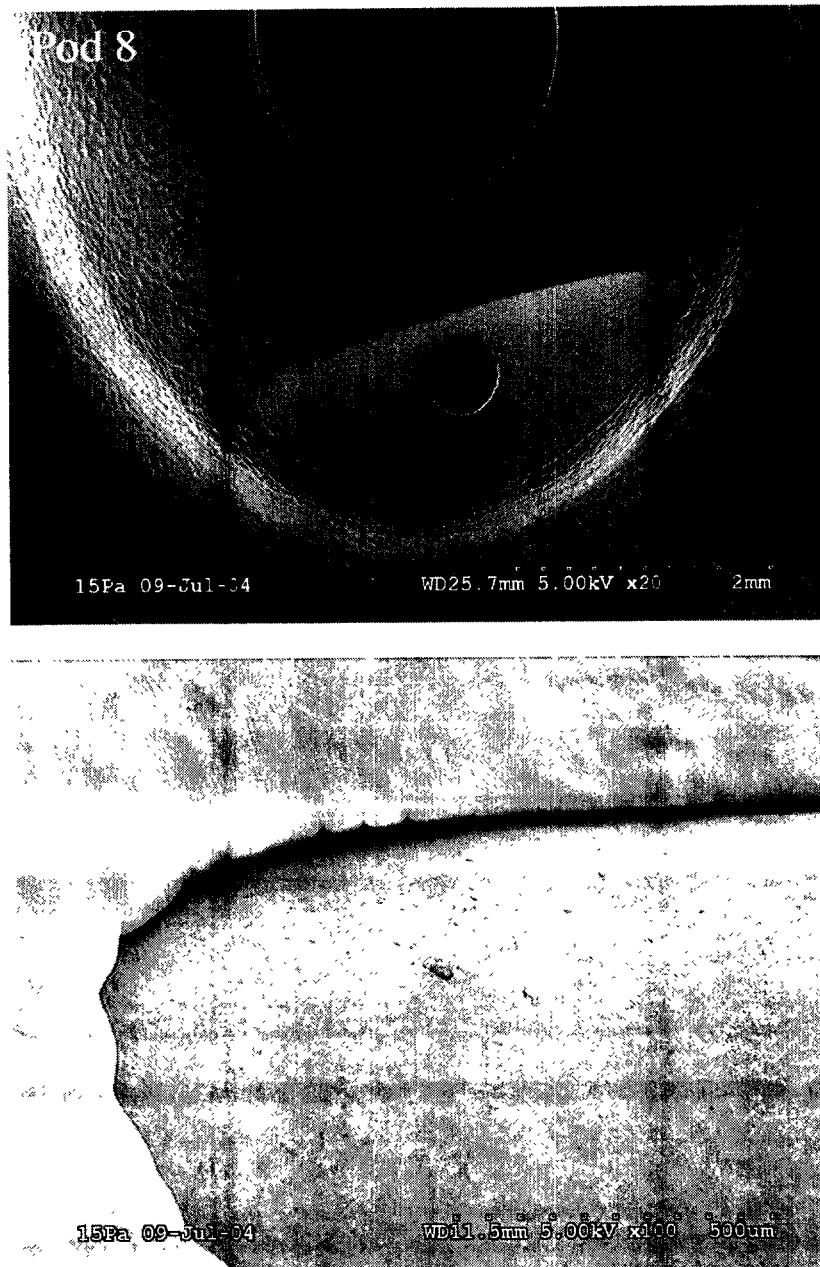


Figure 65. Images collected from Hitachi S3500N variable pressure scanning electron microscope in the areas of pod 8 on the **reprocessed Octopus 4[®] MT-104-13**. The images show little to no contamination on surface of the hypotubing. Note gap between hypotube and pod. The number in the upper left indicates the pod # (see Figure 5). Scale bar in each image.

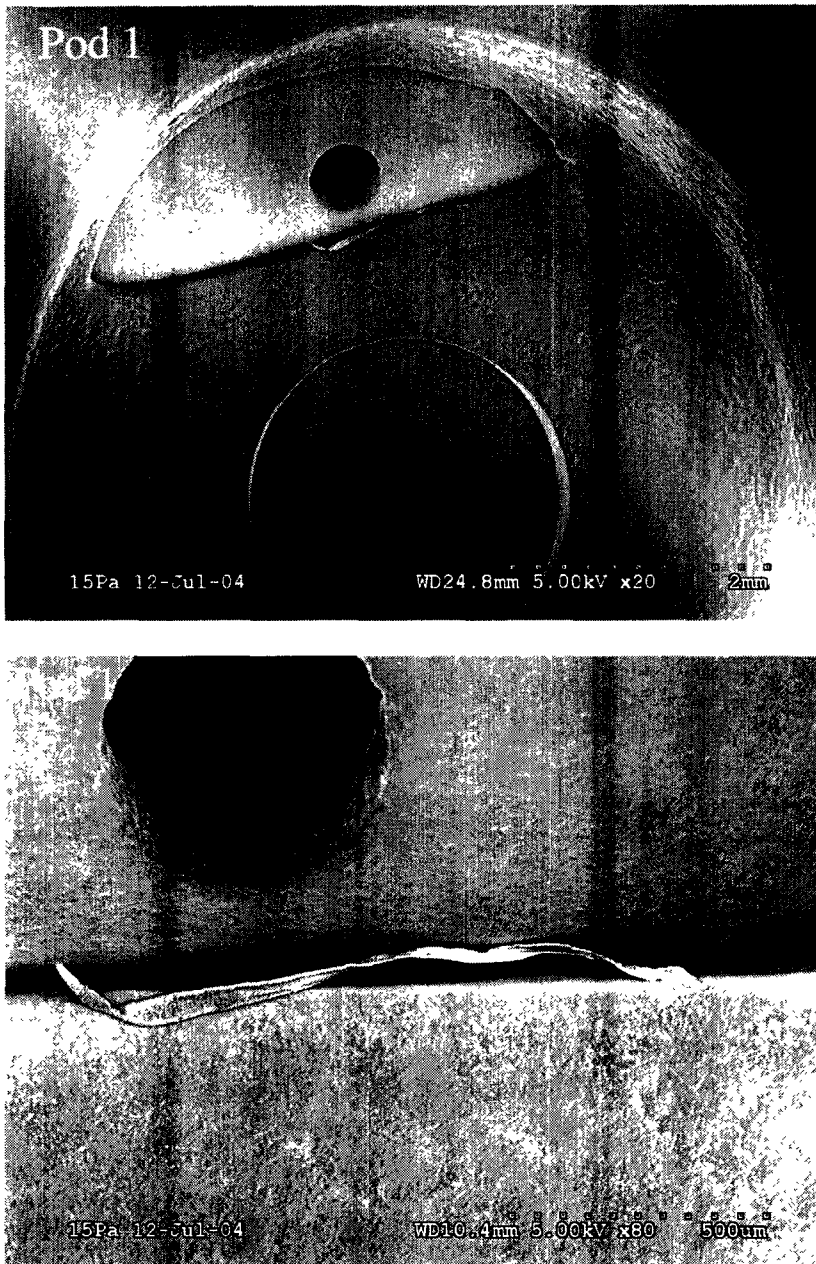


Figure 66. Images collected from Hitachi S3500N variable pressure scanning electron microscope in the areas of pod 1 on the **reprocessed Octopus 4[®] MT-104-16**. The images show gap between hypotube and pod. Note fiber in gap region. The number in the upper left indicates the pod # (see Figure 5). Scale bar in each image.

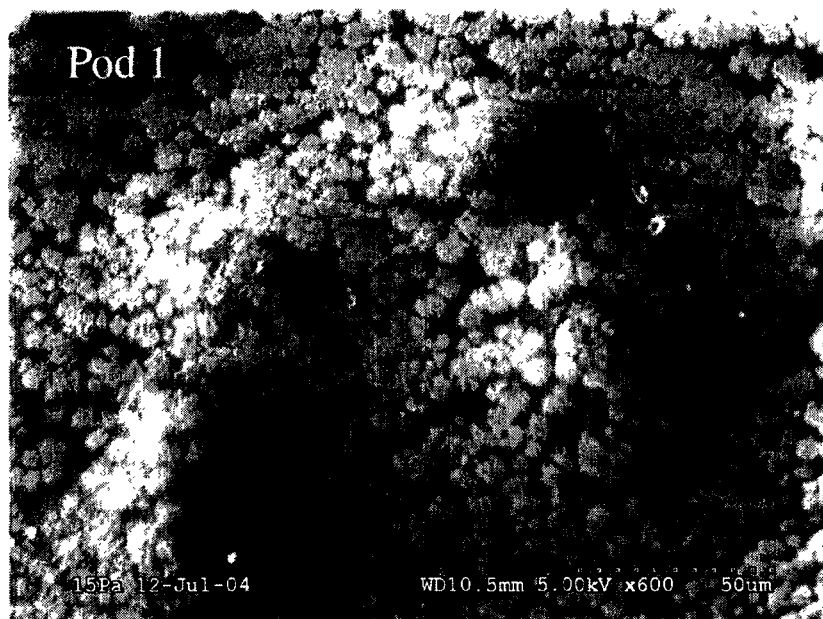


Figure 67. Image collected from Hitachi S3500N variable pressure scanning electron microscope in the area of pod 1 on the **reprocessed Octopus 4[®] MT-104-16**. The images show foreign crystalline substance in pod base. The number in the upper left indicates the pod # (see Figure 5). Scale bar in each image.

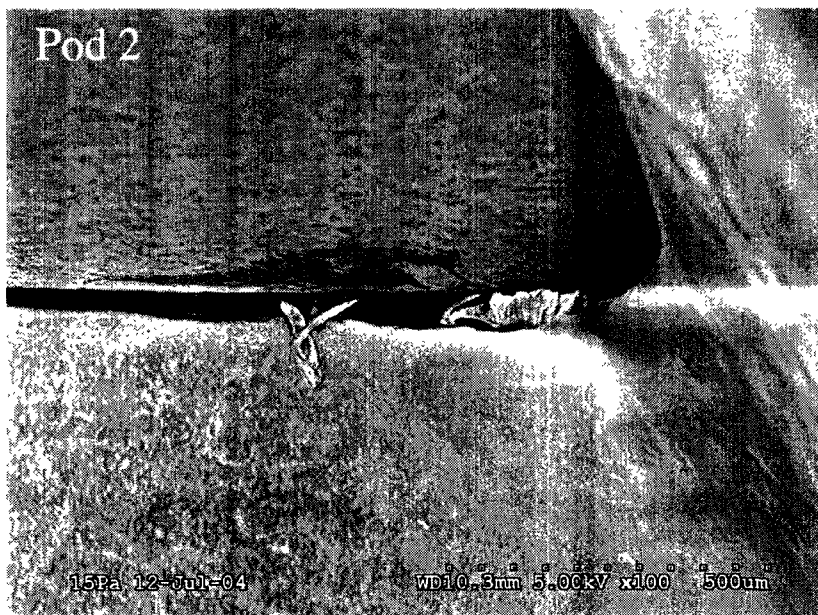
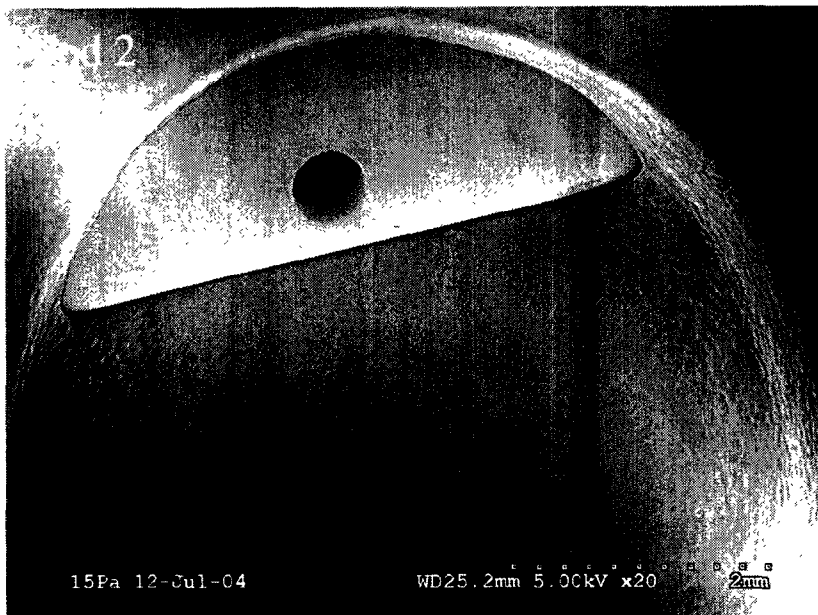


Figure 68. Images collected from Hitachi S3500N variable pressure scanning electron microscope in the areas of pod 2 on the **reprocessed Octopus 4[®] MT-104-16**. The images show gap between hypotube and pod. Note fiber and debris in gap region. The number in the upper left indicates the pod # (see Figure 5). Scale bar in each image.

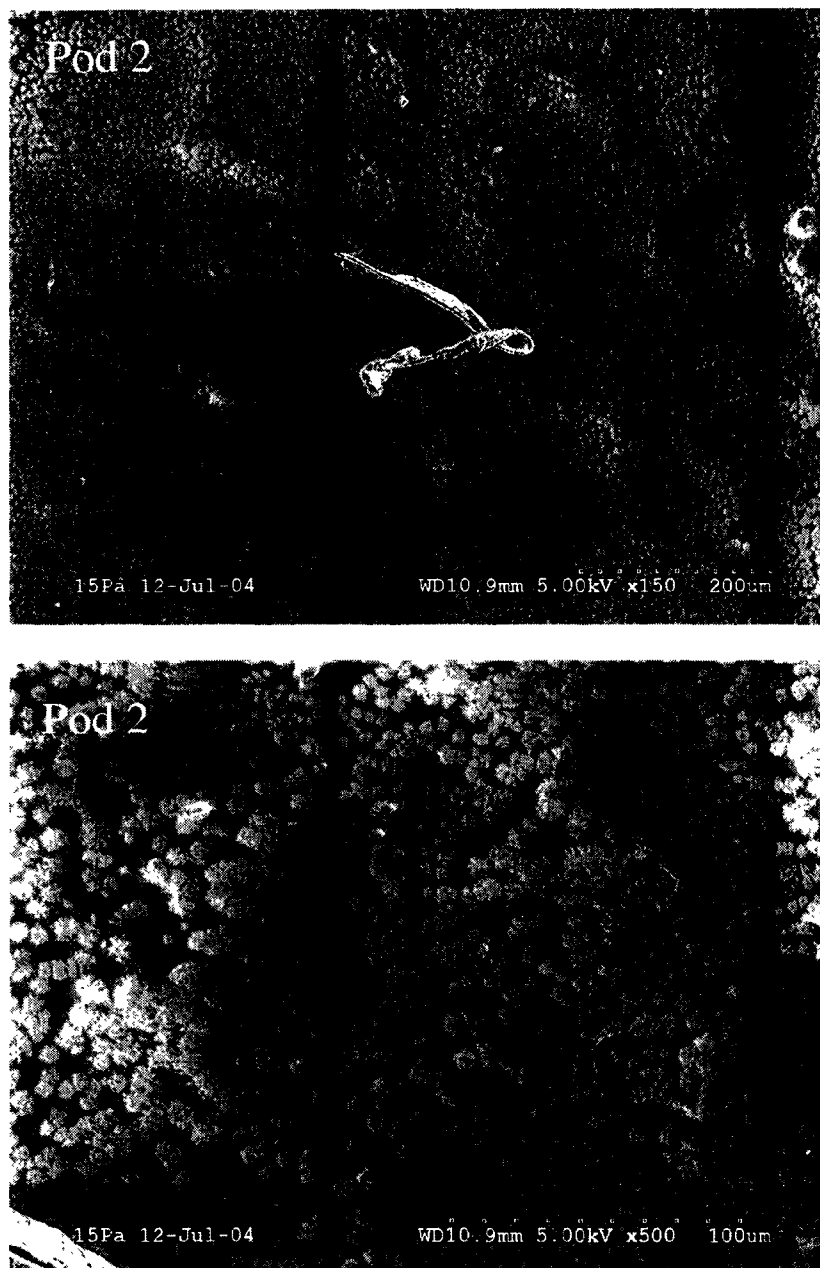


Figure 69. Images collected from Hitachi S3500N variable pressure scanning electron microscope in the area of pod 2 on the **reprocessed Octopus 4[®] MT-104-16**. The images show bioburden and fiber on pod base. The number in the upper left indicates the pod # (see Figure 5). Scale bar in each image.

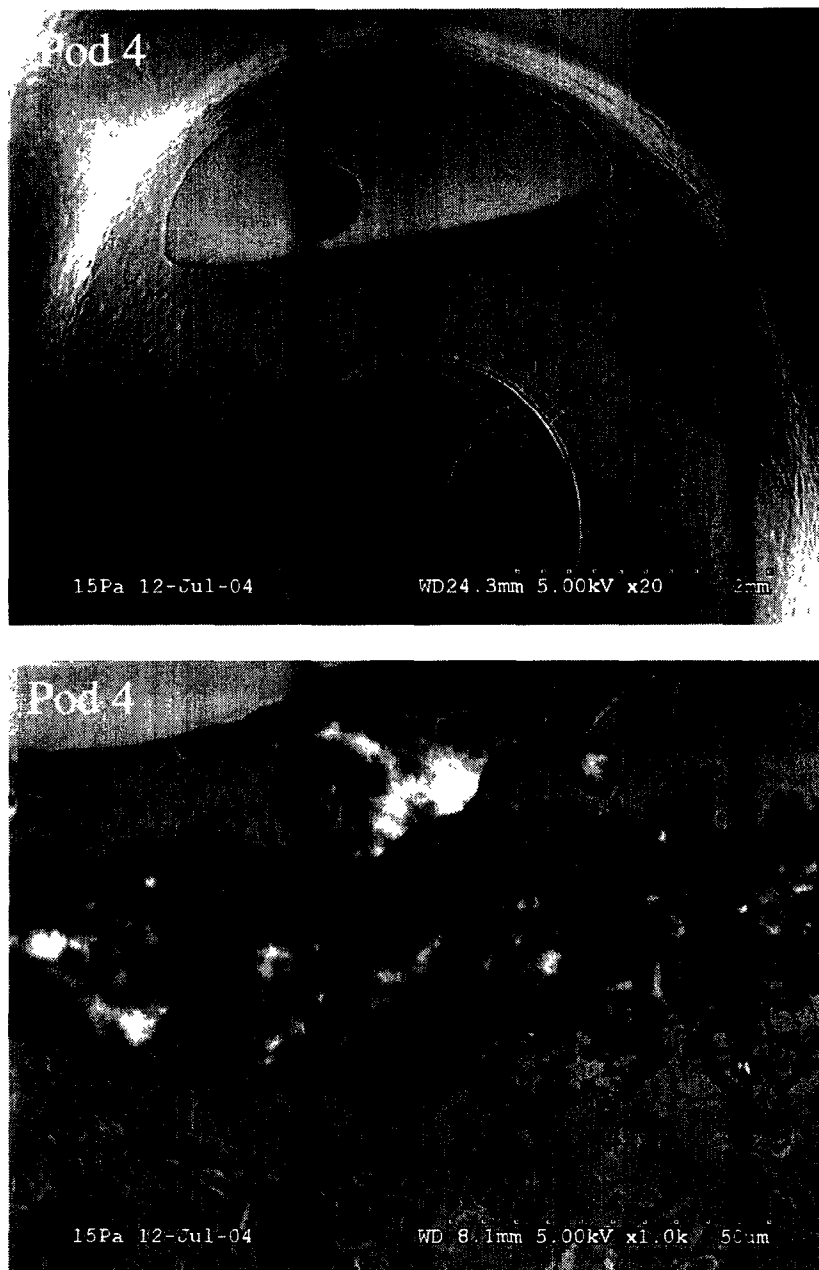


Figure 70. Image collected from Hitachi S3500N variable pressure scanning electron microscope in the area of pod 4 on the **reprocessed Octopus 4[®] MT-104-16**. The images show on hypotube near upper region of tube. The number in the upper left indicates the pod # (see Figure 5). Scale bar in each image.

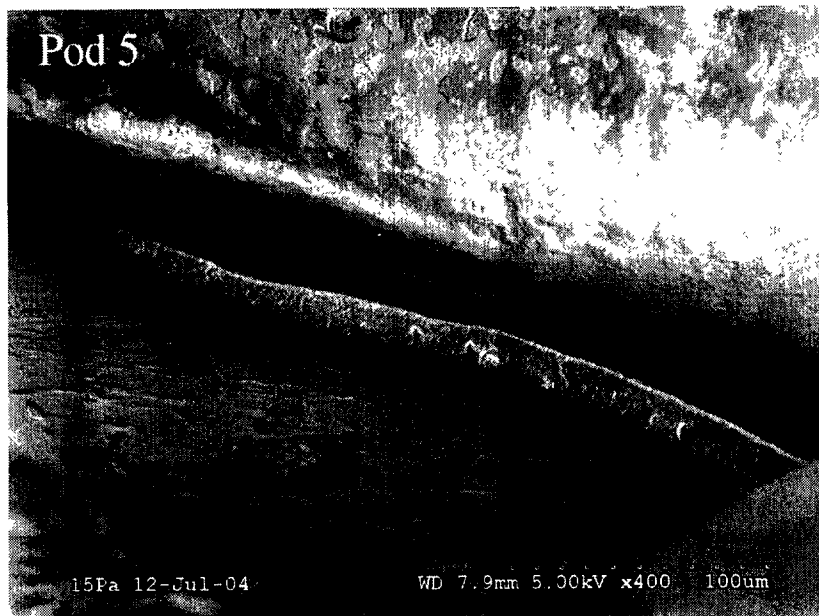
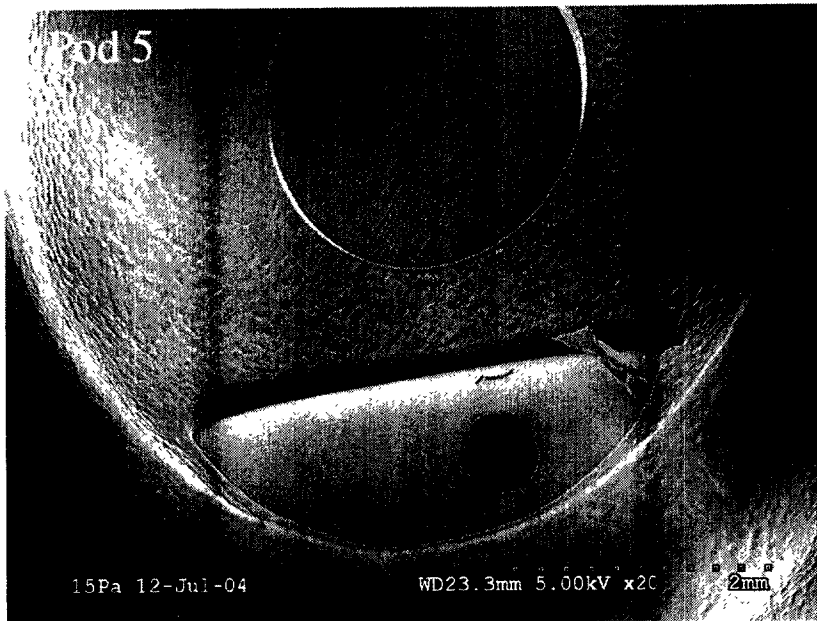


Figure 71. Images collected from Hitachi S3500N variable pressure scanning electron microscope in the areas of pod 5 on the **reprocessed Octopus 4[®] MT-104-16**. The images show gap between hypotube and pod. Note debris in gap region. The number in the upper left indicates the pod # (see Figure 5). Scale bar in each image.

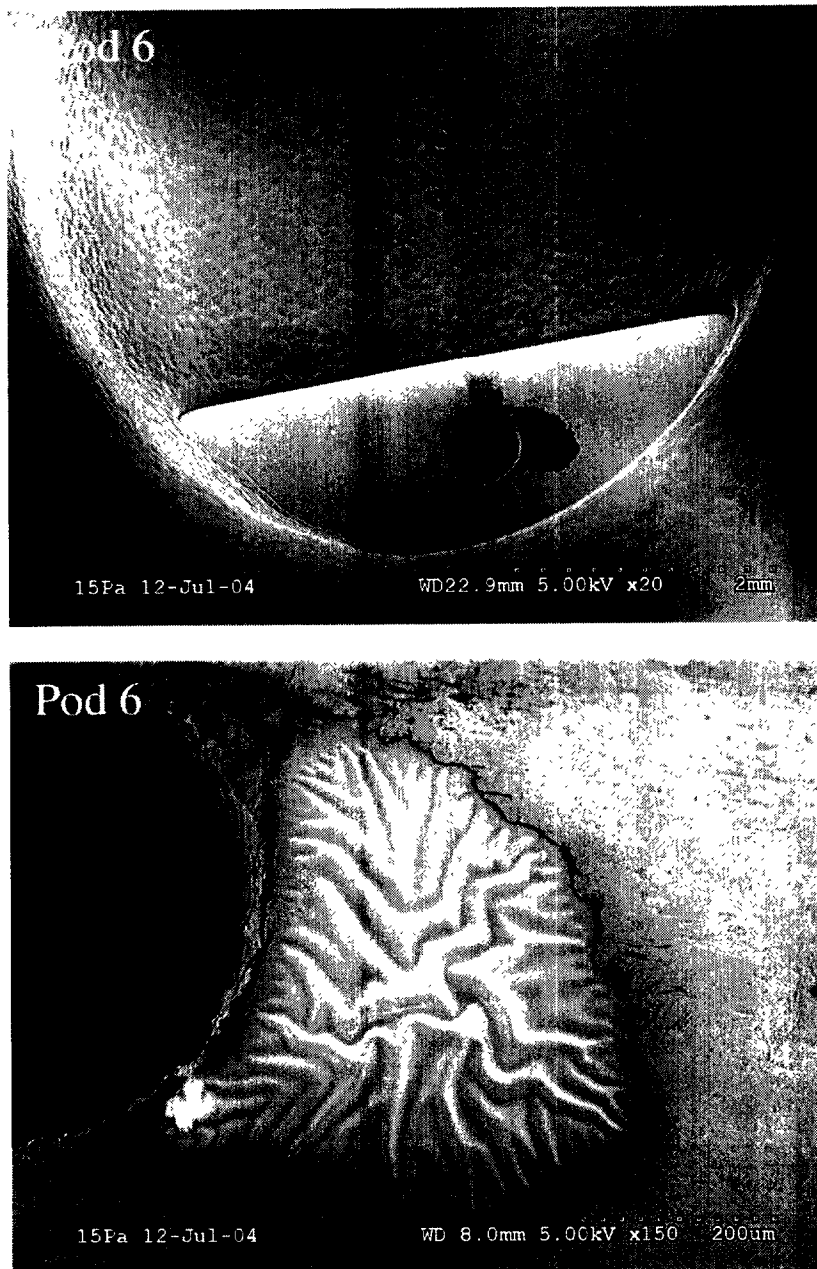


Figure 72. Images collected from Hitachi S3500N variable pressure scanning electron microscope in the areas of pod 6 on the **reprocessed Octopus 4[®] MT-104-16**. Note contamination and dried liquid material near hypotube opening. The number in the upper left indicates the pod # (see Figure 5). Scale bar in each image.

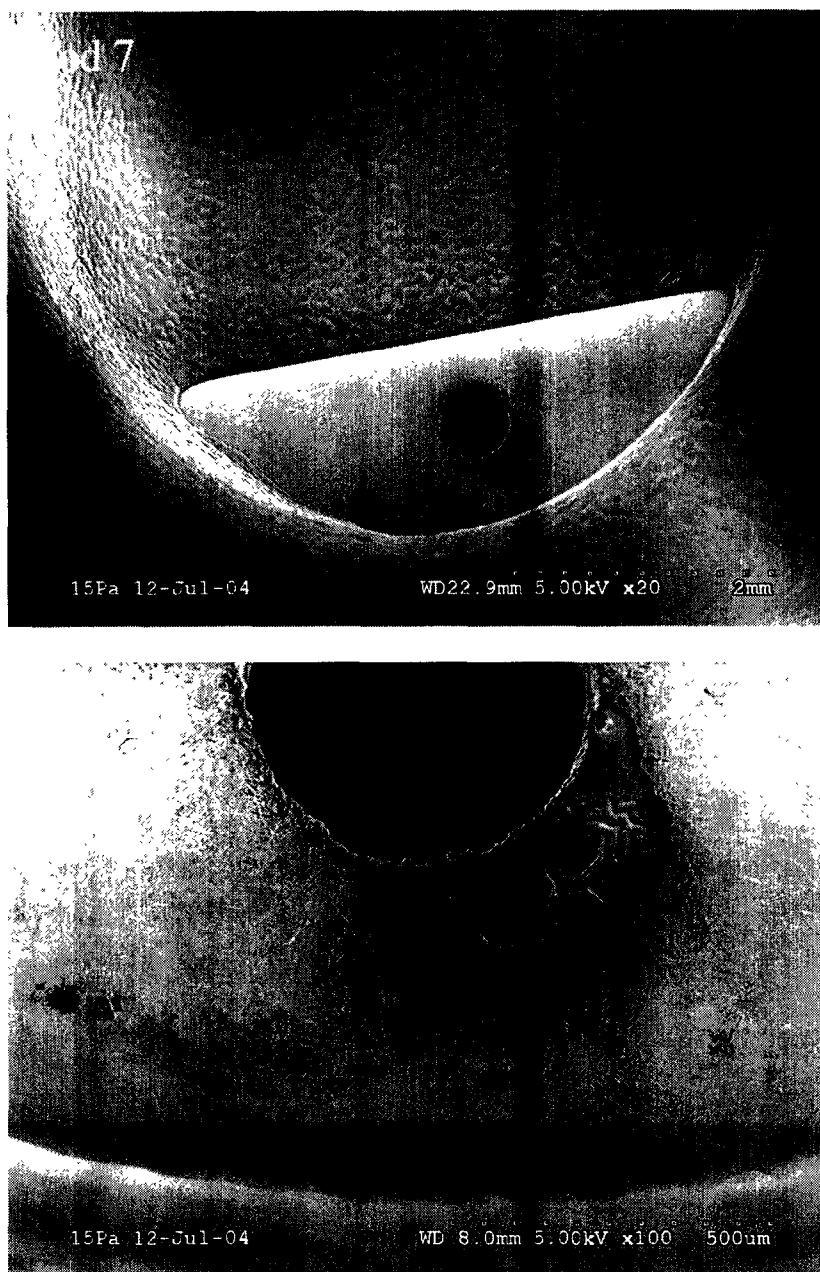


Figure 73. Images collected from Hitachi S3500N variable pressure scanning electron microscope in the areas of pod 7 on the **reprocessed Octopus 4[®] MT-104-16**. Note contamination and dried liquid material near hypotube opening. The number in the upper left indicates the pod # (see Figure 5). Scale bar in each image.

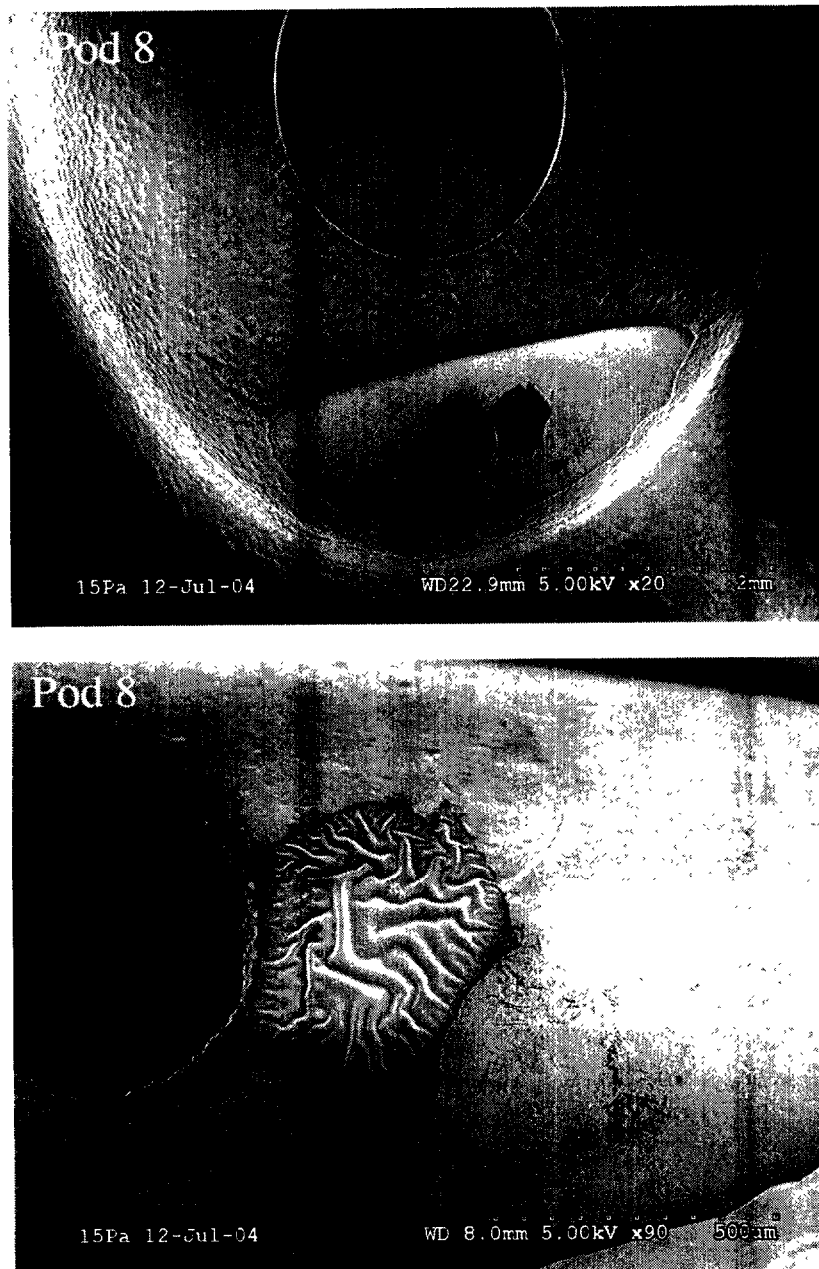


Figure 74. Images collected from Hitachi S3500N variable pressure scanning electron microscope in the areas of pod 8 on the **reprocessed Octopus 4[®] MT-104-16**. Note contamination and dried liquid material near hypotube opening. The number in the upper left indicates the pod # (see Figure 5). Scale bar in each image.



Figure 75. Images collected from Hitachi S3500N variable pressure scanning electron microscope in the areas of pod 8 on the **reprocessed Octopus 4® MT-104-16**. Note contamination and dried liquid material near hypotube opening. There is also debris in the opening of the hypotube. The number in the upper left indicates the pod # (see Figure 5). Scale bar in each image.

Confocal Microscopy DNA and Protein Staining

Following examination by SEM, prior to any additional treatments, each pod examined was imaged using multiple fluorescence excitation and emission wavelengths to note any strong autofluorescence. Areas of contamination exhibited low levels autofluorescence. Images were collected prior to staining. These images represent the unstained control images.

The individual pods of the devices were then probed and examined using the fluorescent DNA probes 4', 6-diamidino-2-phenylindole, dihydrochloride (DAPI, D-1306, Molecular Probes, Inc.), propidium iodide (P-1304, Molecular Probes, Inc.) or Syto 16 (S7578, Molecular Probes, Inc.) or Sypro[®] Orange (S6650, Molecular Probes, Inc. See attached product sheets). The blue fluorescent DAPI nucleic acid stain preferentially stains dsDNA; it appears to associate with AT clusters in the minor groove. DAPI stains nuclei specifically, with little or no cytoplasmic labeling. Propidium iodide (PI) binds to DNA by intercalating between the bases with little or no sequence preference and with a stoichiometry of one dye per 4-5 base pairs of DNA. Syto 16 binds to RNA and DNA in both live and dead eukaryotic cells as well as Gram-positive and Gram-negative bacteria. The Syto 16 has an extremely low intrinsic fluorescence when not bound to nucleic acids. The Syto 16 dye was used at a concentration of 1 μM in distilled water.

Sypro[®] Orange stain is a fluorescent stain for proteins. It offers many advantages, including a fast, one-step staining protocol requiring no destaining; a linear range over three orders of magnitude; and very little protein-to-protein variation in staining. The Sypro[®] Orange stain was used at a concentration of 2 μM diluted in distilled water.

All reagents were applied in the following manner. Approximately 3 μL of the dilute staining solution was added to the metal tubing region within the pods of the reprocessed Octopus[®] devices, taking care not to invade the hole or touch the surface. Following a minimum of 10-15 minutes of incubation the pods were imaged using the same microscope parameters as the control images. The DAPI staining procedure was used to initially and independently confirm the presence of DNA on two of the devices (MT-104-5 and MT-104-7, pod 2 on each). The devices were observed visually for positive staining, no images were collected. Both devices observed had positive indication of DNA.

The staining results from the PI, Syto 16 nucleic acid stains and the Sypro[®] Orange protein stain are included in this report.



Figure 76. Control. Series of optical sections collected from laser scanning confocal microscope through the area of the tube in the untreated pod #5 of the **new Octopus 3[®] MT-104-1**. The images show no appreciable fluorescence from the region. The numbers indicate the optical section.

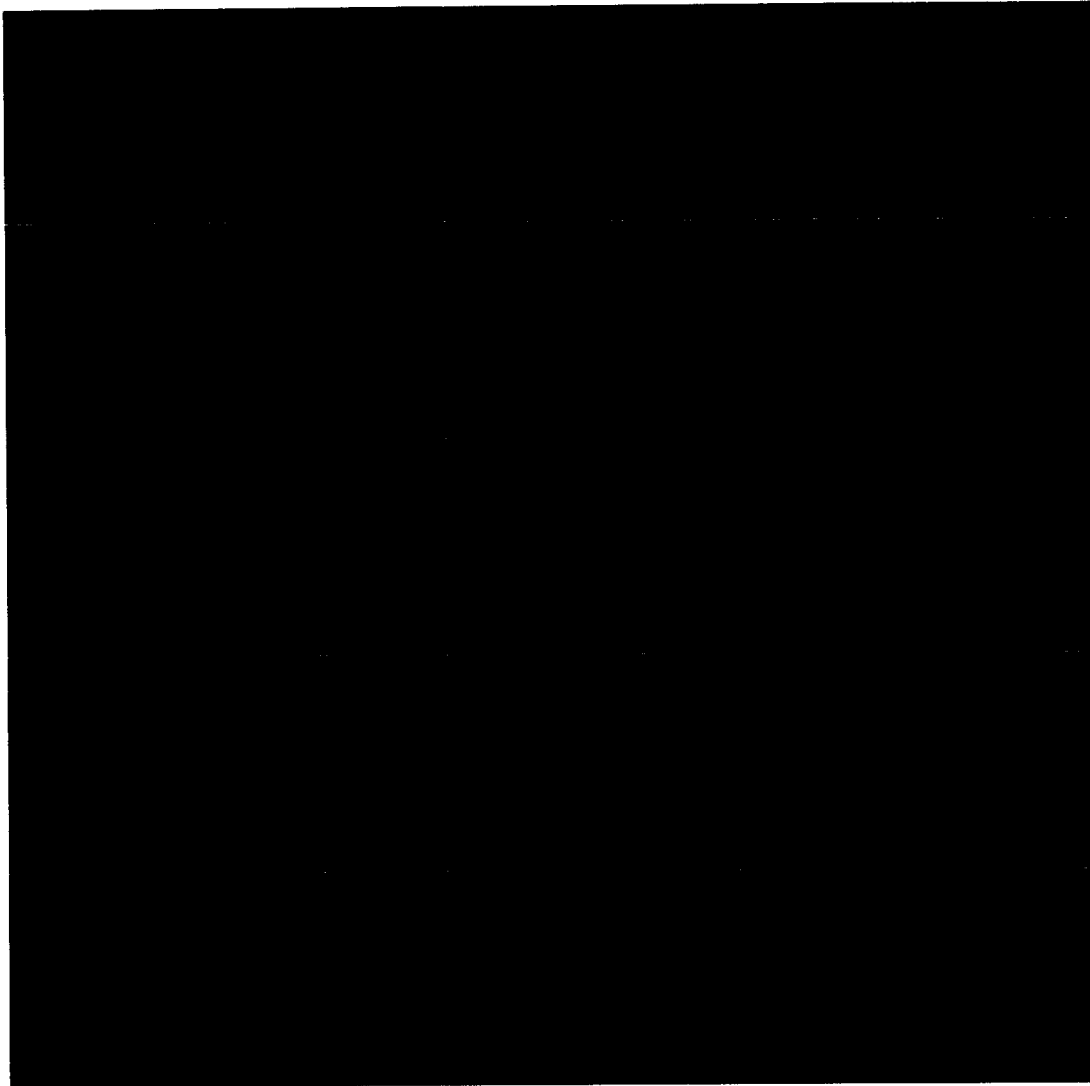


Figure 77. Treated with DNA probe. Series of optical sections collected from laser scanning confocal microscope through the same area of the tube in figure 76 of the **new Octopus 3[®] MT-104-1** following treatment with 500nM of the DNA stain propidium iodide. The images show no fluorescence from the region following staining. The numbers indicate the optical section.

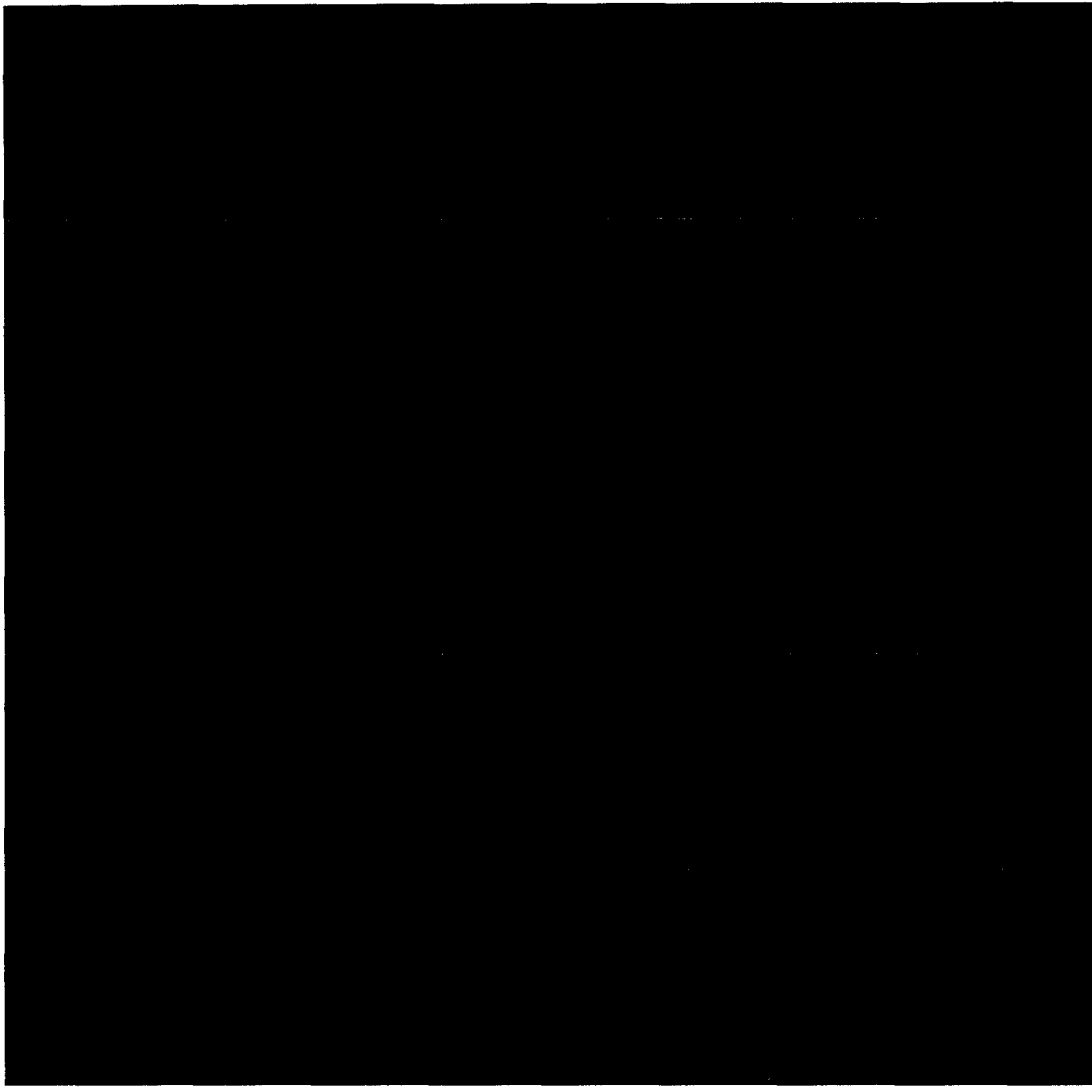


Figure 78. Control. Series of optical sections collected from laser scanning confocal microscope through the area of the tube in pod #5 in the **reprocessed Octopus 3[®] MT-104-3**. The images show low level of autofluorescence in the region of the orifice and additional signals on the surface of the tube. The numbers indicate the optical section.

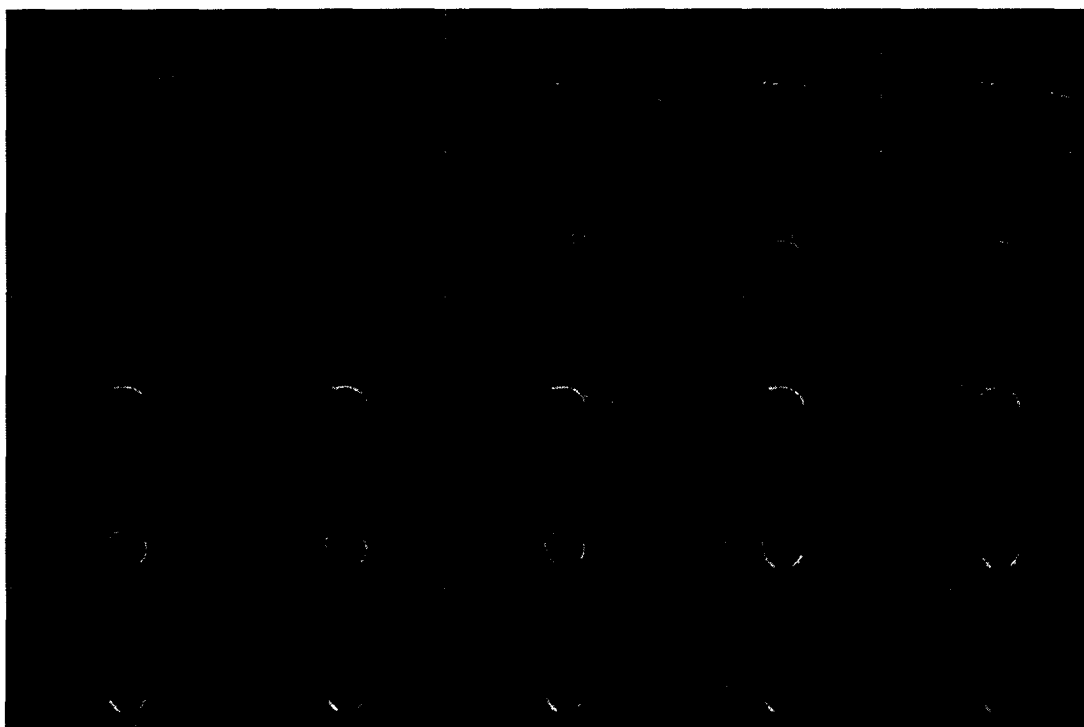


Figure 79. Treated with propidium iodide DNA stain. Series of optical sections collected from laser scanning confocal microscope through the same area of the tube in figure 78 of the **reprocessed Octopus 3[®] MT-104-3** following treatment with 500nM of the DNA stain propidium iodide. The images show significant positive labeling for DNA around the orifice and on the surface of the tubing. This correlates to the SEM images collected prior to staining. The numbers indicate the optical section.

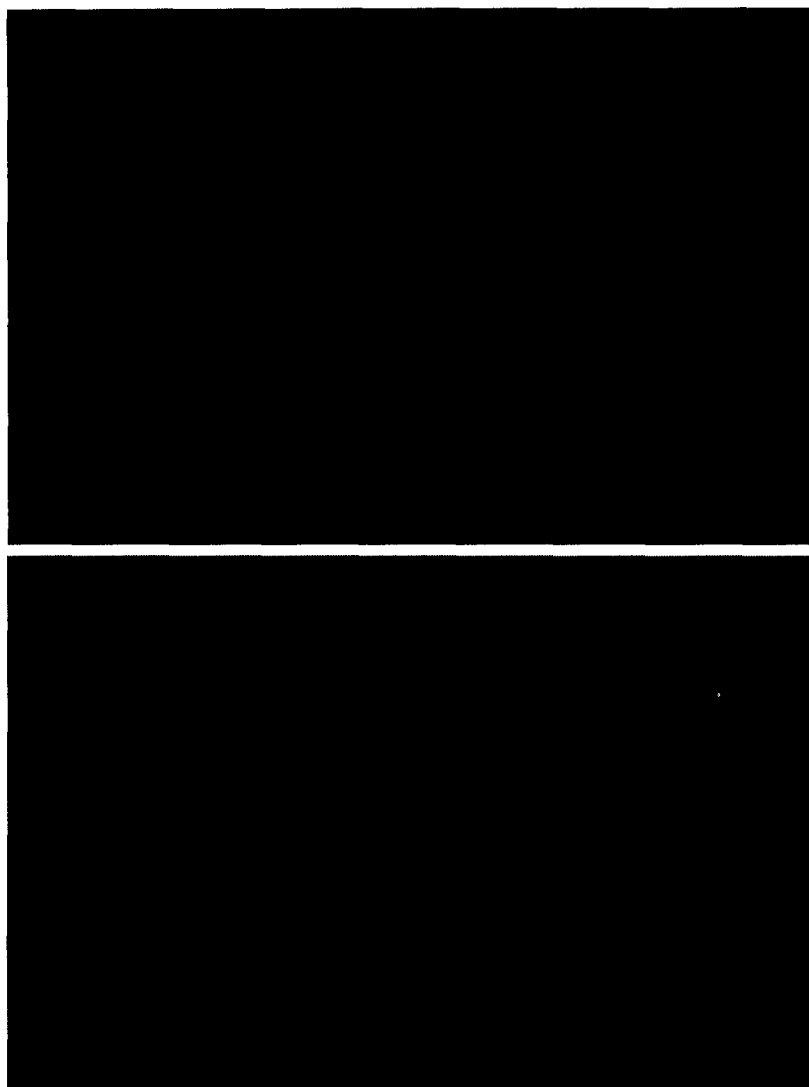


Figure 80. Projections (maximum intensity method) of optical sections used in figures 76 and 77 collected by laser scanning confocal microscope through the area (>0.5 mm thick) of the tube in pod #5 in the **new Octopus 3[®] MT-104-1** before (upper) and following (lower) treatment with 500nM of the DNA stain propidium iodide. The images show no appreciable fluorescence from the region following staining.



Figure 81. Projections (maximum intensity method) of optical sections used in figures 78 and 79 collected by laser scanning confocal microscope through the area (>0.5 mm thick) of the tube in pod #5 in the **reprocessed Octopus 3[®] MT-104-3** before (upper) and following (lower) treatment with 500nM of the DNA stain propidium iodide. The images show significant positive labeling for DNA around the orifice and on the surface of the tubing.

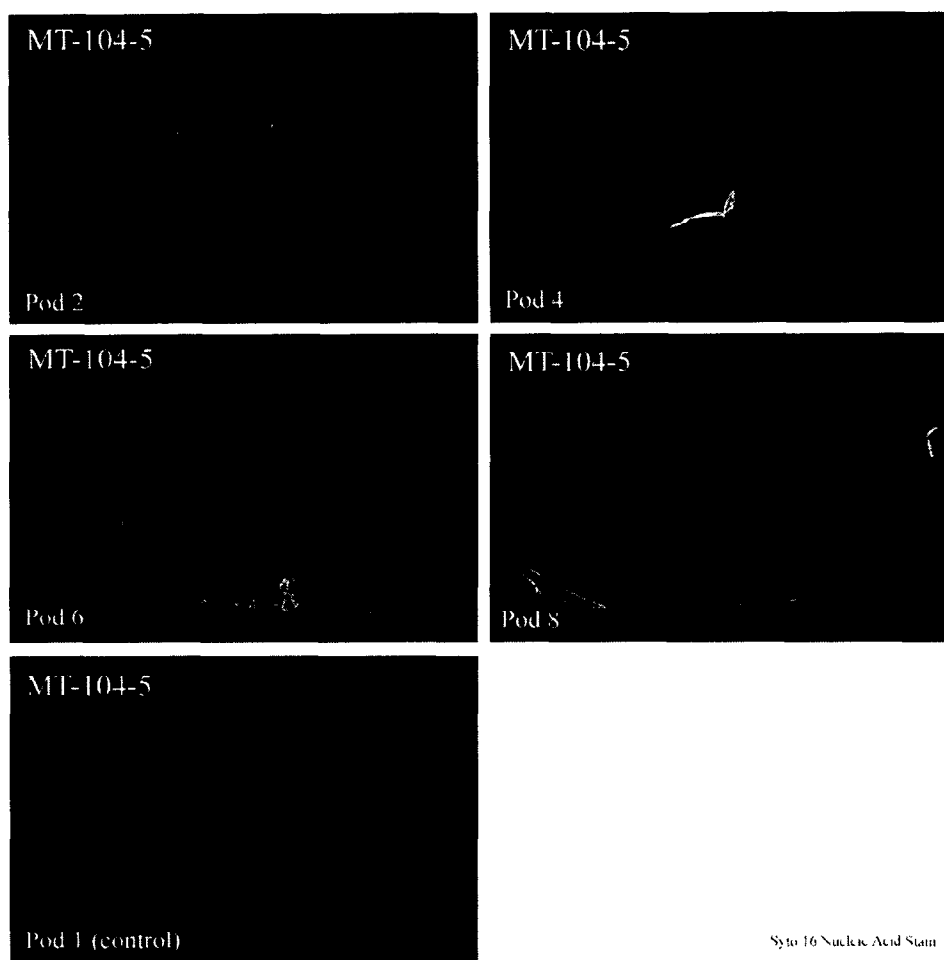


Figure 82. MT-104-5, pod #s 2, 4, 6 and 8 treated with Syto 16 nucleic acid probe. Projections (maximum intensity method) of series of optical sections collected from the laser scanning confocal microscope through the hypotube area of the pod following treatment with 1 μ M of the stain Syto 16. Bright regions indicate positive nucleic acid staining. Pod #1 is an unstained control image through the same area of the hypotube as the other images. The control image shows a low level of autofluorescence.

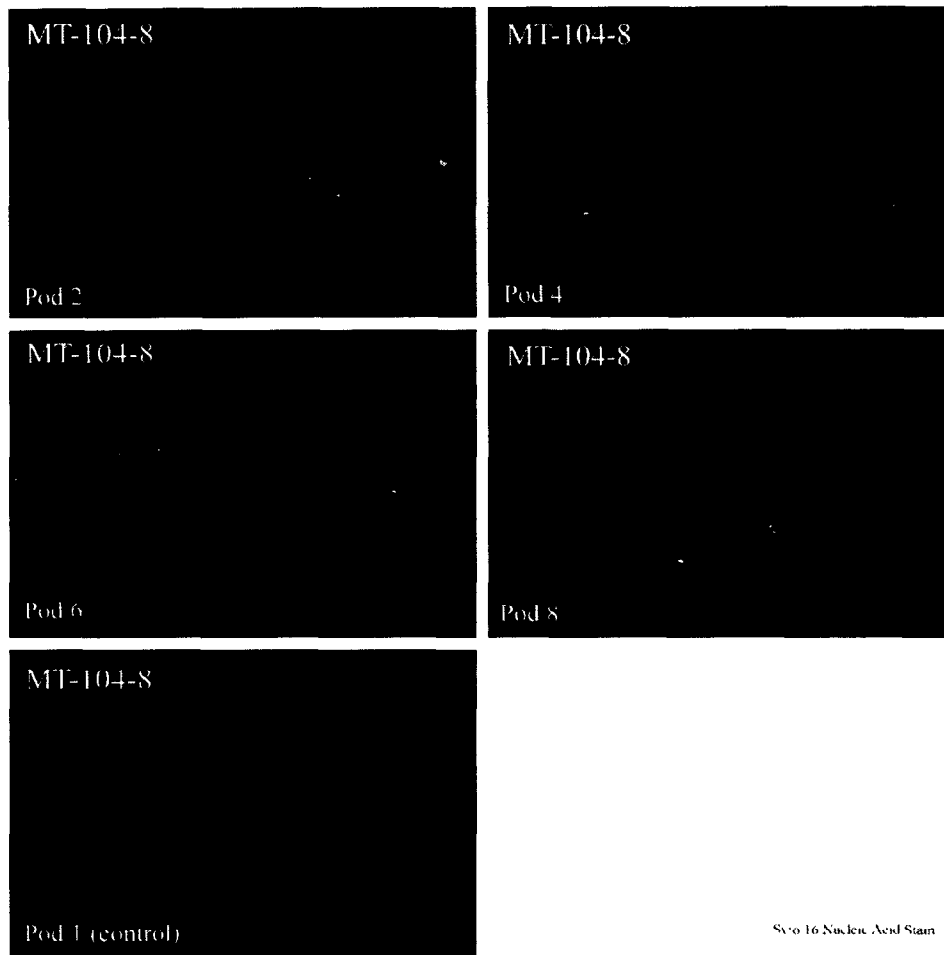


Figure 83. MT-104-8, pod #s 2, 4, 6 and 8 treated with Syto 16 nucleic acid probe. Projections (maximum intensity method) of series of optical sections collected from the laser scanning confocal microscope through the hypotube area of the pod following treatment with 1 μ M of the stain Syto 16. Bright regions indicate positive nucleic acid staining. Pod #1 is an unstained control image through the same area of the hypotube as the other images. The control image shows a low level of autofluorescence.



Figure 84. **Control MT-104-9, pod #6.** Projection (maximum intensity method) of a series of optical sections collected from laser scanning confocal microscope through the area of the tube in the untreated MT-104-9, pod #6 of the reprocessed Octopus 3[®]. The images show a low level of autofluorescence associated with material present in the opening of the hypotube.

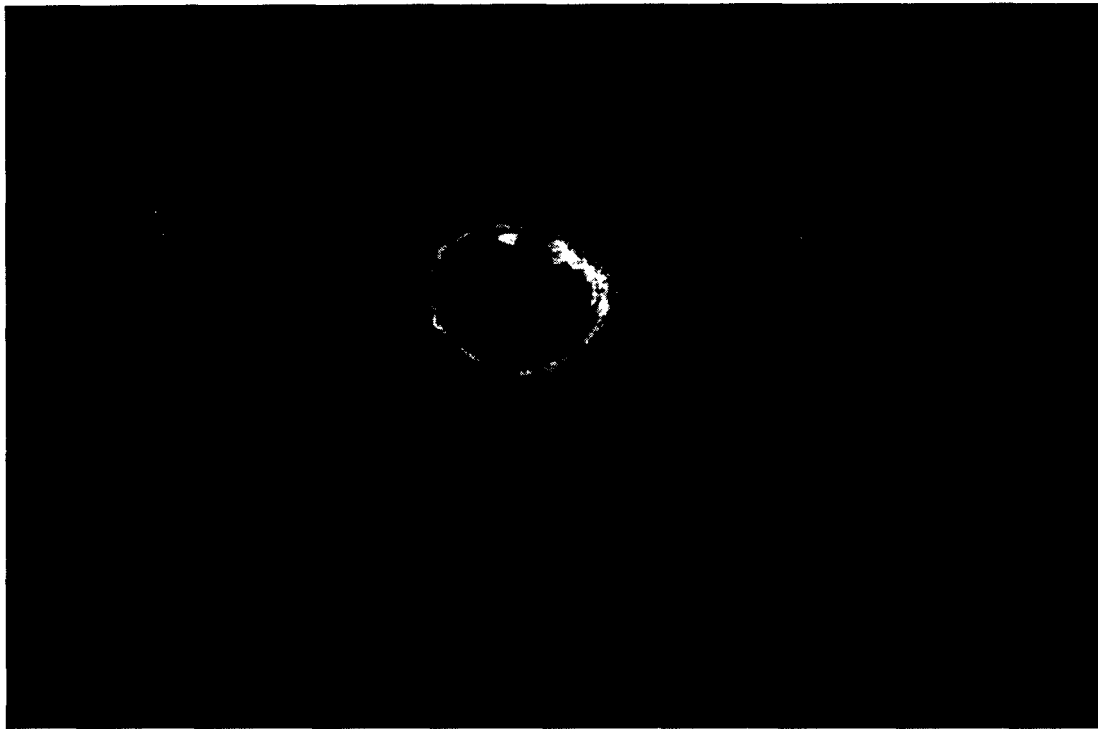


Figure 85. MT-104-9, pod #6 treated with Syto 16 probe. Projection (maximum intensity method) of a series of optical sections collected from laser scanning confocal microscope through the same area of the tube in figure 84 of **MT-104-9, pod #6 of the reprocessed Octopus 3[®]** following treatment with 1 μ M of the stain Syto 16. The images show significant Syto 16 positive labeling around the orifice and on the surface of the tubing. This correlates to the contamination seen in the SEM images collected prior to confocal imaging.



Figure 86. Higher magnification of control MT-104-9, pod #6. Projection (maximum intensity method) of a series of optical sections collected from laser scanning confocal microscope through the area of the tube in the **untreated MT-104-9, pod #6 of the reprocessed Octopus 3[®]**. The images show a low level of autofluorescence associated with the material in the opening of the hypotube.



Figure 87. Higher magnification of MT-104-9, pod #6 treated with Syto 16 probe. Projection (maximum intensity method) of a series of optical sections collected from laser scanning confocal microscope through the same area of the tube in figure 86 of **MT-104-9, pod #6 of the reprocessed Octopus 3[®]** following treatment with 1 μ M of the stain Syto 16. The images show significant Syto positive labeling around the orifice and on the surface of the tubing. This correlates to the SEM images collected prior to staining.



Figure 88. MT-104-9, pod #5 treated with Syto 16 probe. Projection (maximum intensity method) of a series of optical sections collected from laser scanning confocal microscope through the hypotube area of the pod of **MT-104-9, pod #5 of the reprocessed Octopus 3[®]** following treatment with 1 μ M of the stain Syto 16. The images show significant Syto positive labeling around the orifice and on the surface of the tubing. Note positive staining in area of hair-like fiber. This correlates to the foreign material observed in the macro and SEM images collected prior to confocal imaging.

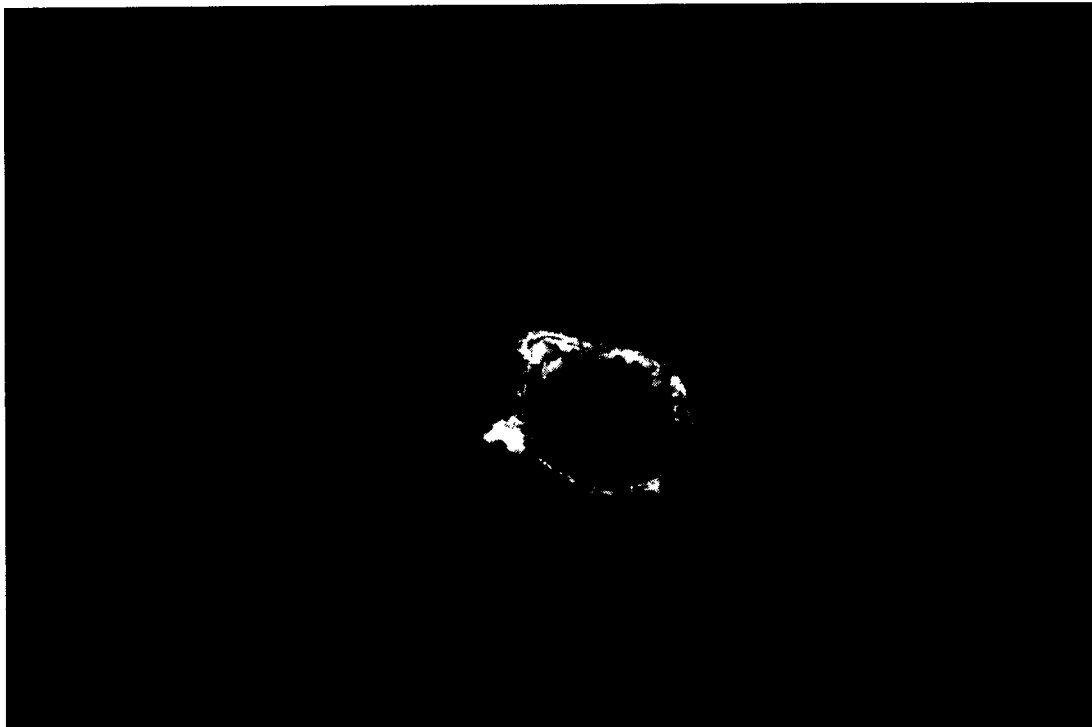


Figure 89. MT-104-9, pod #7 treated with Syto 16 probe. Projection (maximum intensity method) of a series of optical sections collected from laser scanning confocal microscope through the hypotube area of the tube in previous figures of **MT-104-9, pod #7 of the reprocessed Octopus 3[®]** following treatment with 1 μ M of the stain Syto 16. The images show significant positive Syto 16 labeling around the orifice and on the surface of the tubing. This correlates to the foreign material observed in the macro and SEM images collected prior to confocal imaging.

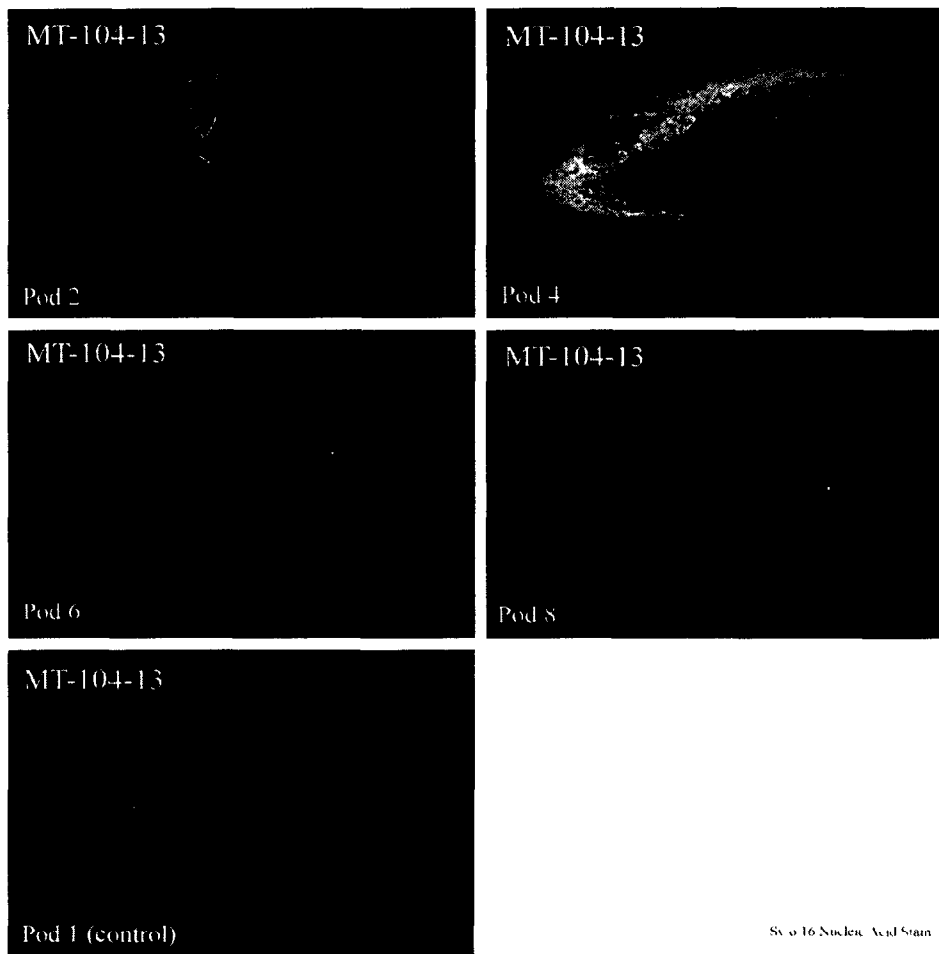


Figure 90. **Reprocessed MT-104-13**, pod #s 2, 4, 6 and 8 treated with Syto 16 nucleic acid probe. Projections (maximum intensity method) of series of optical sections collected from the laser scanning confocal microscope through the hypotube area of the pod following treatment with 1 μ M of the stain Syto 16. Bright regions indicate positive nucleic acid staining. Pod #1 is an unstained control image through the same area of the hypotube as the other images. The control image shows a low level of autofluorescence.

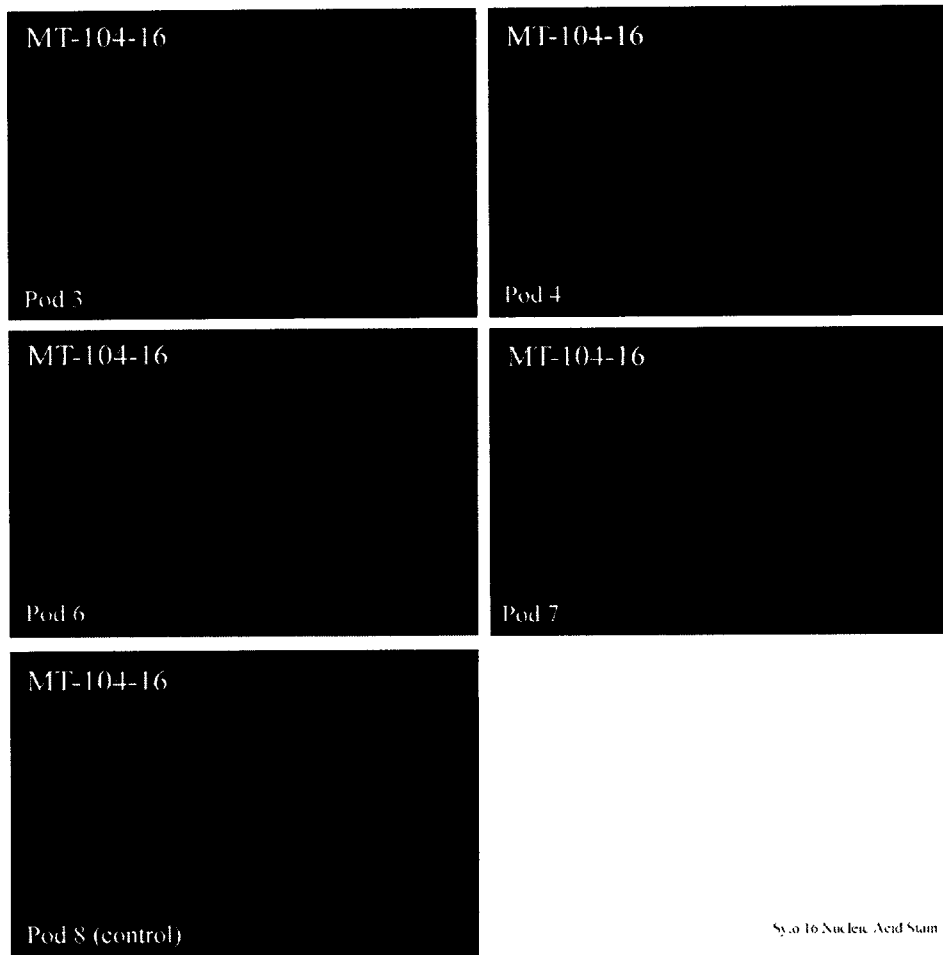


Figure 91. **Reprocessed MT-104-16**, pod #s 3, 4, 6 and 7 treated with Syto 16 nucleic acid probe. Projections (maximum intensity method) of series of optical sections collected from the laser scanning confocal microscope through the hypotube area of the pod following treatment with 1 μ M of the stain Syto 16. Bright regions indicate positive staining. Pod #8 is an unstained control image through the same area of the hypotube as the other images. The control image shows a low level of autofluorescence. Pods # 6 and 8 have a material near the hypotube opening that is not positive for DNA stain.

Sypro[®] Orange Protein Stain



Figure 92. **Reprocessed MT-104-5**, pod #s 3, 5 and 7 treated with Sypro[®] Orange protein stain. Projections (maximum intensity method) of series of optical sections collected from the laser scanning confocal microscope through the hypotube area of the pod following treatment with 2 μ M of the stain Sypro[®] Orange. Bright regions indicate positive staining for protein. Pod #1 is an unstained control image through the same area of the hypotube as the other images. The control image shows a low level of autofluorescence.

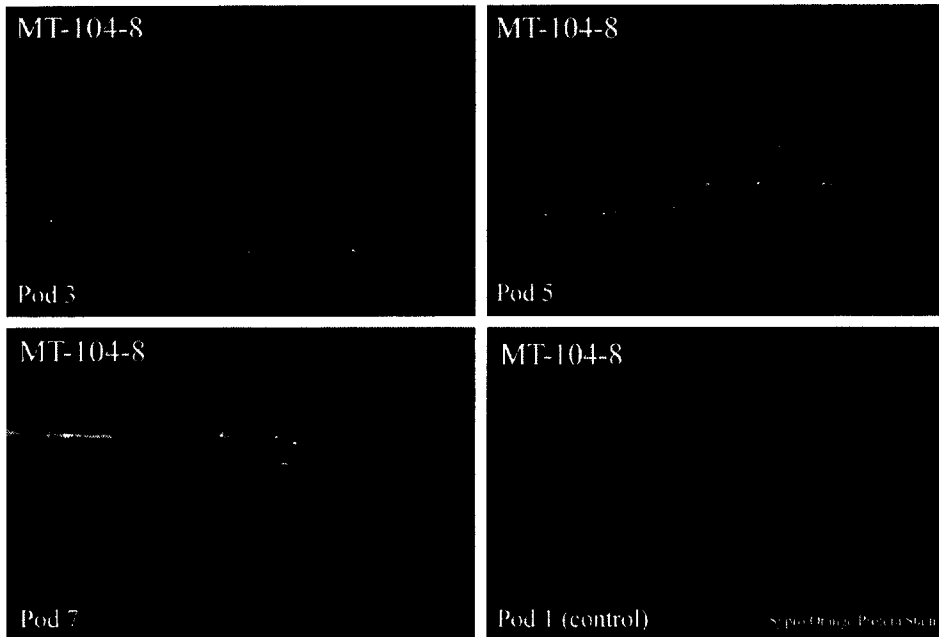


Figure 93. **Reprocessed MT-104-8**, pod #s 3, 5 and 7 treated with Sypro[®] Orange protein stain. Projections (maximum intensity method) of series of optical sections collected from the laser scanning confocal microscope through the hypotube area of the pod following treatment with 2 μ M of the stain Sypro[®] Orange. Bright regions indicate positive staining for protein. Pod #1 is an unstained control image through the same area of the hypotube as the other images. The control image shows a low level of autofluorescence.